ATLSS

Residual Strength and Repair of Damaged and Deteriorated Offshore Structures

Supplement to Area One

MOMENT-THRUST-CURVATURE RELATIONSHIP OF GROUT-FILLED DENTED TUBES

By
A. Ostapenko
T. W. Berger

DISCLAIMER

TABLE OF CONTENTS

ABSTRACT

The moment-thrust-curvature (M-P-Φ) relationship of grout-repaired dented tubular sections was studied by deriving formulas as functions of the level of deformation.

Both materials, steel and concrete, were assumed to have bi-linear elastic-plastic stress-strain relationships except that the grout had no strength in tension and that its post-ultimate strain was limited by the crushing strain. Moreover, it was assumed that the strain distribution in the cross section was planar and that the axial strains in the steel shell and the grout core were fully compatible.

By varying the location of the neutral axis and the value of curvature, the relationship between the axial load and curvature could be defined for a given load eccentricity. The ultimate load was given by the peak of the resultant curve.

The method was applied to analyze six grouted test specimens: three dented and three undented. The resultant ultimate loads were compared with the test loads and the loads according to the formula proposed by Parsanejad. The method tended to give somewhat higher ultimate loads than the test loads.

The method was then used to compute the ultimate loads for seven specimens planned in the testing program proposed for future research.

A FORTRAN computer program was written to facilitate the iterative computations involved in the method.

S1. INTRODUCTION

S1.1 Background

This work was performed in anticipation of funding for Area 4 of the project ("Repair of Dented Members -- Segment Approach") which included tests on short fabricated tubes damaged by deep dents and then repaired by internal grouting.[1] The objective of the tests was to provide experimental information on the moment-thrust-curvature relationship of such tubes in order to verify analytical (finite element) methods. Since the specimens were to be made from the undisturbed portions of the tubular columns tested in a previous project [S4], and some of them were of such dimensions (D = 24.5 in.) that the loads required could have exceeded the capacity of available testing machines, it was necessary to be able to calculate their ultimate strengths in order to design them so that they could be loaded to their maximum capacity. The purpose of the resultant method and the computer program based on it was to provide such a tool.

S1.2 Project Description

The study performed examines tubular members typically used in offshore structures. These structural members are continuously exposed to the possibility of damage from impact by ships or dropped objects. This type of damage is usually in the form of a dent or a combination of a dent and overall out-of-straightness. The main concern is the residual strength of these damaged tubular members. Most of the time, it is not economically advantageous to replace the damaged member and alternative repair methods must be considered. One such method is internal grouting which is finding more frequent use in industry due to its cost effectiveness over other methods, such as underwater welding and clamped sleeves.[S3]

---

[1] Insufficient funding precluded research on Area 4 at the time.

The purpose of internal grouting is to increase the residual strength of a damaged tubular member supplying additional material, but mainly by providing resistance to further distortion of the dented cross section. The following four parameters influencing the strength of the repaired member are studied: diameter-to-thickness ratio (D/t), dent depth-to-diameter ratio (d/D), yield stress of steel (F_y), and ultimate strength of grout (f_g'). A method is formulated for computing the moment-thrust-curvature (M-P-Φ) relationship of a dented, grout-repaired cross section under eccentric loading. To facilitate calculations, the method was incorporated into a computer program.

Chapter 2 describes the method. Chapter 3 describes the material models for grout and steel used in the analysis. Chapter 4 presents the algorithm which was used in the computer program. Chapters 5 and 6 present the results from the analysis of thirteen grout-filled, damaged members. Specifically, Chapter 5 presents the results from the computer program, other analytical methods and experiments and their comparison, and Chapter 6 describes the analysis and a simple parametric study of D/t, d/D, F_y and f_g' based on the results from the thirteen grout-filled dented tubular members which included the projected test specimens.

Finally, Chapter 7 presents the summary, conclusions and recommendations for future studies. Appendix SA provides an address for obtaining the FORTRAN computer program developed for this simplified analysis.

S1.3 Previous Work[1]

The analysis and testing of tubular members repaired by internal grouting has been undertaken by several researchers, notably Parsanejad [S5], Boswell [S2], Ricles [S8],

---

[1] Since the work for this report was performed in 1993, some later publications have not been reviewed.

Renault [S7], and Loh [S3]. A complete state-of-the-art review of the technique of internal grouting as a repair method was conducted by Loh [S3].

Investigation of small-scale specimens by Parsanejad was one of the first endeavors into examining grouting as a repair method for dented tubular members.[S5] An analytical expression was developed to estimate the ultimate capacity of such members.

Ricles investigated both internal grouting methods and clamped sleeve repair of dented tubulars.[S8] Three dented, internally grouted specimens with D/t ratios of 34.5, 46 and 64 and an L/r ratio of 60 were tested.

Boswell and D'Mello conducted tests on grout-filled damaged tubulars with D/t ratios of 23, 29 and 48. Besides the D/t ratio, the following four other parameters were found to have an effect on the behavior and strength: d/D, L/r, scale effects and grout age.

Renault and Quillevere conducted experiments on nine grout-filled, damaged tubes, approximately 15 feet in length, that had a large extent of damage (0.50 and 0.64 dent depth-to-diameter ratio (d/D)) in addition to an initial out-of-straightness.[S7] All of these specimens had a D/t of approximately 22. In addition to testing, a preliminary finite element analysis was performed for both tensile and compressive loadings. It was found from both tests and finite element analysis that the main effect of internal grouting was to prevent or delay the development of a plastic hinge due to local buckling.[S7]

The survey by Loh examined grouting over both the full and partial length of damaged tubulars.[S3] The purpose was to compare current analytical approaches and test data used in determining the ultimate strength of grout-filled tubular members, depending on whether they were fully or partially filled. Additionally, existing technical guidance was summarized and identification of additional work for testing and analysis was proposed.

S1.4 Objectives of Current Study

The objective of the current study is to establish a database for the M-P-ϕ relationship of grout-filled, dented tubular segments and to give an estimate of their residual strength. The resultant M-P-ϕ relationships can then be incorporated into a numerical integration program for the analysis of long columns.

S1.5 Assumptions

To facilitate analysis, the following assumptions were made for a grout-filled dented tube segment to allow for the ease of implementation into a computer program.

1) Strain distribution in the cross section is planar and deformations of steel and concrete are compatible.

2) Steel is assumed to have an elastic-perfectly plastic stress-strain relationship without strain-hardening.(Fig. S3-1)

3) Grout is assumed to be elastic-perfectly plastic with an ultimate strain of 0.003 in./in. Thus, any portion of the grout which reaches this strain can no longer sustain any load or moment.(Fig. S3-2)

4) Grout cannot take any tensile strain, i.e., its modulus of elasticity for tensile loading is zero.

5) In order to preserve the area of the steel, the dented portion of the steel shell is treated as a rectangle extending beyond the edges of the dent as shown in Fig. S1-1. The circular portion of the section is assumed to remain unchanged.

In Figure S1-1, the actual shape of the damaged tube is approximately indicated with heavy dashed lines. The idealized geometry of a dented tube is superimposed using solid lines. It can be seen that near the dented portion, there is distinct bulging of the tube wall with a rather complicated geometry. This is simplified by assuming the shape unchanged

S1-4

below the dent and, to maintain the same cross-sectional area of steel, by replacing the portion above the dent with a flattened, rectangular shape. The additional area extending outside the undamaged portion of the tube is taken into account in calculating the cross-sectional properties, specifically, the moment of inertia, static moment of area and location of the neutral axis.

S2. PROCEDURE OF THE METHOD

S2.1 Introduction

As indicated in Figs. S2-1a and S2-1b, calculation of the total load and moment acting on the cross section is based on first calculating the elastic load and moment for an undamaged cross section, and then subtracting those portions of the load and moment that have yielded or crushed (the yielded area is shown as the triangular portion extending beyond ϵ_{yg} and the crushed portion is shown as the darkened rectangle that has width ϵ_{yg}.) These yielded and crushed portions of the stress diagram for grout over the cross section can be thought of as an *orange wedge*, and, for steel, an *orange rind*.(Figs. S2-2 and S2-3) This terminology of *wedges* and *rinds* is used in subsequent presentation.

S2.2 Cross-Sectional Properties

S2.2.1 Transformed Section

The first step in analyzing a damaged, grout-filled section is to calculate the cross-sectional properties -- area, static moment of area and moment of inertia -- for both the steel shell and grout core assumed to remain elastic.

Figure S2-1 shows that the extent of dent damage is defined by the depth of the dent d and the angle subtended by the dented portion α_d.

$$\alpha_d = \cos^{-1}\left(\frac{R_i - d}{R_i}\right) \tag{S2-1}$$

where R_i is the inner radius.

For a symmetrical cross section, the centroid is at the center of the circle C. As shown in Fig. S2-4, the presence of a dent complicates the analysis since the centroid of the cross section is shifted below the center axis. The location of the centroid is found by taking the first moment of area and dividing by the total area. For simplification purposes, the area of the grout is transformed to an equivalent steel area by dividing it by the modular ratio n.[S6]

Modular Ratio:

$$n = \frac{E_s}{E_g} \qquad (S2-2)$$

Thus, in all subsequent computations, transformation is made to steel by dividing the grout contribution by the modular ratio. Separate calculations are performed for the grout and steel sections to facilitate the analysis of the centroidal shift.

S2.2.2 Grout

For the first moment of area of the grout portion, a simple approach is taken by considering the whole circle and subtracting the portion above the dent as shown by the shaded portion in Fig. S2-1a. By definition, the static moment of area for a circle is, with the lever arm being a function of both r and α,

$$Q = \int_0^\alpha \int_0^{R_i} y(r,\alpha) \; r \; dr \; d\alpha \qquad (S2-3)$$

For a damaged, circular cross section, the static moment of the solid core is

$$Q_g = \int_0^{2\pi} \int_0^{R_i} r^2 \cos\alpha \; dr \; d\alpha \; + \; \frac{2}{3} R^3 \cos\alpha_d \sin^2\alpha_d \; - \; \int_{-\alpha_d}^{\alpha_d} \int_0^{R_i} r \cos\alpha \; dr \; d\alpha \qquad (S2-4)$$

Referring to Fig. S2-5a, the first term is the full circular portion of the grout, the second term is the triangular portion of grout directly below the dent, labeled 'T1', and the third term is the circular wedge of the dented portion, labeled 'T2', that is subtracted. Since the

S2-2

origin and centroid of the circle coincide, the first term drops out and the resulting equation becomes

$$Q_g = \frac{2}{3} R_i^3 \cos^2\alpha_d \sin\alpha_d - \frac{2}{3} R_i^3 \sin\alpha_d \qquad (S2\text{-}5)$$

S2.2.3 Steel

For steel, a simplification is made for the dented portion, as described in Sect. S1.3. The static moment of area for steel after the replacement of the dented portion is

$$Q_s = \int_{\alpha_d-\pi}^{\pi-\alpha_d} R_m^2 \, t \, \cos\alpha d\alpha + 2 \, \alpha_d \, R_m^2 \, t \, \cos\alpha_d \qquad (S2\text{-}6a)$$

where R_m is the mid-thickness radius

$$R_m = R_i + \frac{t}{2} \qquad (S2\text{-}6b)$$

Referring to Figure S2-5b, the first term is the static moment of area for the undamaged circular portion of the tube and the second term is the flattened portion of steel. The resulting equation is

$$Q_s = 2 \, R_m^2 \, t \, [\alpha_d \cos(\alpha_d) - \sin(\alpha_d)] \qquad (S2\text{-}7)$$

S2.2.4 Centroid

As mentioned previously, the steel area is enforced to remain the same, damaged or undamaged. The grout area is decreased by the amount lying above the dent. This reduction gives a slightly smaller area than for an actual dented section which bulged at the sides of the dent. However, the difference is negligibly small. The resulting area equations for steel and grout, respectively, are given by Eqs. S2-8a and S2-8b.

S2-3

$$A_s = 2\pi R_m t \qquad \text{(S2-8a)}$$

$$A_g = R_i^2 \left[\pi - \alpha_d + \cos\alpha_d \, \sin\alpha_d \right] \qquad \text{(S2-8b)}$$

The centroid shift of the damaged cross section is then calculated after transforming the grout contributions to steel properties. The result for the centroidal shift is

$$\bar{y} = \dfrac{\dfrac{Q_g}{n} + Q_s}{\dfrac{A_g}{n} + A_s} \qquad \text{(S2-9)}$$

Figure S2-4 shows the location of the centroid relative to the central axis as well as the sign convention for coordinate axes x and y.

S2.2.5 Moment of Inertia

The basic equation for the moment of inertia about the center is

$$I_{center} = I_{tr,c.g.} + A\bar{y}^2 \qquad \text{(S2-10a)}$$

where

$$I_{tr,c.g.} = \int_{dA_{c.g.}} y^2 \, dA \qquad \text{(S2-10b)}$$

The process of computing the moment of inertia is analogous to the computation of the areas and first moments of area (static moment): the properties are first computed for steel and grout portions with respect to the center, then, transformed to steel and adjusted for the centroidal shift.

The moment of inertia of the steel portion about the center is calculated similarly to the static moment of area, that is, by using the contributions from the undamaged portion and the flattened section.(Fig. S2-5b) The moment of inertia equation for the steel shell is given

S2-4

by Eq. S2-11a.

$$I_s = \int_{-\pi - \alpha_d}^{\pi - \alpha_d} R_m \, t \, (R_m \cos(\alpha))^2 \, d\alpha + 2 \, R_m^3 \, t \, \alpha_d \cos^2(\alpha_d) \qquad \text{(S2-11a)}$$

After integration and setting the limits, the final result is

$$I_s = \frac{R_m^3 \, t}{2} [2 \, \pi - 2 \, \alpha_d - \sin 2 \, \alpha_d + 4 \, \alpha_d \cos^2 \alpha_d] \qquad \text{(S2-11b)}$$

For grout, the moment of inertia about the center is

$$I_g = \int_{-(\pi - \alpha_d)}^{\pi - \alpha_d} \int_0^{R_i} r^3 \cos^2 \alpha \, dr \, d\alpha + \frac{R_i^4 \cos^3 \alpha_d \sin \alpha_d}{2} \qquad \text{(S2-12a)}$$

and after integration,

$$I_g = \frac{R_i^4}{8} [2 \, \pi - 2 \, \alpha_d - \sin \alpha_d + 4 \cos^3 \alpha_d \sin \alpha_d] \qquad \text{(S2-12b)}$$

The transformed moment of inertia with respect to the central axis of the undamaged tube is

$$I_c = I_s + \frac{I_g}{n} \qquad \text{(S2-13a)}$$

and the transformed area is given by Eq. S2-13b

$$A_{tr} = A_s + \frac{A_g}{n} \qquad \text{(S2-13b)}$$

where A_s and A_g are from Eqs. S2-8a and S2-8b, respectively. Thus, the total moment of inertia about the centroid of the damaged section is given by Eq. S2-14.

$$I_{tr,c.g.} = I_c - A_{tr}\,\bar{y}^2 \qquad\qquad \text{(S2-14)}$$

S2.3 Location of Neutral Axis

In order to determine the state of stress in a dented cross section under load with a given eccentricity it is necessary to locate the neutral axis, that is, the location where the stress is zero. For a planar distribution of stresses, the equation for zero stress is

$$\frac{P}{A_{tr,cg}} + \frac{M\,a_{cg}}{I_{tr,cg}} = 0 \qquad\qquad \text{(S2-15a)}$$

where a_{cg} is the y-coordinate from the centroid of the damaged cross section to the neutral axis. With $M = Pe_g$, the equilibrium equation becomes

$$\frac{P}{A_{tr,cg}} + \frac{[P\,e_g]\,a_{cg}}{I_{tr,cg}} = 0 \qquad\qquad \text{(S2-15b)}$$

where e_g is the given eccentricity. Then, Eq. S2-15c gives

$$P\left| \frac{1}{A_{tr,cg}} + \frac{e_g\,a_{cg}}{I_{tr,cg}} \right| = 0 \qquad\qquad \text{(S2-15c)}$$

Since $P \neq 0$, it follows that $\Rightarrow [\ ] = 0$

Figure S2-4 shows the location of the neutral axis with respect to the center and with respect to the distance separating the two axes, a_{cg}. The solution for a_{cg} is given by Eq. S2-16.

$$a_{cg} = \frac{-I_{tr,cg}}{A_{tr,cg}\,e_g}$$

$$\qquad\qquad \text{(S2-16)}$$

$$|a_{cg}| = \frac{I_{tr,cg}}{A_{tr,cg}\,e_g}$$

Then, the distance of the neutral axis from the center of the undamaged tube is

$$a = a_{cg} + \bar{y}$$ (S2-17)

S2.4 Equations for Moment and Axial Load

To analyze a grout-filled, dented tube, it is necessary to calculate the load and moment for both the grout core and steel shell acting on the cross section for a certain state of strain. First, equations are derived for an undented cross section. Then, they are adjusted to consider dent damage and various physical states, such as tension, compression, crushing and yielding. Closed-form solutions are derived for each physical state.

S2.4.1 Elastic Load and Moment for an Undamaged Section

The elastic load and moment are calculated by considering the state of stress at the central axis of the undamaged cross section. Figure S2-6 shows the elastic stress condition in an undamaged cross section, and it can be seen that both load and moment are dependent on the value of curvature ϕ and the location of the neutral axis a. The total elastic load is independent of the centroid location. However, the location of the neutral axis and the amount of curvature determine the value of the elastic load and moment. The neutral axis is assumed to be located at some distance a below the central axis. Taking axial equilibrium over the entire undamaged area, the elastic load is the elastic stress at the centroid times the total area of the undamaged tube.

$$P_e = \sigma_e A_{tr}$$ (S2-18)

The equation for the elastic load of a grout-filled tube is given by Eq. S2-19.

$$P_e = P_g + P_s = \sigma_s A_s + \sigma_g A_g$$

$$P_g = \phi E_g a \left(\pi R_i^2 \right)$$

$$P_s = \phi E_s a \left(2\pi R_m t \right)$$

(S2-19)

For a grouted tube, the total elastic moment is

$$M_e = M_g + M_s$$

$$M_g = E_g I_g \phi$$

$$M_s = E_s I_s \phi$$

(S2-20a)

or

$$M_e = E_s \left[I_s + \frac{I_g}{n} \right] \phi$$

(S2-20b)

In this formulation, the moment of inertia for the grout and steel are not combined into a transformed moment of inertia.

S2.4.2 Grout Under Tension and in the Dented Region

In Sect. S1.3, it was assumed that the grout cannot take any tensile strain. Therefore, if the neutral axis is located within the cross section, the tensile grout load and moment must be deducted from Eqs. S2-19 and S2-20b.(Fig. S2-7) Also, the grout portion that would exist in the dented portion if the tube were undamaged, must be deducted as well to find the total elastic load and moment acting on the damaged cross section.(Fig. S2-1a)

The approach for both regions is exactly the same, with the difference being the limits of integration for the angle. The tension region is subtended by an angle denoted 'α_{na}' and, from Sect. S2.1, the dented portion is subtended by an angle denoted 'α_d'.(Fig. S2-1a) The equations presented in this section are applicable for either the tension or dented region of the grout core.

The equation for the grout load in tension is given by Eq. S2-21a.

$$P_{gt} = 2 \, \phi \, E_g \int_0^{\alpha_{na}} \int_{\frac{R_i \cos(\alpha_{na})}{\cos(\alpha)}}^{R_i} \left[r^2 \cos(\alpha) - r \, R_i \cos\alpha_{na} \right] dr \, d\alpha \qquad \text{(S2-21a)}$$

The final result after integration is

$$P_{gt} = \frac{\phi \, E_g \, R_i^3}{3} \left[2 \sin(\alpha_{na}) - 3 \, \alpha_{na} \cos(\alpha_{na}) + \cos^2(\alpha_{na}) \sin(\alpha_{na}) \right] \qquad \text{(S2-21b)}$$

For the dented portion, only a change of limits for the angle is required

$$P_{gd} = 2 \, \phi \, E_g \int_0^{\alpha_d} \int_{\frac{R_i \cos(\alpha_d)}{\cos(\alpha)}}^{R_i} \left[r^2 \cos(\alpha) - r \, R_i \cos\alpha_d \right] dr \, d\alpha \qquad \text{(S2-22a)}$$

with the final result being

$$P_{gd} = \frac{\phi \, E_g \, R_i^3}{3} \left[2 \sin(\alpha_d) - 3 \, \alpha_d \cos(\alpha_d) + \cos^2(\alpha_d) \sin(\alpha_d) \right] \qquad \text{(S2-22b)}$$

The moment of the grout in the tension region is given by the following equation:

$$M_{gt} = 2 \, \phi \, E_g \int_0^{\alpha_{na}} \int_{\frac{R_i \cos(\alpha_{na})}{\cos(\alpha)}}^{R_i} \left[r^3 \cos^2(\alpha) - r^2 \, R_i \cos(\alpha_{na}) \cos(\alpha) \right] dr \, d\alpha \qquad \text{(S2-23a)}$$

After integrating, the result is

$$M_{gt} = \frac{\phi E_g \, R_i^4}{24} \left[6\alpha_{na} - 5 \sin(2\alpha_{na}) + 4 \cos^3(\alpha_{na}) \sin(\alpha_{na}) \right] \qquad \text{(S2-23b)}$$

Similarly, the moment equation for the grout within the dented portion is given by Eq. S2-24a.

$$M_{gd} = 2 \, \phi \, E_g \int\limits_{0}^{\alpha_d} \int\limits_{\frac{R_i \, \cos(\alpha_d)}{\cos(\alpha)}}^{R_i} \left[r^3 \, \cos^2(\alpha) - r^2 \, R_i \, \cos(\alpha_d) \, \cos(\alpha) \right] dr \; d\alpha \qquad \text{(S2-24a)}$$

The final result for the moment of the grout within the dented portion is

$$M_{gd} = \frac{\phi E_g \, R_i^4}{24} \left[6\alpha_d - 5 \, \sin(2\alpha_d) + 4 \, \cos^3(\alpha_d) \, \sin(\alpha_d) \right] \qquad \text{(S2-24b)}$$

S2.4.3 Effect of Denting

Since the area of steel before and after denting is the same, the axial load is not affected by denting. However, the moment is reduced because the lever arm of the flattened portion becomes smaller. Figures S2-8a and S2-8b show the area modified by denting and the necessary parameters for calculating the lever arm.

Since the formulation is based on finding the total stress acting over an undamaged tube and subtracting appropriate grout stress wedges and steel stress rinds, the effect of denting will be considered by assuming the stress to consist of two parts: a constant block portion acting over the dented steel area and a triangular stress wedge.(Fig. S2-8a) The moment for the block portion is calculated by multiplying the strain at the mid-depth of the flattened segment by the elastic modulus and the lever arm of the dented area, even if the steel fibers in the dented portion have already yielded. The moment for the triangular wedge, shown in Fig. S2-8a, is calculated by using Eq. S2-37b developed later in Sect. S2.4.5 for steel under tension. The appropriate angle to be substituted into Eq. S2-37b in Sect. S2.4.5 is the dent angle, α_d.

The lever arm is found by dividing the first moment of area by the area of the arc subtended by the dent angle. The equation for the lever arm with respect to the center axis is given by Eq. S2-25a.

$$\bar{y}_{arc,c} = \frac{\int_{-\alpha_d}^{\alpha_d} R_m^2\, t\, \cos(\alpha)\, d\alpha}{2\,\alpha_d\, R_m\, t} \qquad \text{(S2-25a)}$$

The result of this equation is

$$\bar{y}_{arc,c} = \frac{R_m\, \sin(\alpha_d)}{\alpha_d} \qquad \text{(S2-25b)}$$

Once the lever arm for the constant stress region acting on the dent portion is found, the moment is then calculated by multiplying this value by the steel load in the segment.

If the fibers in the flattened segment have not yielded, the moment for the dented portion is calculated based on the elastic strain in the dented portion. The moment is the sum of two parts: an elastic block and an elastic wedge.(Fig. S2-8b) Equation S2-37b, described in Sect. S2.4.5, accounts for the elastic wedge. The equation for the elastic block of the moment is given by Eq. S2-26a.

$$M_d = 2\,\phi\, E_s\, R_m^2\, t \left[\sin(\alpha_d) - \alpha_d\, \cos(\alpha_d) \right]\left(R_m + a - d \right) + \text{Eq.2-37b} \qquad \text{(S2-26a)}$$

However, once the flattened segment experiences yielding, the moment is the yield load multiplied by the lever arm from Eq. S2-25b. The portion of the elastic stress wedge beyond yield is accommodated for by Eq. S2-37b described in Sect. S2.4.5.3. The equation for the yield load of the dented portion multiplied by the lever arm is

$$M_d = 2\, R_m^2\, t \left[\sin(\alpha_d) - \alpha_d\, \cos(\alpha_d) \right] F_y + \text{Eq. 2-37b} \qquad \text{(S2-26b)}$$

This is the total loss in moment due to denting.

S2.4.4 Summary: Total Elastic Load and Moment

The total elastic load and moment acting on the damaged cross section are found by first finding the elastic equations for the undamaged portion (Sect. S2.4.1 -- with the grout portion in tension subtracted if the neutral axis is located within the cross section,

Sect. S2.4.2). Then, the damage is accommodated by subtracting the equations derived for the grout portion within the dented region (Sect. S2.4.2) and the loss in moment due to denting of the steel (Sect. S2.4.3).

Summarizing,

Load, P_e:

$$P_e = P_g + P_s - P_{gt} - P_{gd} \qquad \text{(S2-27)}$$

and

Moment, M_e:

$$M_e = M_g + M_s - M_{gt} - M_{gd} - M_d \qquad \text{(S2-28)}$$

S2.4.5 Strain Beyond the Yield Condition

If the strain in the grout and steel is elastic, the load and moment are calculated by Eqs. S2-27 and S2-28. However, as the strain in the grout and/or steel reaches yield, different equations are necessary. This section considers three inelastic cases that develop as the curvature increases, and, consequently, the strain in each material becomes greater than the yield level. The three cases are: yielded grout (compression), yielded steel (compression or compression and tension), and crushing of grout. The equations for each of these cases are then deducted from Eqs. S2-27 and S2-28 to find the total load and moment acting on the dented cross section.

S2.4.5.1 Yielded Grout Under Compression

Figures S2-9a and S2-9b show the general stress states of compression, above and below the central axis C, acting over a portion of the grout. The angle defining the location of the yielded grout region α_{gc}, is shown in Figs. S2-9a and S2-9b. The value of α_{gc} depends on whether the distance c from the neutral axis to the closest yielded fiber is above or below the central axis. Mathematically, α_{gc} is found using Eqs. S2-29a or S2-29b.

For $c \leq a$

$$\alpha_{gc} = \cos^{-1}\left(\frac{a - c}{R_i}\right) \qquad \text{(S2-29a)}$$

or

for $c \geq a$

$$\alpha_{gc} = \cos^{-1}\left(\frac{c - a}{R_i}\right) \qquad \text{(S2-29b)}$$

If the yielded grout region lies above the central axis ($c \geq a$), the equations for grout under tension (Eqs. S2-21 and S2-23) are used by substituting the angle α_{gc} for α_d. On the other hand, if the yielded grout region lies below the central axis ($c \leq a$), equations for the load and moment must be derived by considering the neutral axis location *and* the angle α_{gc}. All the equations derived here are valid even if the neutral axis is outside the cross section, the entire cross section is in compression, and significant yielding has occurred.

When the yielded portion extends below the central axis ($c \leq a$), the total compressive area of the grout core consists of two parts: a pie wedge-shaped portion of a circle and a triangle.(Fig. S2-10) In this case, the value of c is less than a and Eq. S2-29a is used for the angle limit in the integral below. The total load is found by integrating the stress over these two areas as shown in Eq. S2-30a.

$$P_{gc} = 2 \, \phi \, E_g \left[\int_{\alpha_{gc}}^{\pi} \left[r \cos\alpha - R_i \cos\alpha_{gc} \right] r \, dr \, d\alpha \; + \right.$$

$$\left. \int_0^{[R_i \sin\alpha_{gc}]} \int_0^{[R_i \cos\alpha_{gc} - \cot\alpha_{gc} \, x]} -(y) \, dy \, dx \right] \qquad \text{(S2-30a)}$$

The first integral is for the wedge portion and the second integral is for the triangular portion between the central and neutral axes.(Fig. S2-10) Integration of the above equation yields

the solution for the total compressive load of the grout

$$P_{gc} = \frac{\phi \, E_g \, R_i^3}{3} \Big[3 \, \alpha_{gc} \, \cos(\alpha_{gc}) - 3 \, \pi \, \cos(\alpha_{gc}) - 2 \, \sin(\alpha_{gc}) - \cos^2(\alpha_{gc}) \, \sin(\alpha_{gc}) \Big] \qquad \text{(S2-30b)}$$

Determination of the moment proceeds in a similar way. Using the same integration limits as for the load, the moment equation becomes

$$M_{gc} = 2 \, \phi \, E_g \left[\int_{\alpha_{gc}}^{\pi} \int_0^{R_i} \Big[r^3 \cos^2\alpha - R_i \, r^2 \cos\alpha_{gc} \cos\alpha \Big] \, dr \, d\alpha \right.$$

$$\left. + \int_0^{[R_i \sin\alpha_{gc}]} \int_0^{[R_i \cos\alpha_{gc} - \cot\alpha_{gc} \, x]} \Big[R_i \cos\alpha_{gc} \, y - y^2 \Big] \, dy \, dx \right] \qquad \text{(S2-31a)}$$

The two integrals are for the full undamaged portion and the triangular portion below the dent, respectively.(Fig. S2-10) The final result from this integration formula yields Eq. S2-31b.

$$M_{gc} = \frac{\phi \, E_g \, R_i^4}{24} \Big[6\pi - 6 \, \alpha_{gc} + 5 \sin 2\alpha_{gc} - 4 \cos^3 \alpha_{gc} \sin \alpha_{gc} \Big] \qquad \text{(S2-31b)}$$

If c is greater than a (Fig. S2-9a), then α_{gc} from Eq. S2-29b is substituted for α_d in Eqs. S2-21 and S2-23, as stated above.

S2.4.5.2 Yielded Steel Shell Under Compression

The computation of the axial load of steel in compression is found in the same manner as for grout. Figures S2-11a and S2-11b show the area under consideration. The angle α_{sc} in the figures is the angle measured from the central axis to the closest yielded steel fiber. As with the grout described above, α_{sc} may have two values depending on the distance f from the yielded fiber closest to the neutral axis.

For $f \leq a$

$$\alpha_{sc} = \cos^{-1}\left(\frac{a - f}{R_i}\right) \qquad \text{(S2-32a)}$$

or

for $f \geq a$

$$\alpha_{sc} = \cos^{-1}\left(\frac{f - a}{R_i}\right) \qquad \text{(S2-32b)}$$

In the case that the closest yielded steel fiber is above the central axis (Fig. S2-11a), Eq. S2-32b is substituted into Eq. S2-35b, the equation for steel load (tension), described in Sect. S2.4.5.3, is used to find the load and moment for the steel shell under compression.

If the yielded steel fiber closest to the neutral axis is located below the central axis, and using Eq. S2-32a is used, the compressive load acting on the steel shell is given by Eq. S2-33a.

$$P_{sc} = 2 \phi E_s \int_{\alpha_{sc}}^{\pi} \int_{R_i}^{R_o} \left[r^2 \cos(\alpha) - r R_m \cos(\alpha_{sc}) \right] dr \, d\alpha \qquad \text{(S2-33a)}$$

The total load acting in compression on the steel shell, with the location of the neutral axis below the central axis of the undamaged tube but within the cross section, is found by integrating the above expression.

$$P_{sc} = 2 \phi E_s R_m^2 t \left[\alpha_{sc} - 2 \pi \cos(\alpha_{sc}) - \sin(\alpha_{sc}) \right] \qquad \text{(S2-33b)}$$

The higher-order terms involving the thickness are ignored since, in most cases, the diameter is much greater than the thickness, $D \gg t$.

The calculation for the moment proceeds similarly as for grout in compression.

$$M_{sc} = 2 \phi E_s \int_{\alpha_{sc}}^{\pi} \int_{R_i}^{R_o} (r^3 \cos^2(\alpha) \; r^2 \cos(\alpha) \; R_m \cos(\alpha_{sc}) \; dr \; d\alpha \tag{S2-34a}$$

and, after integration, the result is Eq. S2-34b.

$$M_{sc} = \frac{\phi E_s R_m^3 t}{2} \left[(2\pi - 2\alpha_{sc} - \sin(2\alpha_{sc}) + 4 \cos(2\alpha_{sc}) \sin(\alpha_{sc}) \right] \tag{S2-34b}$$

Again, the terms involving the thickness with the order higher than two are ignored.

S2.4.5.3 Yielded Steel Shell Under Tension

For the case where the location of the neutral axis is within the cross section, the strain in the steel fibers below the neutral axis is tension.(Fig. S2-12) The contribution of these steel fibers to the load is expressed by Eq. S2-35a

$$P_{st} = 2 \phi E_s \int_{0}^{\alpha_{st}} \int_{R_i}^{R_o} \left[(r^2 \cos(\alpha) - r R_m \cos(\alpha_{st}) \right] dr \; d\alpha \tag{S2-35a}$$

where α_{st} is the angle defining the extent of the steel region that has yielded. Angle α_{st} is found in a similar fashion as α_{gc} and α_{sc}, but here the distance from the yielded fiber to the central axis is the distance from the neutral axis to the central axis and is denoted by 'b' as shown in Fig. S2-12.

$$\alpha_{st} = \cos^{-1}\left(\frac{b}{R_i}\right) \tag{S2-36}$$

The final result after integration gives Eq. S2-35b.

$$P_{st} = \frac{\phi E_s R_m^3 t}{2} \left[(2\alpha_{st} + \sin(2\alpha_{st})) - 4 \cos(\alpha_{st}) \sin(\alpha_{st}) \right] \tag{S2-35b}$$

The moment equation for steel in tension is given by Eq. S2-37a.

$$M_{st} = \frac{\phi \, E_s \, R_m^3 \, t}{2} \left[2 \, \alpha_{st} + \sin(\alpha_{st}) - 4 \cos(\alpha_{st}) \sin(\alpha_{st}) \right] \qquad \text{(S2-37b)}$$

Then, integration gives Eq. S2-37b for the magnitude of the moment in the tension region of the steel shell.

$$M_{st} = 2 \, \phi \, E_s \int_0^{\alpha_{st}} \int_{R_i}^{R_o} \left[r^3 \cos^2(\alpha) - R_m \, r^2 \cos(\alpha_{st}) \cos(\alpha) \right] dr \, d\alpha \qquad \text{(S2-37a)}$$

S2.4.5.4 Crushing of Grout

When the strain in the grout becomes larger than the ultimate strain, the grout no longer contributes to either the load or moment and is considered to have zero stress. Figures S2-13a and S2-13b show the point w above which the grout has crushed. As can be seen in Fig. S2-13a, the grout has yielded above point "v" since the strain exceeds the f_g'/E_g value. The amount of grout that has exceeded f_g' before crushing is shown by the triangular wedge marked 'gy.' The amount of grout that carries f_g' is denoted by 'gc'. The grout that has crushed is shown by the dark, rectangular-shaped stress block labelled gc. The equations are developed by considering the stress state of the grout as being at or below the yield level (f_g'). It should be noted that it is the strain that controls this state, not stress, although the stress acting on the crushed portion is still easily calculated given curvature, location of the neutral axis and the necessary material properties.

In order to develop the equations for load and moment at the crushed condition, it is assumed that the stress is constant over the portion that has crushed. Similarly to the development of the equations for the yielded grout and steel under compression, two equations are necessary for the crushing of grout -- one for grout crushing above the central axis and one for below.

Distance g is defined to be the distance from the closest crushed fiber to the location of the neutral axis. Angle α_{gcr} defines the extent of crushing. If g is greater than a,

(Fig. S2-13b) then α_{gcr} results in Eq. S2-38a.

For g ≤ a

$$\alpha_{gcr} = \cos^{-1}\left(\frac{a - g}{R_i}\right) \tag{S2-38a}$$

or, for Fig. S2-13a,

for g ≥ a

$$\alpha_{gcr} = \cos^{-1}\left(\frac{g - a}{R_i}\right) \tag{S2-38b}$$

The load over a crushed portion when g < a is calculated from Eq. S2-39a

$$P_{gcr} = 2 f'_g \left[\int_{\alpha_{gcr}}^{\pi} \int_0^{R_i} r\, dr\, d\alpha + \int_0^{[R_i \sin\alpha_{gcr}]} \int_0^{[R_i \cos\alpha_{gcr} - \cot\alpha_{gcr}\, x]} dy\, dx\right] \tag{S2-39a}$$

where $\sigma_{cr,g}$ is the stress acting on the crushed section. Integration then yields the final result per Eq. S2-39b.

$$P_{gcr} = f'_g R_i^2 \left[\pi - \alpha_{gcr} + \cos\alpha_{gcr} \sin\alpha_{gcr}\right] \tag{S2-39b}$$

To find the crushing load when g > a, the following equation yields the appropriate result in Eq. S2-40a.

$$P_{gcr} = 2 \int_0^{\alpha_{gcr}} \int_{\left[\frac{R_i \cos(\alpha_{gcr})}{\cos(\alpha)}\right]}^{R_i} f'_g\, r\, dr\, d\alpha \tag{S2-40a}$$

The final result for the crushed load is found from the above equation

$$P_{gcr} = f'_g R_i^2 \left[\alpha_{gcr} - \cos(\alpha_{gcr}) \sin(\alpha_{gcr})\right] \tag{S2-40b}$$

The moment of the crushed portion when g < a (Fig. S2-13a) is determined by

integrating the following equation Eq. S2-41a:

$$M_{gcr} = 2 \left[\int_{\alpha_{gcr}}^{\pi} \int_{0}^{R_i} f'_g \; r^2 \cos(\alpha) \; dr \; d\alpha \right.$$

$$\left. + \int_{0}^{[\; R_i \sin(\alpha_{gcr}) \;]} \int_{0}^{[\; R_i \cos(\alpha_{gcr}) \; - \; \cot(\alpha_{gcr}) \; x \;]} f'_g \left[R \cos(\alpha_{gcr}) - y \right] dy \; dx \right]$$

(S2-41a)

After integration, the solution reduces to Eq. S2-41b.

$$M_{gcr} = - \left[\frac{2 \, f'_g \; R_i^2 \; \sin^3(\alpha_{gcr})}{3} \right]$$

(S2-41b)

Finally, the equation to find the moment of the crushed portion when $g > a$ is Eq. S2-42a.(Fig. S2-13b)

$$M_{gcr} = 2 \, f'_g \int_{0}^{\alpha_{gcr}} \int_{\left[\frac{R_i \cos(\alpha_{gcr})}{\cos(\alpha)} \right]}^{R_i} r^2 \cos(\alpha) \; dr \; d\alpha$$

(S2-42a)

The result after integrating Eq. S2-42a becomes Eq. S2-42b.

$$M_{gcr} = \frac{2 \, f'_g \; R_i^2 \; \sin^3(\alpha_{gcr})}{3}$$

(S2-42b)

As expected, the tensile moment is equal to the absolute value of the compressive moment. The difference in sign arises due to the choice of sign convention, tension -- positive, compression -- negative.

S3. MATERIAL PROPERTIES

The assumptions used for both the grout and steel material models are described in Sect. S1.3.

S3.1 Grout

S3.1.1 Modulus of Elasticity for Grout

As an approximation, the modulus of elasticity for grout is calculated from the ACI equation recommended for concrete (§ 8.5.1 of Ref. S1).

$$E_g = \frac{w_g^{1.5} \; 33 \sqrt{f'_g}}{1000} \quad [\text{ksi}] \tag{S3-1}$$

Where w_g is the unit weight of grout.

S3.1.2 Stress-Strain Curve for Grout

The assumed stress-strain curve for grout is shown in Fig. S3-1. Besides making a simplifying assumption for the value of the modulus of elasticity of the grout, the material model for grout is assumed to be linearly elastic-perfectly plastic. However, once the strain in the grout attains the value of the ultimate strain, $\epsilon_{cr} = 0.003$, the grout is assumed to be crushed and unable to carry any additional stress. Further developments in analysis will require better knowledge of the stress-strain (σ-ϵ) relationship for grout.

S3.2 Steel

S3.2.1 Stress-Strain Curve for Steel

Steel is assumed to have a linearly elastic-perfectly plastic stress-strain relationship, as shown in Figure S3-2. Strain hardening effects are not taken into consideration nor is

strain reversal. Once the strain in any portion of the steel shell becomes greater than the yield strain, the slope of the stress-strain curve becomes zero up to an infinite strain value.

It is recommended that for subsequent development of the material model of steel, strain hardening effects be considered. Since the steel shell within the vicinity of the dent is plastified, this portion of the steel may pick up additional load due to strain-hardening. Thus, the inelastic behavior of the damaged, grout-filled specimen may be better represented.

S4. ALGORITHM FOR SIMPLIFIED ANALYSIS OF DENTED GROUT-REPAIRED TUBE SECTIONS

A computer program was developed for performing the analysis of dented, grout-filled tubes. The logic of the program is to determine the load vs. curvature relationship for a given tubular section with the eccentricity set to have a specified value (e_g). Then, with the preset eccentricity, the curvature and the location of the neutral axis are the two variables which define the state of stress in the cross section. The computational procedure calculates the initial location of the neutral axis and (Sec. S2-2), by iteratively varying the curvature, computes the moment and axial load which give the required eccentricity ($M/P = e_g$). Then, by changing the location of the neutral axis, the relationship between the load and curvature is computed. The flowchart of the steps required for performing this work is shown in Fig. S4-1. The section below explains the relevant steps of the computer program used for these calculations (Appendix SA).

S4.1 Required Input

First, the appropriate geometrical and material properties of each specimen are read in. Figure S4-2 shows an example input file for data. The program reads in the specimen name and then the needed geometrical and material properties as well as the date of analysis. The geometrical properties required are: outside diameter (D), thickness (t), dent depth (d/D), and the preset eccentricity (e/D). The diameter and thickness values are in inches.

Then, the material properties are read in. These properties include the modulus of elasticity of steel (E_s), the unit weight of grout (w_g), the yield stress of grout (f_g') and steel (F_y), and the ultimate strain of grout (ϵ_u). All the yield stress and modulus of elasticity units are in ksi.

S4.2 Computational Procedure

With the value of eccentricity specified, a trial location of the neutral axis is chosen. Then, the computer program determines the yield curvature for steel and for grout and selects the smaller of them as the starting curvature for the next step. The initial location of the neutral axis is changed next and the total axial load and moment are calculated for the starting curvature. The eccentricity is determined by dividing the moment by the load. With the neutral axis kept at the same location, the curvature is increased by a certain percentage of the starting value, and a new value for eccentricity is calculated. If this eccentricity is not within a prescribed tolerance of the specified eccentricity, a third value of curvature is calculated by linear interpolation. If, after this step, the tolerance for eccentricity is still not reached, interpolation is repeated until the desired convergence is achieved. The resultant axial load and curvature give one point of the load-curvature relationship. Figure S4-3 shows a sample plot of eccentricity vs. curvature for a fixed location of the neutral axis. The details of the interpolation are discussed further in the next section. The neutral axis is changed, and a new load and curvature are found in a similar way, until the load associated with the converged eccentricity value is less than a certain percentage of the maximum load value, or the curvature has reached the value that is three times the value at the ultimate condition. The program stops execution at this step.

This procedure is repeated for each location of the neutral axis until there comes a certain point where any increase in curvature, results in an increase in eccentricity. Then, it becomes necessary to reverse the change in the location of the neutral axis. For example, if the distance between the central axis and the location of the neutral axis is being decreased, then the change in location of the neutral axis is reversed and the distance is made to increase. This behavior is a result of the tension and compression regions no longer being in equilibrium, and in consequence, for an increasing curvature, convergence of the eccentricity can only be achieved through reversing the change of the location of the neutral axis.

Since the M-ϕ and P-ϕ relationships are linear in the elastic region, discussion here is mainly concerned with the inelastic behavior. To construct the complete P-ϕ ($M=Pe$) curves, the following ranges of stress conditions must be considered:

1) Steel and grout, both elastic.

2) Grout, inelastic under compression.

3) Steel, inelastic under compression.

4) Grout crushing.

5) Grout, inelastic under tension.

6) Steel, inelastic under tension.

A more specific discussion for each stress state is presented next.

S4.2.1 Elastic Range

The program does not calculate any intermediate points for the elastic range of the P-ϕ curve of grout or steel since it is known to be linear. For an initial location of the neutral axis, first yielding in either the grout or steel in the damaged portion is the starting point for the computational process.

S4.2.2 Inelastic Range

As the first step in the inelastic analysis for each set of values of curvature and location of the neutral axis, the cross section is assumed to be undamaged and fully elastic with the corresponding linear distribution of stresses. Then, the load and moment contributions of the grout-core in the dent portion are subtracted. Since the steel area remains the same, dented or undented, only the moment adjustment for the dent area is subtracted. In Sect. S1.3, it was assumed that the grout portion in tension carries no load or moment. Thus, these contributions are subtracted from the elastic load and moment (Sect. S2.3.4). If the neutral axis lies outside the inner diameter, there will be no subtraction for grout under tension. A flag in the code determines whether this subtraction is necessary. This completes the determination of the total *elastic* load, given by Eq. S2-27 in

Sect. S2.3.4, and moment of the damaged cross section (Eq. S2-28 also in Sect. S2.3.4). Next, these values are adjusted for inelastic effects.

If grout under compression has yielded, then the portion exceeding the yield stress, f_g', is subtracted. The shape of this yielded portion is similar in shape to an "orange wedge," shown in Fig. S2-2. The program determines whether the yielded portion extends below the central axis. If so, the formulas for load and moment developed for grout in compression are used (Eqs. S2-30 and S2-31). If not, the formulas for grout in tension are used (Eqs. S2-21 and S2-23). It should be noted that the volume of this wedge is exactly equal to the load, and the moment is equal to the first moment of the wedge volume.

If the strain in the damaged steel shell exceeds the yield level in the tension or compression regions, the location of the yielded portion is checked to determine whether the load and moment equations for compression or tension should be subtracted from the elastic values. If the neutral axis lies within the cross section below the central axis, the yielded compression portion may extend below the central axis. Then, the load and moment for steel under compression must be used for the values of the load and moment to be subtracted from the *elastic* values (Eqs. S2-33 and S2-34); otherwise, the values for tension must be used (Eqs. S2-35 and S2-37).

If the curvature is increased to the point where the strain in the grout exceeds the crushing value (0.003 in./in.), the corresponding contributions of the load and moment must be subtracted from the values computed up to this point.(Sect. S2.3.5.4 and Eqs. S2-39, S2-40, S2-41 and S2-42)

Finally, the only time steel in tension can yield is when the neutral axis lies within the cross section of the tube. The program checks the strain in this region, and, if yielding has occurred, the load and moment values developed for steel in tension (Eqs. S2-35 and S2-37) are subtracted from the total load and moment.

S4.3 Load-Curvature Pattern

The change from one yield condition to another is often quite noticeable in the P-ϕ curve. Figure S4-11 shows a typical P-ϕ curve. (The M-ϕ curve could just as well have been presented, since in this analysis, the moment is a direct function of the load, $M = Pe$.) This curve has five distinct parts: elastic, inelastic - grout yielding, inelastic -compression yielding of steel, inelastic - tension yielding of steel, and the crushing of grout above the crushing strain. As each of these yielding conditions is reached, a distinct kink appears in the P-ϕ curve. Point 1 designates the end of the linearly elastic region and the start of the grout inelastic region. The yielding of steel in the compression region is signified by Point 2. Point 3 marks the peak, that is, the ultimate load. After this point, the grout strain under the dent is greater than the crushing strain, and the grout in this area can no longer sustain any load or moment. The curve levels off, and proceeds with gradually reducing load until another kink occurs (Point 4), albeit not as distinct as the others. This point signifies yielding of the steel in the tension region below the neutral axis. After this point, the curve continues until the total load is less than or equal to a preset minimum value (Point 5) or the curvature has reached a value that is greater than three times the curvature value at the ultimate condition. It should be pointed out that the yielding of the grout does not always occur first. If the yield curvature for the steel in the dent section is less than that for the grout in this region, Points 2 and 3 would represent the yielding of the steel and then the grout.

S4.4 Interpolation Procedure

Figures S4-4 to S4-10 illustrate the interpolation procedure used in the computer program to determine the curvature, moment and load for a prescribed eccentricity. Specimen P3P10 of Table S2-1 is chosen for a numerical example with the location of the neutral axis a fixed at 8.94 inches, that is, $a/R = 0.72$ with the neutral axis within the cross

section. This specimen had $D = 24.66$ in., $t = 0.321$ in., $d = 2.45$ in., $F_y = 59.3$ ksi, $f'_g = 3$ ksi, and $e = 2.45$ in.

Figure S4-4 shows the anticipated plot of the eccentricity (e) vs. curvature (Φ) relationship for $a = 8.94$ in. Each point on the curve has an axial load P associated with it (or M since $M = Pe$). The task is to compute the values of Φ and P for a given value of eccentricity e_g, which is indicated by a vertical line intersecting the curve. Since the relationship among a, Φ, e and P ($M = Pe$) is very nonlinear, an iterative procedure must be used. A trial value of curvature Φ_1 is assumed (conveniently, a slightly larger value of Φ than described in Sect. S4.2.1). Then, the corresponding value of eccentricity e_1 is determined from the procedure of Sect. S4.2.2. This point is marked on the curve. This value of eccentricity is compared to the given input value e_g. If the calculated value for the eccentricity e_1 is within a prescribed tolerance taken with respect to e_g (currently set into the program to be $\pm 0.1\%$), then the location of the neutral axis is changed and the procedure begins again. Usually, this is not the case, and the search must continue.

Figure S4-5 shows the second point of the procedure. This point is obtained by incrementing the start curvature Φ_1 by $\Delta\Phi$ which is chosen to be 10% of Φ_1. Figure S4-5 shows that the calculated eccentricity e_2 is still not within the tolerance ($\pm 0.1\%$) of e_g. Therefore, the procedure is continued in order to determine a third point closer to e_g.

Using the values of e_1 and e_2 together with their respective curvature values, the third value of Φ_3 is found by using linear interpolation.(Fig. S4-6) The new value of eccentricity e_3, marked as Point 3 in the figure, is computed but it is still not within $\pm 0.1\%$ of the given value e_g, and the procedure is continued.

Figure S4-7 shows the fourth calculated value (Point 4) for the eccentricity as well as Points 1, 2 and 3 and their respective curvature values. Since e_3 was greater than e_g, the two closest values of eccentricity are selected and linear interpolation is used to compute the next value of curvature, Φ_4. If the corresponding eccentricity is greater than e_g, then the two

closest values to e_g are again chosen and the linear interpolation procedure is repeated until e_4 is less than or within $\pm 0.1\%$ of e_g.

If after reaching the condition where two points are straddling the input value for eccentricity (Fig. S4-7), the program switches to a different search procedure. A sorting algorithm determines which point in Fig. S4-7 is farthest away from the desired point e_g and discards it. Thus, in this example, Point 1 is farthest away and is replaced in memory by Point 2. Then, if two points are straddling e_g, another sort routine is used to determine the two closest of the remaining values that are straddling. In the case that the two closest points are to the left of e_g, the program discards the one that is farthest away from e_g. This method assures that at least two points straddle e_g.

After obtaining the two closest values that straddle e_g, the next point is found by taking the average curvature of these two straddling points. Point 5 in Fig. S4-8 is found in this manner. Φ_5 is the average of Φ_4 and Φ_2. This procedure continues as Point 6 in Fig. S4-9 is found by averaging the curvatures of Points 4 and 5, and finally, in Fig. S4-10, the final converged point is found by averaging Φ_5 and Φ_6 ($\Phi_{final} = 0.27 \times 10^{-3}$ in.$^{-1}$). The corresponding value of eccentricity, $e = 2.449$ in., is within the prescribed tolerance of $\pm 0.1\%$. At this point the program writes to an output file the corresponding values for eccentricity (Fig. S4-2b), the location of neutral axis, load, moment and curvature. Then, the neutral axis location is changed and the last curvature value ($\Phi_{final} = 0.27 \times 10^{-3}$ in.$^{-1}$ in this case) is used for the start curvature of this location of the neutral axis.

S5. COMPARISON WITH OTHER METHODS AND RESULTS

S5.1 Analytical Solution from Parsanejad

Parsanejad has developed an analytical expression for estimating the ultimate capacity of grout-filled damaged tubular members based on first yielding of the steel in the dent area from beam-column analysis.[S5] Parsanejad's equation was used to calculate the ultimate load for all specimens, and they are compared with the method proposed in Chapter S2. This equation is presented here in Eq. S5-1a.

$$\left[\frac{\sigma_u}{\sigma_y}\right]^2 - \left[\frac{1+k}{\lambda^2} + m\right]\left[\frac{\sigma_u}{\sigma_y}\right] + \frac{m}{\lambda^2} = 0 \qquad \text{(S5-1a)}$$

$$\text{where } \lambda = \sqrt{\frac{\sigma_y}{\sigma_{euler}}}$$

$$k = \frac{A_{tr,c.g.}\ e_t}{z_{tr}} \qquad \text{(S5-1b)}$$

$$m = \frac{A_{tr,c.g.}}{A_{tr}}$$

Equation S5-1a above is solved for σ_u (and P_u since $P_u = \sigma_u A_{tr,c.g.}$) using the parameters listed in Eq. S5-1b where

λ is the reduced slenderness parameter.

k is the nondimensionalized parameter consisting of transformed area A_{tr} multiplied by the total lateral displacement ($e_t = e_g + \delta + y$, where e_g is the prescribed eccentricity.

δ is the out-of-straightness.

y is the distance between the centroids of the dented steel cross section and the undamaged cross section) and divided by the transformed section modulus taken with respect to the dented side.

m is the nondimensionalized parameter consisting of the ratio of the transformed area of the dented cross section $A_{tr,c.g.}$ to that of the undented cross section A_{tr}.

S5.2 Comparison with Experimental Results from Ref. S8

Table S5-1 lists the material and geometrical properties of the three specimens (A3, B3, C3) tested by Ricles.[S8] The dent depth for all three specimens was the same -- 0.1D. The axial load was applied with an end eccentricity of 0.2D. In the analysis, the given eccentricity was taken as the sum of the lateral displacement at the ultimate (peak) load and the applied end eccentricity $e_g(=0.2D)$, which were given in the reference.

Table S5-2 compares the ultimate loads computed using the proposed method to experiments and the analytical method from Ref. S5 (Eq. S5-1a). As shown in the table, the proposed method tends to overestimate the ultimate load in most cases when compared to experimental results, as well as to the results from the method of Ref. S5 (Eq. S5-1a). The non-dimensionalizing value P_y in the table is defined by Eq. S5-2.

$$P_y = A_s F_y + A_g f'_g \tag{S5-2}$$

Table S5-3 lists the ultimate loads and corresponding curvature for each specimen. Figures S5-1 through S5-3 give the load vs. curvature curves calculated for Specimens A3, B3 and C3.

S5.2.1 Specimen A3

Figure S5-1 shows the computed P-ϕ curve for Specimen A3 of Table S5-1. For a curvature of 0.564×10^{-3} in.$^{-1}$, the calculated ultimate load was 198.2 kips (0.46P_y). The ultimate axial load from experiment was 191 kips (0.44P_y). The program overestimated the

ultimate load by about +3.7%. In comparison, Eq. S5-1a predicted a lower-bound value of 143 kips ($0.33P_y$) for the ultimate load, that is -25.2% lower than the experimental load.

S5.2.2 Specimen B3

Figure S5-2 shows the computed P-ϕ curve for Specimen B3 of Table S5-1. For a curvature of 0.609×10^{-3} in.$^{-1}$, the ultimate load was 133.8 kips, that is, $0.39P_y$. The test load was 117 kips ($0.34P_y$). Thus, the program overestimated the ultimate load by +14.4%. Equation S5-1a gave an ultimate load of 110 kips, or $0.32P_y$, that is, an error of -6.0%.

S5.2.3 Specimen C3

Figure S5-3 shows the computed P-ϕ curve for Specimen C3 of Table S5-1. The ultimate load was estimated to be 192.8 kips ($0.47P_y$) at a curvature of 0.581×10^{-3} in.$^{-1}$. The experimental load was 122 kips ($0.29P_y$). The program overestimated the ultimate load by +58.0%. Equation S5-1a showed very good correlation of -1.0% with respect to the test in this instance, giving an ultimate load of 121 kips ($0.29P_y$).

S5.2.4 Summary

Three specimens tested by Ricles had different D/t ratios but the same relative dent depths and end eccentricities.[S8] For an increasing D/t ratio, the ultimate load decreased for the tests. The program overestimated the ultimate load from +3.7% for Specimen A3 to +58.0% for Specimen C3.

S5.3 Analysis of Proposed Specimens

Seven short, dented and grouted specimens proposed for testing in the current research program at Lehigh University are analyzed in this section. These specimens are to be made from the following previously tested dented specimens of Ref. S4: P1P, P2P, P3P, E1, D1, and D3. A new specimen will be made by cutting off a still-undamaged portion of an old specimen, denting it and then grouting it. There will be one new specimen from each

of the old except that two will be made from P3P. The proposed specimens and their test parameters are listed in Table S5-1. For convenience, the specimen names were kept as those of the original specimens (but they may be changed later) except for P3P05 and P3P10 where the extensions of 05 and 10 refer to the level of denting d/D. Since experiments have not yet been performed on these specimens, comparison will be made only with Eq. S5-1a.[S5]

S5.3.1 'P', 'E' and 'D' Specimens

Four fabricated and three salvaged specimens were analyzed by the proposed formulation with D/t ratios ranging from 28.18 for Specimen E1 to 76.32 for Specimen P3P. Table S5-1 lists the parameters of these specimens and Table S5-3 gives their computed ultimate loads and the corresponding curvatures. Figures S5-4 through S5-10 present the load vs. curvature curves for each specimen calculated by the proposed formulation. The peak values from these curves are compared against the ultimate loads calculated by Eq. S5-1a.[S5]

S5.3.1.1 Specimen P1P

Figure S5-4 shows the computed P-ϕ curve of Specimen P1P generated from the program. A peak load of 803.3 kips, that is, $0.59P_y$, was reached at a curvature of 0.212×10^{-3} in.$^{-1}$. Equation S5-1a gave an ultimate load of 752.5 kips ($0.55P_y$) which differs by $+6.76\%$ from the proposed result.

S5.3.1.2 Specimen P2P

Figure S5-5 shows the computed P-ϕ curve of Specimen P2P generated from the program. A peak load of 1275.8 kips ($0.49P_y$) was reached at a curvature of 0.214×10^{-3} in.$^{-1}$. In comparison, the ultimate load calculated by Eq. S5-1a was 1084.4 kips ($0.42P_y$). The difference between the two methods is slightly larger than that for Specimen P1P. The calculated difference with respect to Eq. S5-1a is $+17.6\%$.

S5.3.1.3 Specimen P3P

Figure S5-6 shows the computed P-ϕ curve of Specimen P3P with a 5% dent depth generated from the program. A peak load of 2166.9 kips ($0.48P_y$) was reached at a curvature of 0.127×10^{-3} in.$^{-1}$. Equation S5-1a yielded an ultimate value of 2513.9 kips ($0.55P_y$), giving a difference of -11.6%.

Figure S5-7 shows the computed P-ϕ curve of Specimen P3P with a 10% dent depth generated from the program. A peak load of 2064.9 kips ($0.45P_y$) was reached at a curvature of 0.143×10^{-3} in.$^{-1}$. Equation S5-1a yielded a value of 2138.8 kips ($0.47P_y$), giving a very reasonable deviation of -3.58%.

S5.3.1.4 Specimen E1

Figure S5-8 shows the computed P-ϕ curve of Specimen E1 generated from the program. A peak load of 602.4 kips ($0.52P_y$) was reached at a curvature of 0.383×10^{-3} in.$^{-1}$. Equation S5-1a gave a peak value of 388 kips ($0.34P_y$), yielding a difference of 55.1%.

S5.3.1.5 Specimens D1 and D3

Figure S5-9 shows the computed P-ϕ curve of Specimen D1 generated from the program. A peak load of 623.9 kips ($0.55P_y$) was reached at a curvature of 0.358×10^{-3} in.$^{-1}$. Equation S5-1a gave a peak value of 474.7 kips, that is, $0.42P_y$. The resulting difference with respect to Eq. S5-1a was 31.4%.

Figure S5-10 shows the computed P-ϕ curve of specimen D3 generated from the program. A peak load of 880.5 kips, or $0.57P_y$, was reached at a curvature of 0.280×10^{-3} in.$^{-1}$. For Specimen D3, Eq. S5-1a yielded an ultimate value of 630.4 kips ($0.41P_y$), giving a deviation of 39.7%.

S5.4 Comparisons with Undamaged, Grout-Filled Specimens

Three undamaged specimens tested with an eccentric load by Wimpey Offshore were analyzed, and the results are compared to the tests.[S3]   The geometric and material properties of these specimens are listed in Table S5-1 and the computed and experimental ultimate loads in Table S5-2. Figures S5-11 through S5-13 show the computed P-ϕ curves for these undamaged, grout-filled Specimens W1, W3 and W5, respectively. The ultimate experimental load and the ultimate load calculated by Eq. S5-1a are shown as well. As expected, the formulation is more accurate for shorter than longer specimens. The computed result for the shorter specimen, Specimen W1, is quite respectable -- 10.1% greater than experimental.

S6. PARAMETRIC STUDY

S6.1 Parametric Study

Table S5-1 lists the geometrical and material properties for the thirteen specimens analyzed in this study. From the analysis of these specimens a preliminary and simple parametric study for the effect of D/t, d/D, F_y and f'_g is performed here. (No attempt was made in this study to explore the use of any combined parameters which may lead to more consistent correlations.) In each graph, comparison is made between the proposed formulation (Eq. S5-1a) and the test results. The results from Eq. S5-1a are marked with an X-filled square, the proposed formulation with a filled triangle and experiments with an X.

S6.2 Diameter-to-Thickness Ratio (D/t)

A significant parameter for the ultimate strength is the D/t ratio. As seen in Table S5-1, the D/t ratio ranged from approximately 16 to 77. Figure S6-1 shows the effect of D/t ratio on the nondimensionalized ultimate strength for all specimens analyzed in this study. It appears that the proposed formulation correlates better for the specimens with D/t ratios between 20 and 50 than for the specimens with D/t below 20 or above 50. However, more data is needed to make a more accurate conclusion.

S6.3 Dent Depth-to-Diameter Ratio (d/D)

The depth of the dent is a significant parameter that affects the ultimate strength of a repaired, dented tubular member. Figure S6-2 shows that the nondimensionalized ultimate load calculated from the proposed formulation correlates well with the results from Eq. S5-1a

and tests for d/D = 0.05 to 0.15. However, for undented specimens (d/D = 0) and specimens with d/D greater than 0.15, the difference is greater.

S6.4 Yield Stress

The yield stresses of grout (f'_g) and steel (F_y) affect the ultimate load. Figure S6-3 shows a plot of steel yield stress versus the nondimensionalized ultimate load. It appears that the proposed method compares better with Eq. S5-1a and experiments for lower values of yield stress ($<$ 60 ksi). Only one specimen was analyzed with the highest yield stress value of 70.9 ksi, and the values for the nondimensionalized ultimate load from the proposed method and Eq. S5-1a differed significantly. More specimens with higher yield stresses are needed for further study.

Figure S6-4 shows the effect the grout yield stress has on the nondimensionalized ultimate strength. For a grout yield stress below approximately 7 ksi, the difference between experiments (Eq. S5-1a) and the proposed formulation is at most 25% with respect to the proposed formulation. At yield stress levels above 7 ksi, the two methods and experiments have greater discrepancy.

S7. SUMMARY, CONCLUSIONS AND RECOMMENDATIONS FOR FUTURE RESEARCH

S7.1 Summary and Conclusions

The moment-thrust-curvature (M-P-Φ) relationship of grout-repaired dented tubular sections was studied by deriving formulas as functions of the level of deformation. The steel tube was assumed to have a bi-linear stress-strain relationship with unlimited straining at the yeild stress level (F_y). The grout core was idealized to have a bi-linear elastic-plastic stress-strain relationship with the straining at the ultimate (yield) level (f_c') limited by the crushing strain. The grout was assumed to have no strength in tension. Furthermore, the strain variation in the cross section was assumed to be planar and the axial strains in the steel shell and the grout core to be fully compatible

The formulas were developed as functions of the limiting positions of the neutral axis (within or outside of the cross section) and of the level of curvature to initiate yielding in steel and/or yielding or crushing in the grout.

A trial-and-error procedure based on a gradual change of the location of the neutral axis (N.A.) and the value of curvature was used to determine the axial load and curvature for a preset load eccentricity. A series of such solutions for an increasing value of the load eccentricity provided data for plotting the load vs. curvature relationship of the cross section. The peak of the curve defined the ultimate axial load P_u.

Although the computations involved CAN be performed manually or, more efficiently, by using a programmable calculator for some individual case, a FORTRAN computer program was written to carry out the calculations of the many cases of this study.

After developing the method, a simplified analysis was performed to calculate the ultimate strength, and comparison was made with the available experimental data and an analytical method. Thirteen full-scale, grout-filled, dented and undented specimens under eccentric loading were studied to investigate the moment-thrust-curvature (M-P-Φ) relationship and ultimate strength. Then, a simple parametric study was performed on the following four parameters: diameter-to-thickness ratio (D/t), extent of damage (d/D), steel yield stress (F_y), and grout yield stress (f_g'). In this study, the D/t ratio ranged from 16 to 77, the d/D ratio from 0.0 (no dent) to 0.2, F_y from 33 to 71 ksi and f_g' from 3 ksi to slightly greater than 10 ksi.

In determining the ultimate load, P_u, the results from the proposed method were found to be less conservative than the results from experiments and Eq. S5-1a. However, when the length effects were included, the results from the numerical procedure correlated very well with the results from experiments and the analytical method. In the best case, for Specimen A3, the method predicted the ultimate load to within approximately 4% of the experimental and 38% of the load calculated by Eq. S5-1a. In the worst case, for undented Specimen W5, the procedure overestimated the experimental ultimate load by a large amount. Equation S5-1a also overestimated the ultimate load, but not by as much. This specimen had the lowest D/t ratio of all the specimens analyzed. It also had the highest steel yield stress value among all the specimens (70.9 ksi) and one of the highest for grout (9.29 ksi).

The proposed procedure was not conservative in estimating the ultimate load. It appears from the parametric study that the procedure better predicts the ultimate load for specimens having a D/t = 20 to 60, a d/D = 0.05 to 0.15, a steel yield stress F_y = 30 to 60 ksi, and a grout yield stress f_g' less than 7 ksi.

S7.2 Recommendations for Future Research

To more adequately estimate the ultimate load and generate the M-P-Φ relationship for grout-filled, dented tubular members, the following work is recommended:

1) More testing needs to be done to extend the database of knowledge about the parameters (D/t, d/D, F_y, f_g') that affect the ultimate strength of grout-filled tubular members. Then, a more comprehensive parametric study can be done. Currently, seven specimens are proposed for testing at Lehigh University. These specimens have already been analyzed in this study.

2) An improved algorithm for determining the M-P-Φ relationship should be developed, for one, by including a more realistic stress-strain relationship for grout and to consider the possibility of local buckling in the steel shell. Currently, the material model for grout is assumed to be elastic-perfectly plastic with the elastic modulus determined from the ACI formula.[S1] Since the stress-strain relationship for grout is known to be nonlinear, it is important to model the actual behavior of the grout.

S8. ACKNOWLEDGMENTS

S9. REFERENCES

[S1]   ACI Committee 318

"Building Code Requirements for Reinforced Concrete (ACI 318-89)", American Concrete Institute, Detroit, MI, 1971.

[S2]   Boswell, L.F., and D'Mello, C.A.

"Residual and Fatigue Strength of Grout-Filled Damaged Tubular Members", OTH 89 314, Offshore Technology Report, United Kingdom, DEn, 1990.

[S3]   Loh, J.T.

"Grout-Filled Undamaged and Dented Tubular Steel Members", Exxon Production Research Co., Houston, Texas, 1991.

[S4]   Ostapenko, A., Wood, B.A., Chowdhury, A., and Hebor, M.F.

"Residual Strength of Damaged Tubular Members in Offshore Structures", Volume 1, Report 93-03, ATLSS-Lehigh University, Bethlehem, PA, 1993.

[S5]   Parsanejad, S.

"Strength of Grout-Filled Tubular Members," J. Struct. Div., ASCE, 113(3), 590-603, 1987.

[S6]   Popov, E.P.

"Mechanics of Materials", 2nd. ed. Englewood Cliffs, NJ: Prentice-Hall, Inc., 1976.

[S7]   Renault, J.P. and Quillevere, J.P.

"Offshore Structures: Repair of Dented Members by Internal Grouting", Proceedings of the Ninth International Conference on Offshore Mechanics and Arctic Engineering - Volume III, Part B (Materials Engineering), Houston, TX, 1990.

[S8]   Ricles, J.R.,Gillum, T., and Lamport, W.

"Residual Strength and Grout Repair of Dented Offshore Tubular Bracing-Phase 1 Study", ATLSS Report No. 92-14 (October), ATLSS-Lehigh University, Bethlehem, PA, 1992.

S10. NOMENCLATURE

a — Distance from the location of neutral axis to horizontal axis passing through the center of the undamaged cross section. [in.]

a_d — Distance from the location of the neutral axis to the centroid of the damaged$_d$ cross section. [in.]

A_g — Area of grout core. [in.^{2}]

A_s — Area of the steel shell for a damaged, circular cross section. Assumed to be equal to the undamaged cross section. [in.^{2}]

A_{tr} — Area of undamaged transformed cross section. [in.^{2}]

$A_{tr, c.g.}$ — Area of damaged transformed cross section. [in.^{2}]

b — Distance from the location of the neutral axis to the closest yielded steel fiber in the tension region. [in.]

c — Distance from the location of the neutral axis to closest yielded grout fiber in the compression region. [in.]

d — Dent depth. [in.]

D — Diameter. [in.]

e_g — Prescribed end eccentricity. [in.]

e_t — Total end eccentricity including out-of-straightness and centroid shift of damaged cross section. ($e_t = e_g + \delta + y$) [in.]

E_g — Modulus of elasticity of grout from ACI formula, Ref. S1. [ksi]

E_s — Modulus of elasticity of steel. [ksi]

f — Distance from the location of the neutral axis to the closest yielded steel fiber in the compresion region. [in.]

f_{exp} Maximum stress due to the ultimate experimental load P_u. [ksi]

f'_g Yield stress of grout. Used in calculations. [ksi]

F_u Ultimate tensile stress of steel. [ksi]

F_y, σ_y Yield stress of steel. Used in calculations. [ksi]

g Distance from location of the neutral axis to the closest crushed grout fiber. [in.]

I_c Transformed moment of inertia with respect to the central axis of the undamaged tube. [in.⁴]

I_{center} Transformed moment of inertia of damaged cross section about the center of the undamaged cross section. [in.⁴]

I_g Moment of inertia of the grout area for the damaged cross section. [in.⁴]

I_s Moment of inertia of the steel shell for the damaged cross section. [in.⁴]

$I_{tr.\ c.g.}$ Transformed moment of inertia about the centroid of the damaged cross section. [in.⁴]

k Nondimensionalized parameter that is the product of the transformed damaged area and total eccentricity divided by the transformed section modulus taken with respect to the dent side. (Ref. S5)

l Length of tube. (Ref. S5) [in.]

m Nondimensionalized parameter that is the ratio of the transformed area of the damaged cross section to the undented cross section. (Ref. S5)

M_{gcr} Moment of crushed grout portion. [k-in.]

M_d Steel moment lost due to dent. [k-in.]

M_c Elastic moment acting on undamaged cross section. [k-in.]

M_g Elastic moment contribution of undamaged grout area. [k-in.]

M_{gc} Moment of yielded grout portion in compression. [k-in.]

M_{gd} Moment of dented portion. [k-in.]

M_{gt} Moment of yielded grout portion in tension. [k-in.]

M_s Elastic moment contribution of undamaged steel area. [k-in.]

M_{sc} Moment of yielded steel portion in compression. [k-in.]

M_{st} Moment of yielded steel portion in tension. [k-in.]

n Nondimensionalized ratio of the steel elastic modulus to the grout elastic modulus.

P_e Total elastic load acting on undamaged cross section. [kips]

P_g Elastic load contribution of undamaged grout area. [kips]

P_{gc} Load of yielded grout portion in compression. [kips]

P_{gd} Load of dented portion. [kips]

P_{gcr} Load of crushed grout portion. [kips]

P_{gt} Load of grout portion in tension. [kips]

P_s Elastic load contribution of steel area. [kips]

P_{sc} Load of yielded steel portion in compression. [kips]

P_{st} Load of yielded steel portion in tension. [kips]

P_y Yield load. [kips]

Q First moment of area (static moment of inertia) of corroded cross section. [in.^{3}]

Q_g First moment of area for the solid grout core of a damaged, circular cross section. [in.^{3}]

Q_s First moment of area for the steel shell of a damaged, circular cross section. [in.^{3}]

R_i Inner radius. [in.]

R_m Mid-thickness radius. [in.]

r_{tr} Transformed radius of gyration of damaged cross section. [in.]

t Thickness. [in.]

w_g Grout weight. [pci - lbs./in.^{3}]

y Centroid shift. (Distance between centroid of the damaged cross section and center of the undamaged cross section) [in.]

$y_{arc,c}$ Lever arm of steel portion above flattened segment in dented area. [in.]

z_{tr} Transformed section modulus taken with respect to dented side. (Ref. S5) [in.^{3}]

α Nondimensionalized parameter used in local buckling formulas.

α_d Angle subtending dented portion of damaged cross section. [rads.]

α_{gc} Angle subtended by yielded portion of grout in compression. [rads.]

α_{gcr} Angle subtended by crushed portion of grout. [rads.]

α_{na} Angle defining the location of the neutral axis when the neutral axis is located within the cross section. [rads.]

α_{sc} Angle subtended by yielded portion of steel in compression. [rads.]

α_{st} Angle subtended by yielded portion of steel in tension. [rads.]

δ Out-of-straightness. [in.]

ϵ_{cr} Ultimate, or crushing, strain of grout. ($\epsilon_{cr}= 0.003$) [in./in.]

ϵ_u Ultimate strain of grout. [in./in.]

ϵ_{yg} Yield strain of grout. [in./in.]

ϵ_{ys} Yield strain of steel. [in./in.]

λ Reduced nondimensionalized slenderness parameter. (Ref. S5)

ϕ Curvature. [in.$^{-1}$]

ϕ_{ys} Yield curvature of steel for the undamaged cross section. [in.$^{-1}$]

σ_e Euler buckling stress. ($\sigma_e = \pi^2 E_s r_{tr}/L^2$, Ref. S5)

σ_g Elastic grout stress. [ksi]

σ_s Elastic steel stress. [ksi]

σ_u Ultimate stress. ($\sigma_u = P_u A_{tr, c.g.}$, Ref. S5) [ksi]

TABLES

Table S5-1: Material and Geometric Properties of Specimens.

Spec.	Ref. No.	Test	D (in.)	t (in.)	L tube (ft)	dent (in.)	End Ecc. (in.)	D/t	d/D	Area (in^2)	Fy (ksi)	f'g (ksi)
1	2	3[1]	4	5	6	7	8	9	10	11	12	13
P1P	--	P	15.13	0.260	12.00	0.75	1.50	58.19	0.05	179.90	42.70	3.00
P2P	--	P	17.22	0.375	12.00	2.38	1.70	45.91	0.14	233.05	57.13	3.00
P3P05	--	P	24.66	0.321	12.00	1.23	2.45	76.82	0.05	477.79	59.30	3.00
P3P10	--	P	24.66	0.321	12.00	2.45	2.45	76.82	0.10	477.79	59.30	3.00
E1	--	P	10.57	0.375	10.00	2.08	1.04	28.18	0.20	87.93	53.27	3.00
D1	--	P	10.54	0.360	10.00	1.55	1.04	29.28	0.15	87.45	54.19	3.00
D3	--	P	13.77	0.444	10.00	2.17	1.36	31.02	0.16	149.27	43.95	3.00
A3	S8	E	8.75	0.247	14.90	0.86	3.02	35.42	0.10	60.21	34.80	4.38
B3	S8	E	8.73	0.187	14.91	0.86	3.73	46.67	0.10	59.88	33.40	3.88
C3	S8	E	8.71	0.135	15.01	0.86	2.79	64.52	0.10	59.62	39.40	6.90
W1	S3	E	8.56	0.118	7.08	0.00	2.1	72.57	0.00	57.61	60.60	10.15
W3	S3	E	6.71	0.177	11.03	0.00	1.62	37.94	0.00	35.46	58.60	8.45
W5	S3	E	6.28	0.374	14.63	0.00	1.43	16.79	0.00	31.20	70.90	9.29

1 - Legend for Column 3

P - Proposed for testing

E - Tested previously

Table S5-2: Ultimate Load Comparison between Experiments and Analytical Methods.

SPECIMEN	TEST	Pu / Py		P analysis / P test	
		PARSANEJAD[1]	PROPOSED	PARSENEJAD[1]	PROPOSED
P1P	-	0.554	0.591	-	-
P2P	-	0.419	0.493	-	-
P3P05	-	0.551	0.475	-	-
P3P10	-	0.469	0.453	-	-
E1	-	0.338	0.524	-	-
D1	-	0.416	0.547	-	-
D3	-	0.411	0.574	-	-
A3 }Ref. S8	0.440	0.330	0.457	0.750	1.037
B3	0.340	0.318	0.388	0.936	1.144
C3	0.294	0.291	0.465	0.991	1.580
W1 }Ref. S3	0.424	0.367	0.467	0.866	1.101
W3	0.317	0.344	0.514	1.086	1.621
W5	0.164	0.282	0.507	1.717	3.081
ALL SPECIMENS — Average		0.392	0.497	1.057	1.594
ALL SPECIMENS — Std. Dev.		0.086	0.053	0.312	0.703
PROPOSED SPECIMENS — Average		0.451	0.523	-	-
PROPOSED SPECIMENS — Std. Dev.		0.073	0.048	-	-
TESTED SPECIMENS — Average		0.322	0.466	1.057	1.594
TESTED SPECIMENS — Std. Dev.		0.029	0.041	0.312	0.703

1 - From Ref. S5.

Table S5-3: Nondimensionalized Ultimate Load and Corresponding Nondimensionalized Curvature Calculated by Proposed Formulation.

Specimen	Ultimate Load (P_u/P_y)	Curvature ϕ_u/ϕ_{ys}
P1P	0.591	1.13
P2P	0.493	0.97
P3P, 0.05	0.475	0.79
P3P, 0.1	0.453	0.89
E1	0.524	1.14
D1	0.547	1.02
D3	0.574	1.32
A3	0.457	2.06
B3	0.388	2.44
C3	0.465	1.98
W1	0.467	0.96
W3	0.514	0.96
W5	0.507	0.77

where $\phi_{ys} = \dfrac{F_y}{(E_s R)}$ and ϕ_u is the curvature at the ultimate condition.

FIGURES
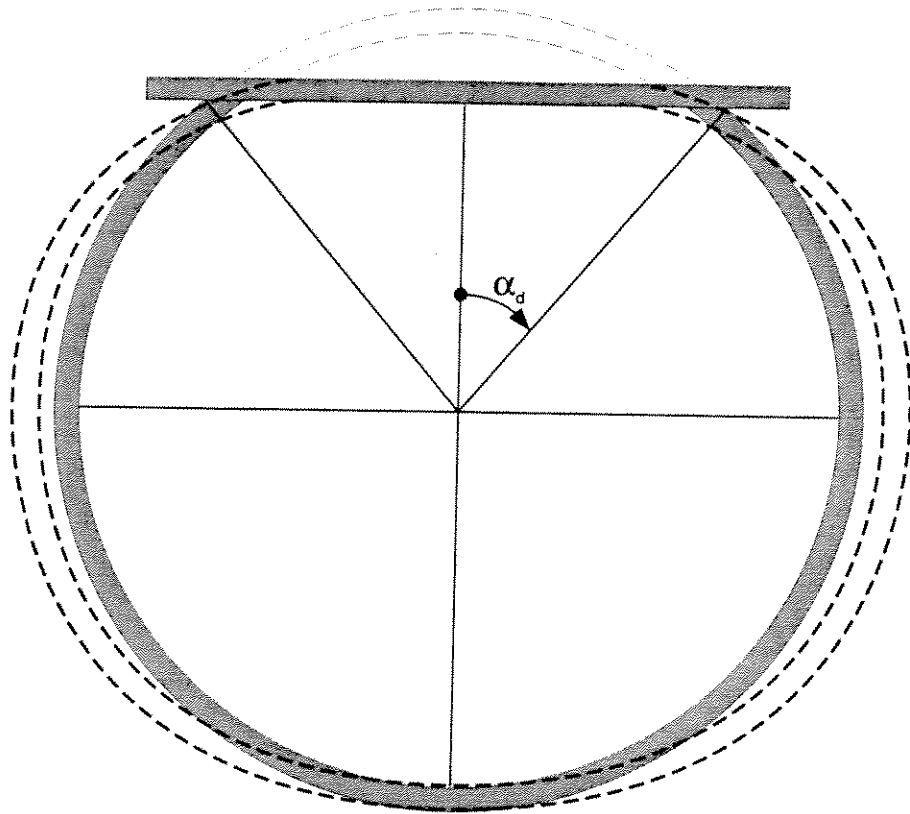
Figure S1-1 Idealization of Dented Cross Section of a Tubular Member
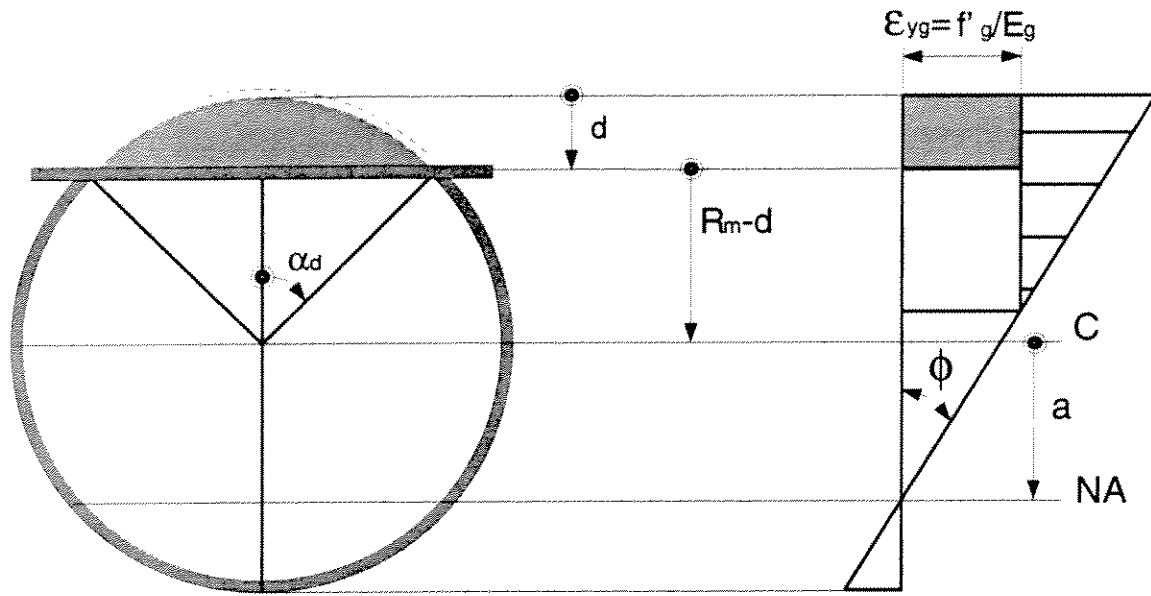
Figure S2-1a: Grout in dented portion.
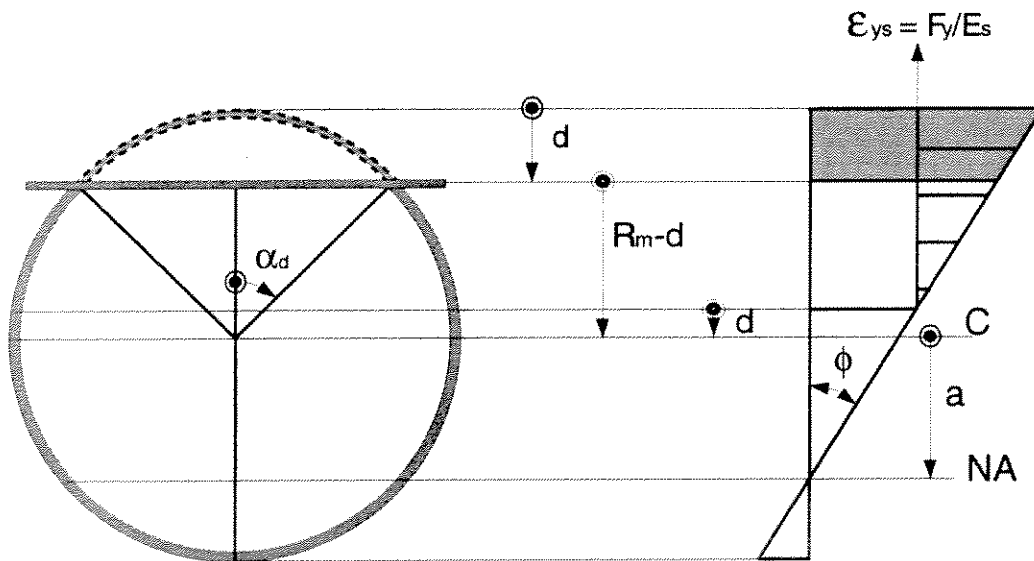
Figure S2-1b: Steel in dented portion.
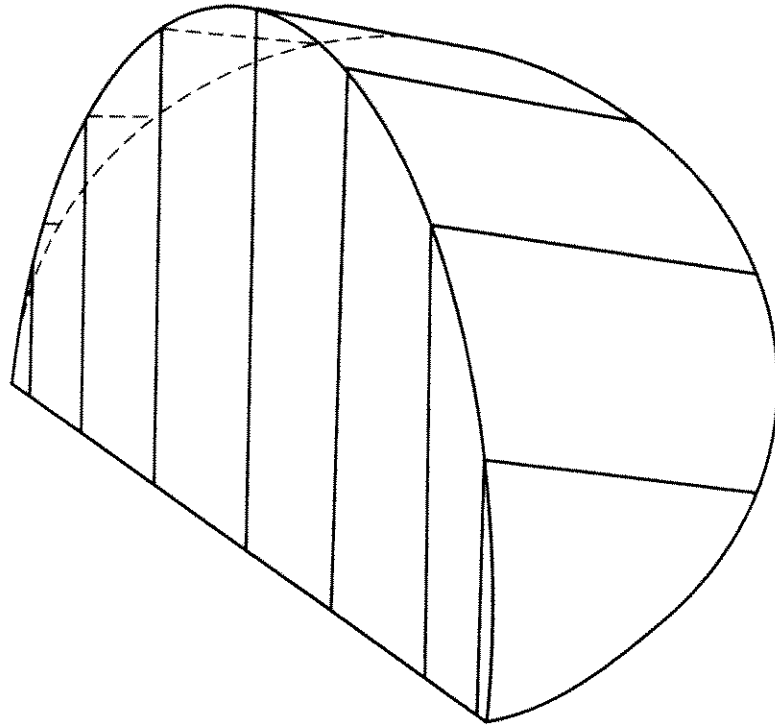
Figure S2-2: Grout stress **wedge**.
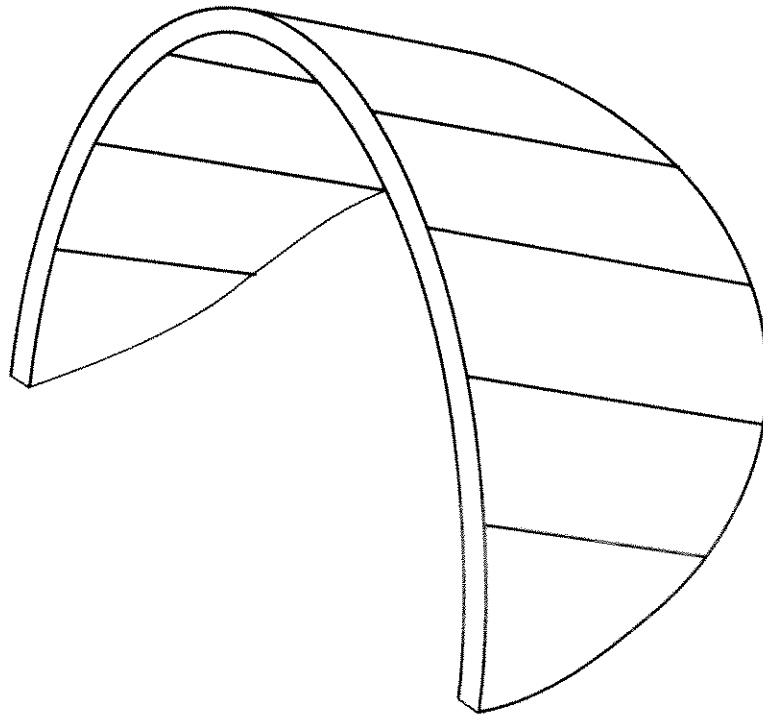
Figure S2-3: Steel stress **rind**.
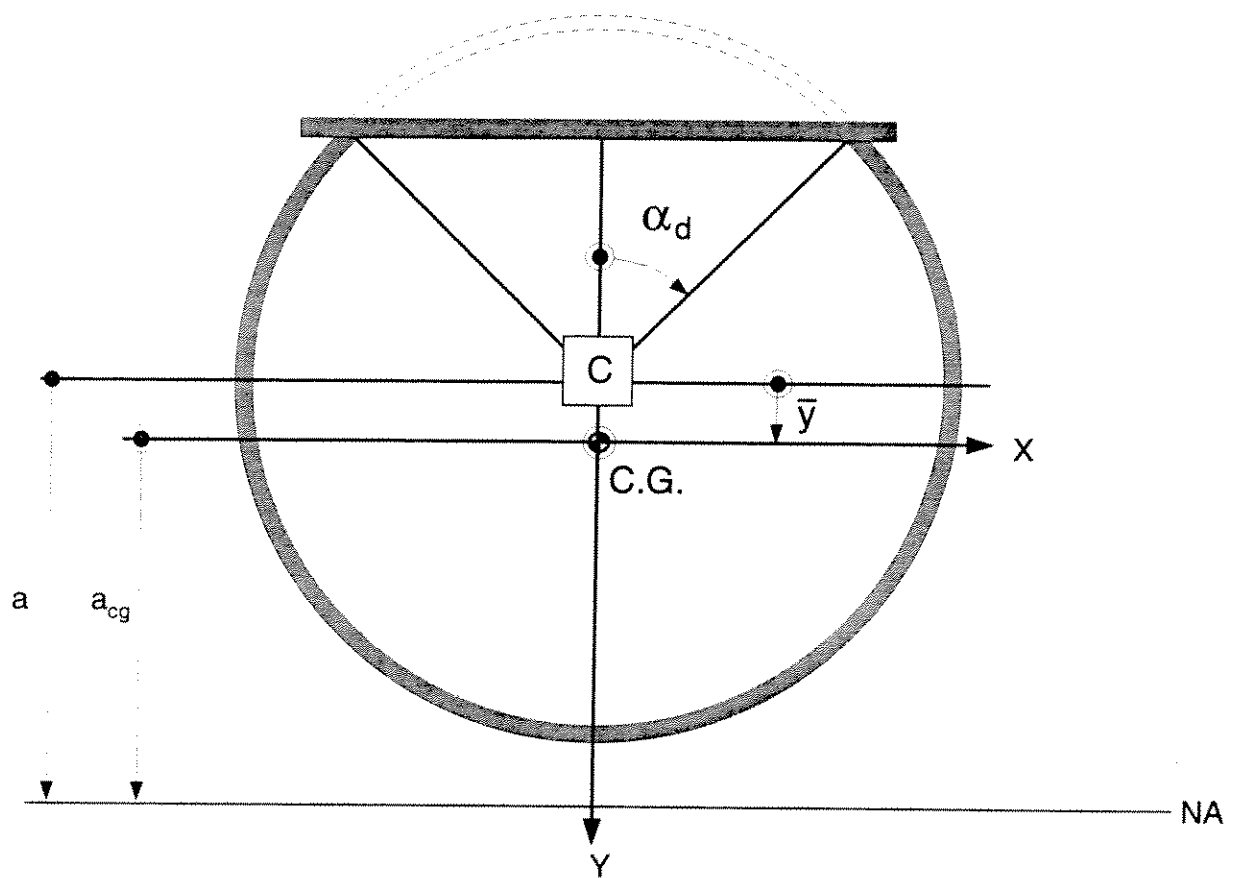
Note: C - Center of Undamaged Tube.

Figure S2-4: Location of Centroid (c.g.) for a Damaged Tube.
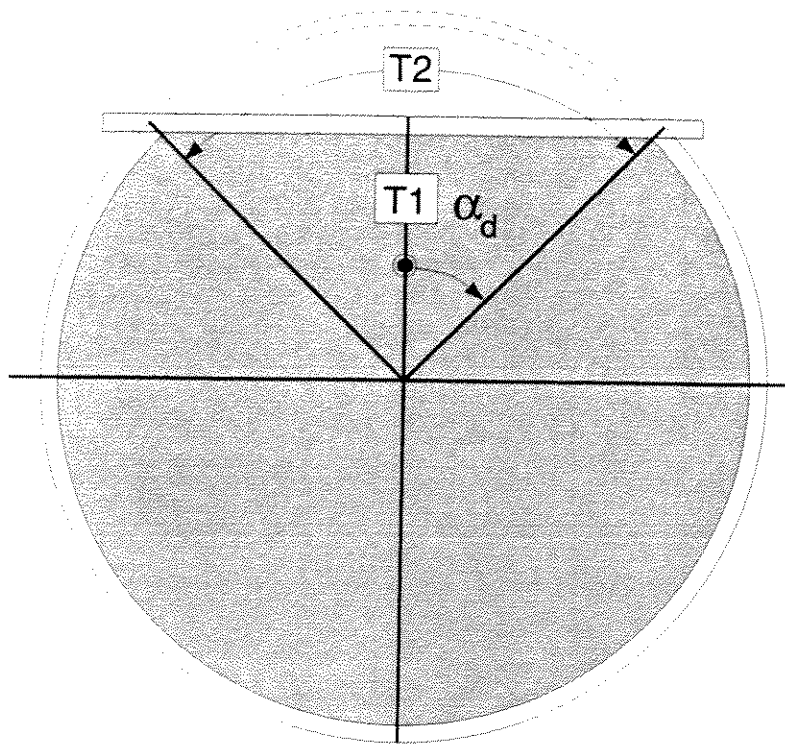
Figure S2-5a: Grout Area of Damaged Tube.
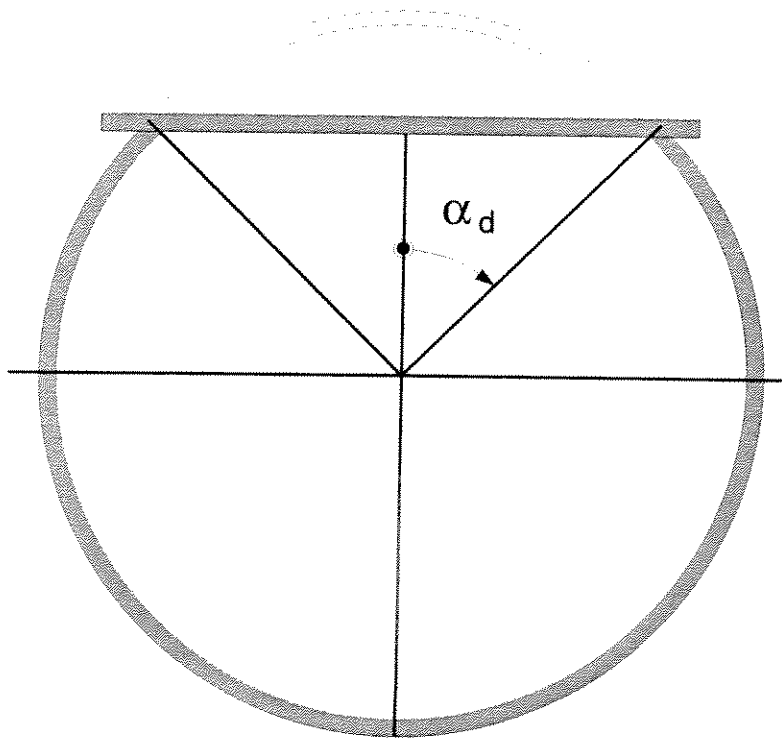
Figure S2-5b:Preserved Steel Area of Damaged Tube.
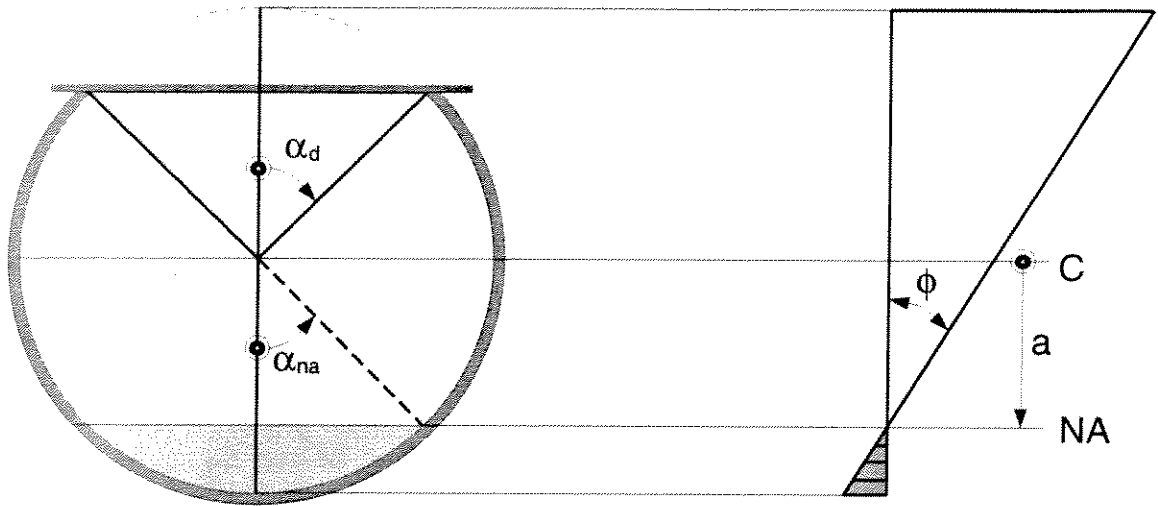
Figure S2-7: Tension Region for Grout.

$$\varepsilon_{max}=\phi E_s(R_m+a)$$

$$\varepsilon_y=\phi_y/E_s$$
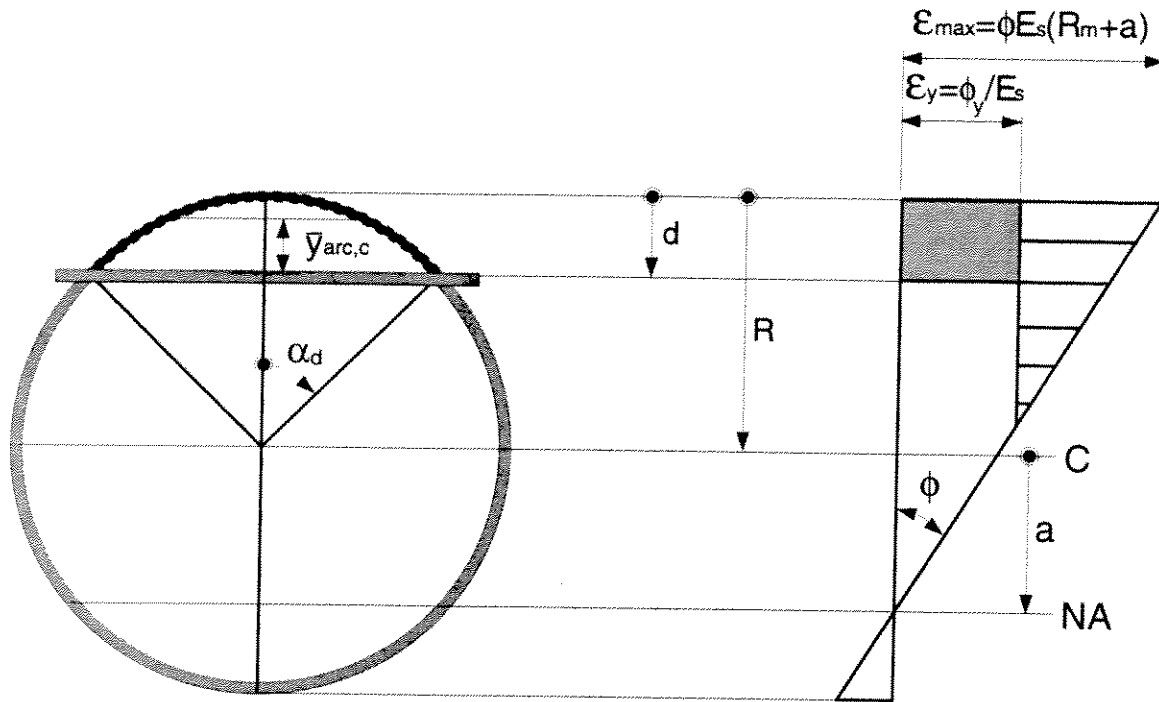
Note: $\bar{y}_{arc,c}$ = lever-arm for steel rind in dented portion.

Figure S2-8a: Loss of Steel Moment Due to Dent -- Inelastic Conditon.

$$\varepsilon_y=f_y/E_s$$
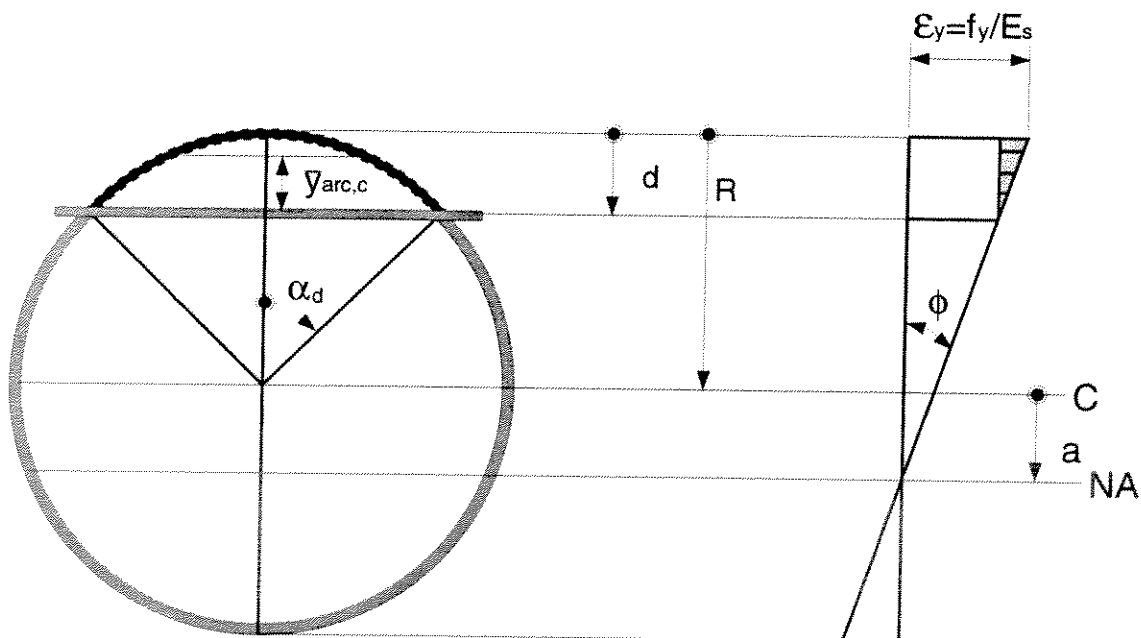
Note: $\bar{y}_{arc,c}$ = lever-arm for steel rind in dented portion.

Figure S2-8b: Loss of Steel Moment Due to Dent -- Elastic Condition.
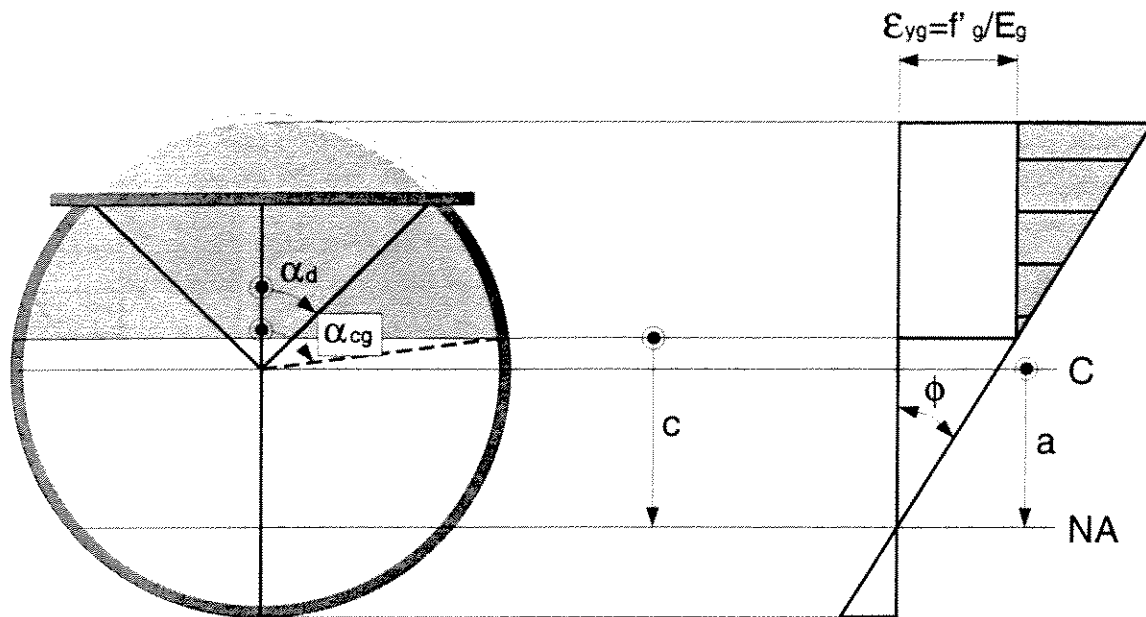
Figure S2-9a: Compression Region for Grout Above the Central Axis.
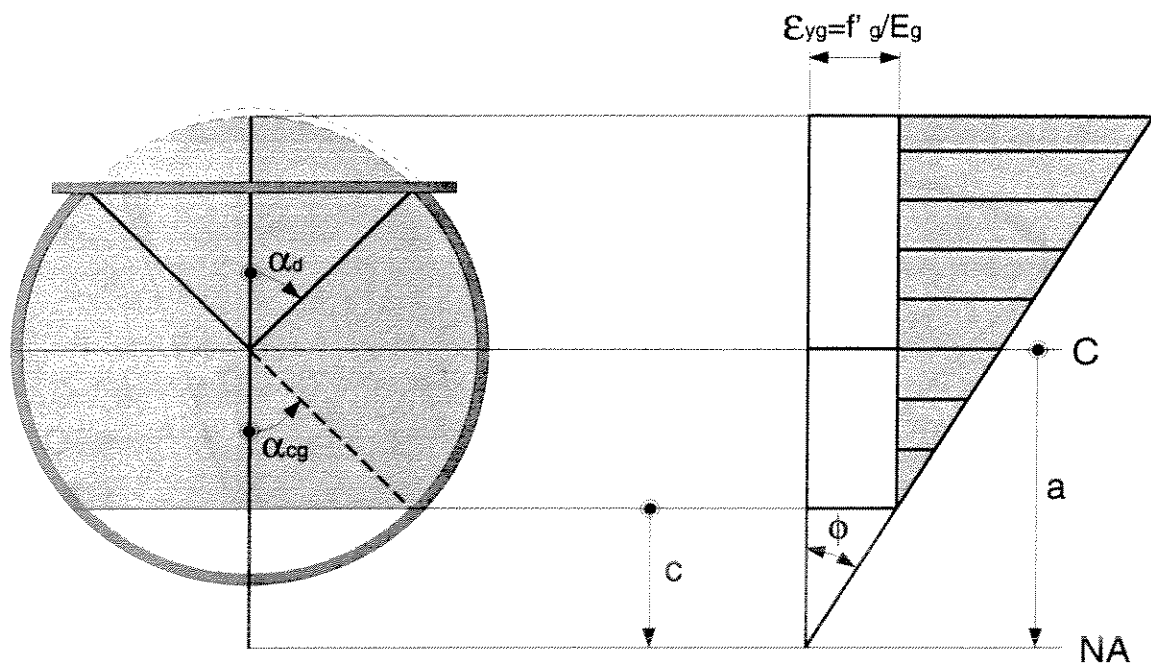
Figure S2-9b: Compression Region for Grout Extending Below Central Axis.
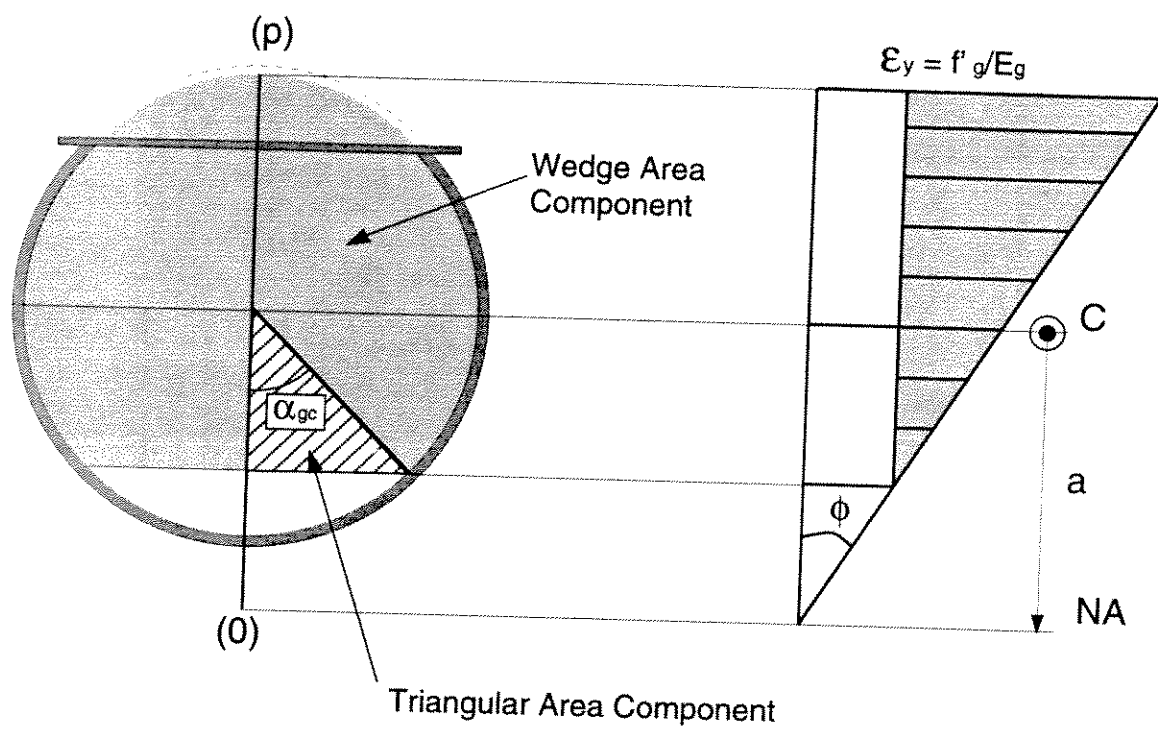
Figure S2-10: Components of Grout Compressive Area.
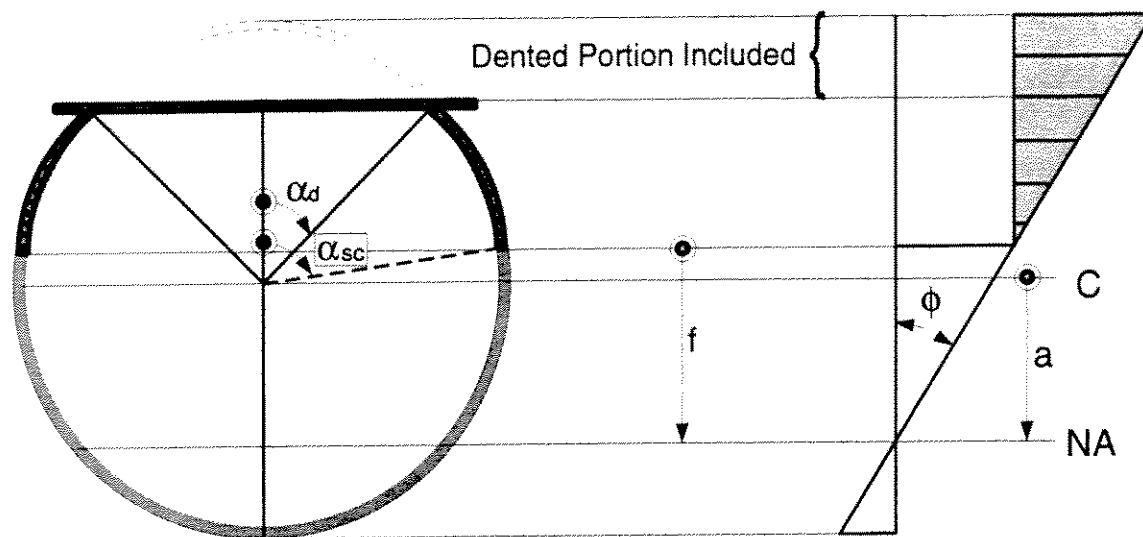
Figure S2-11a: Compression Region for Steel, a < f.
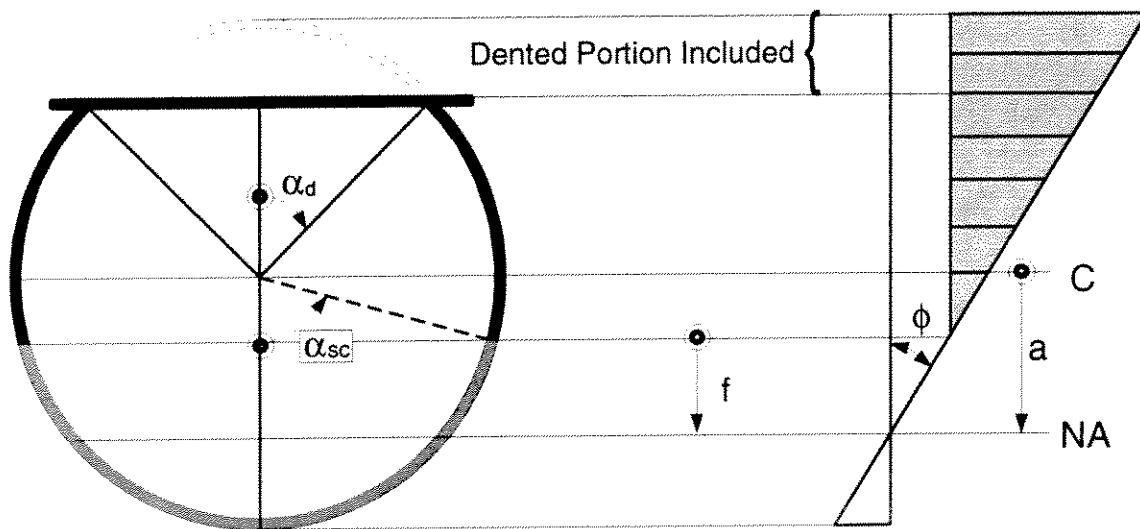
Figure S2-11b: Compression Region for Steel, a > f.
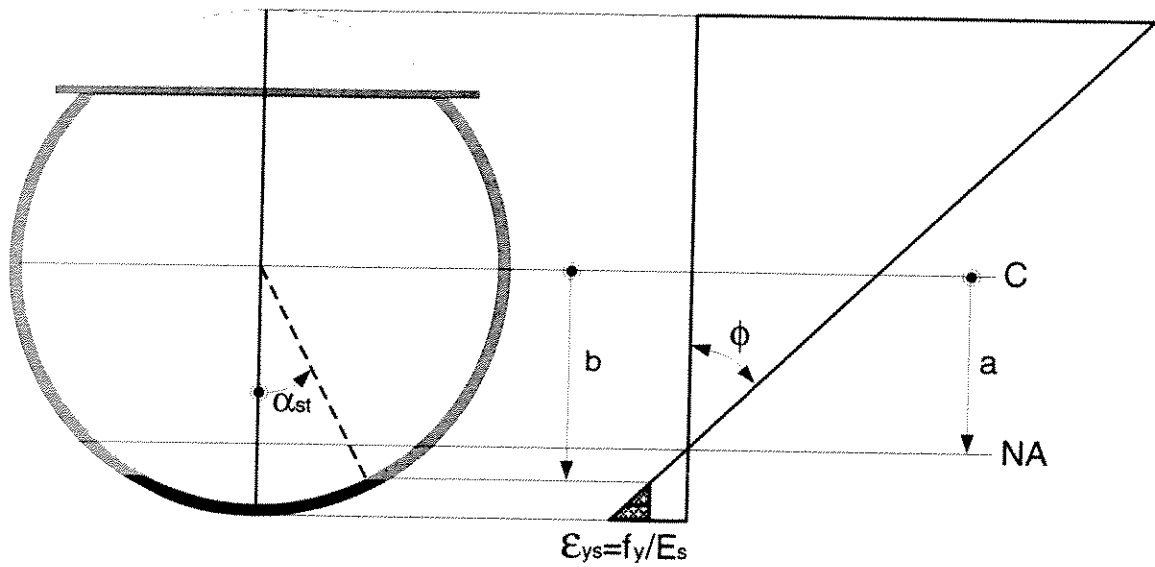
Figure S2-12: Tension Region for Steel.
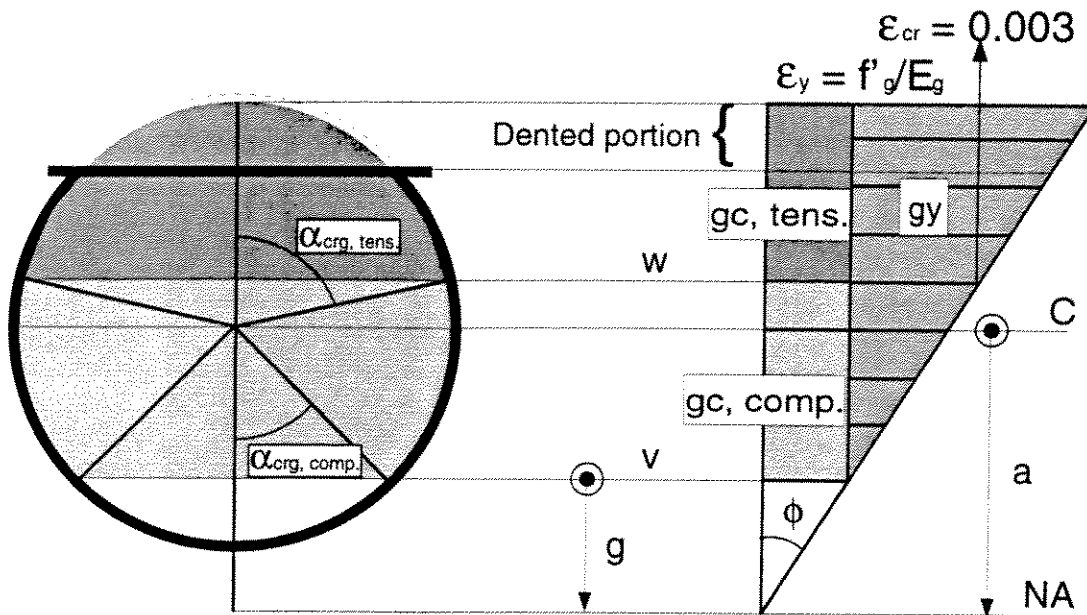
Note: Equation for grout crushing in compression region includes portion marked above by gc, tens.

Figure S2-13a: Crushing of Grout -- Neutral Axis Lies Outside Cross Section.
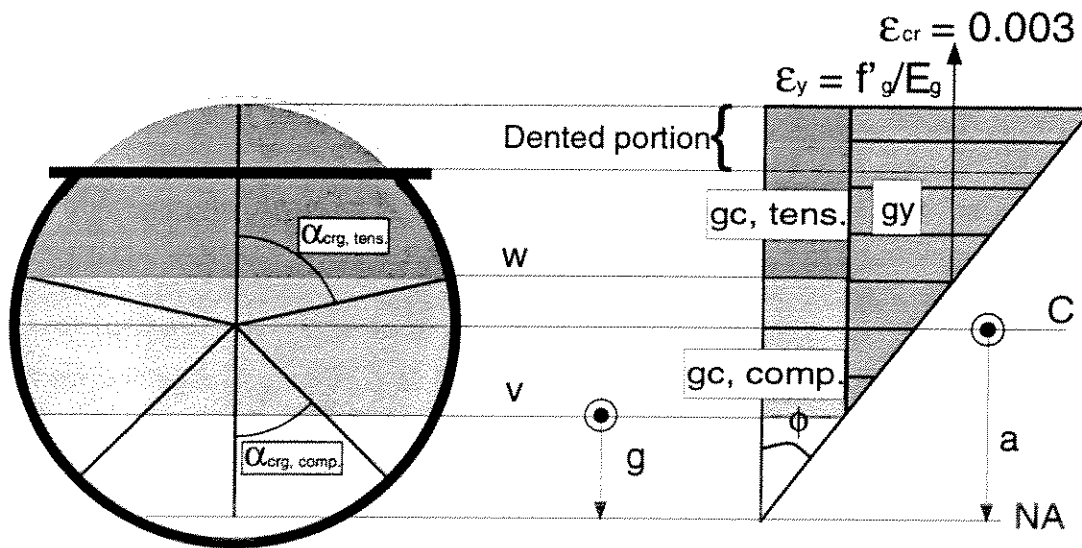
Figure S2-13b: Crushing of Grout -- Neutral Axis Lies Within Cross Section.
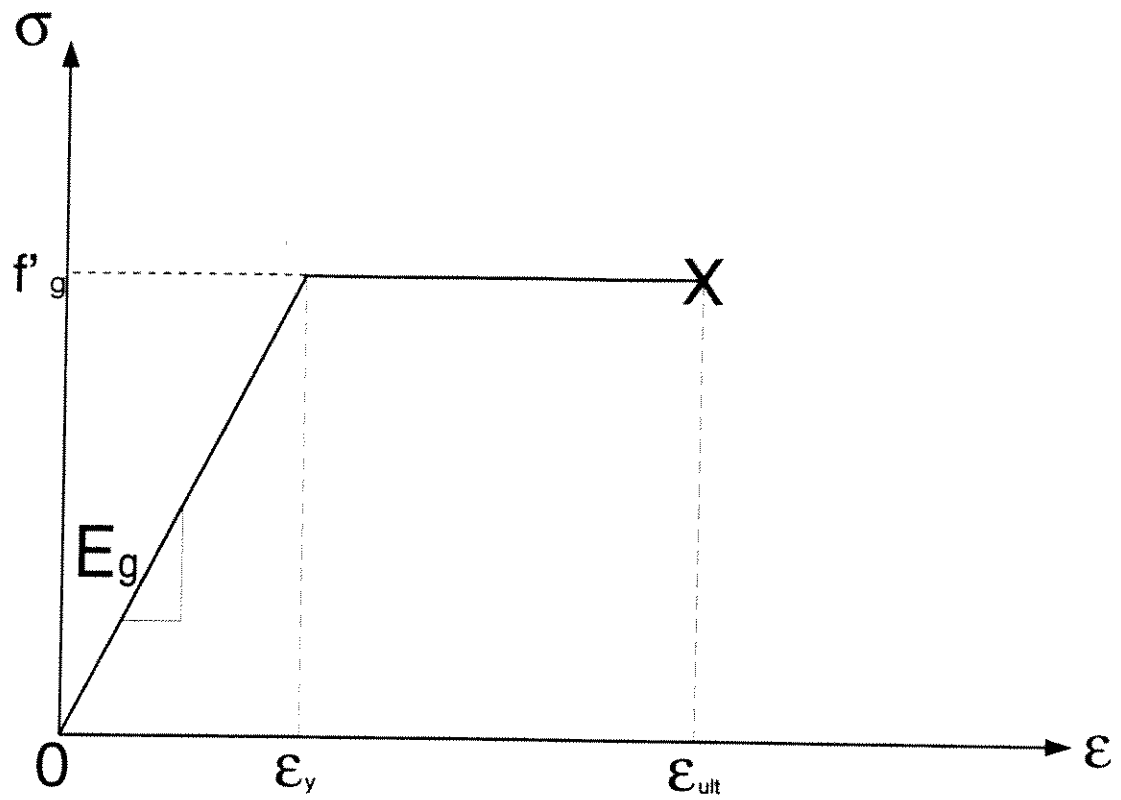
Figure S3-1: Material Model Used for Grout.
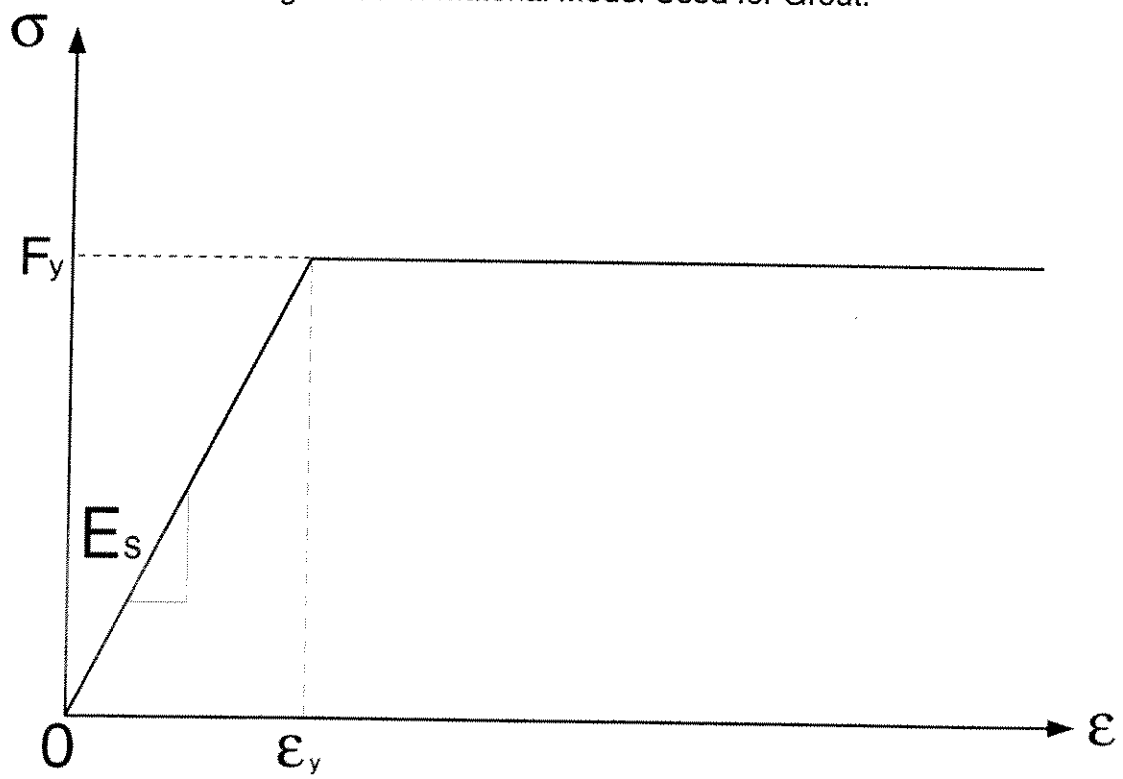
Figure S3-2: Material Model Used for Steel.
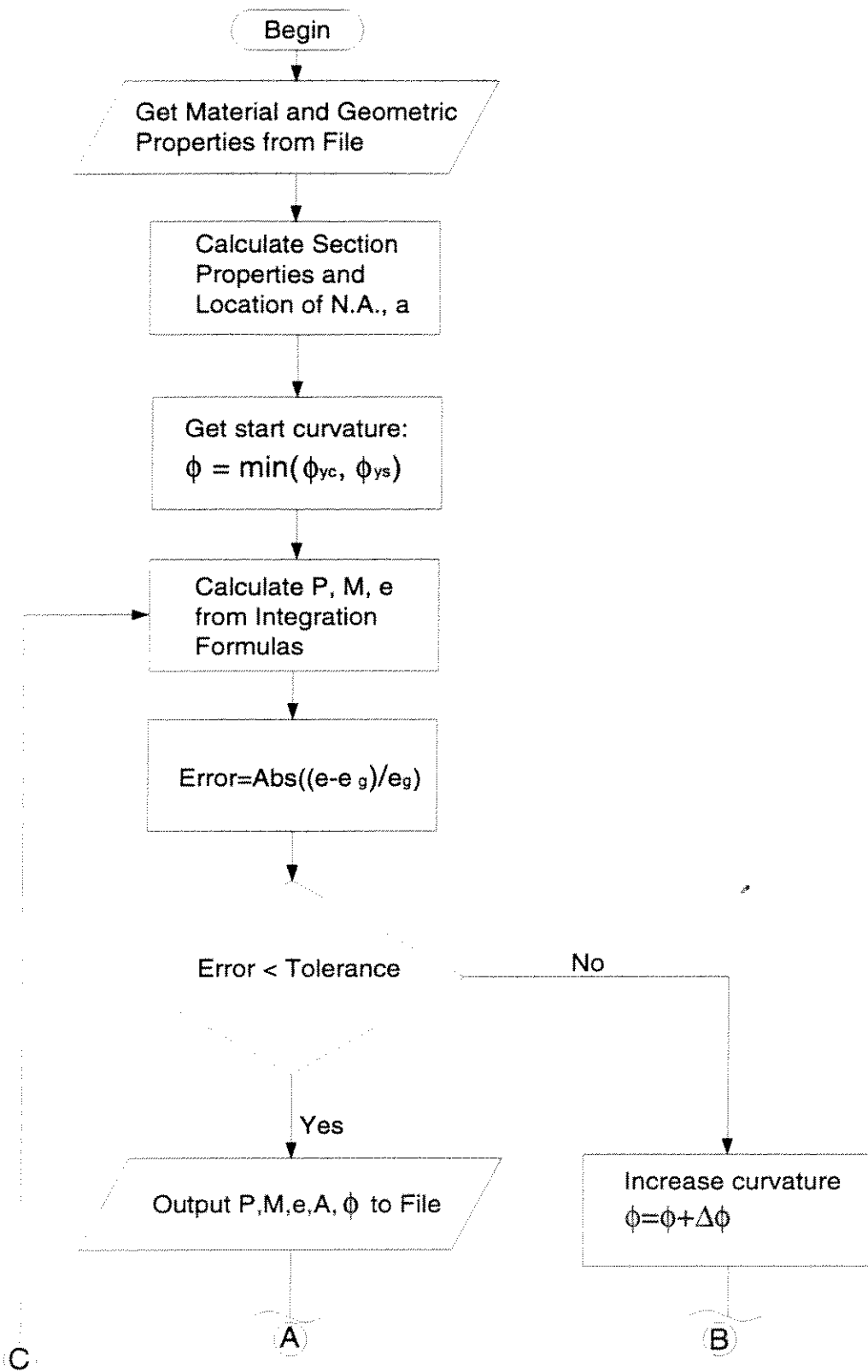
Figure S4-1a: Flowchart of Computer Program, 'SIMGT.F'.
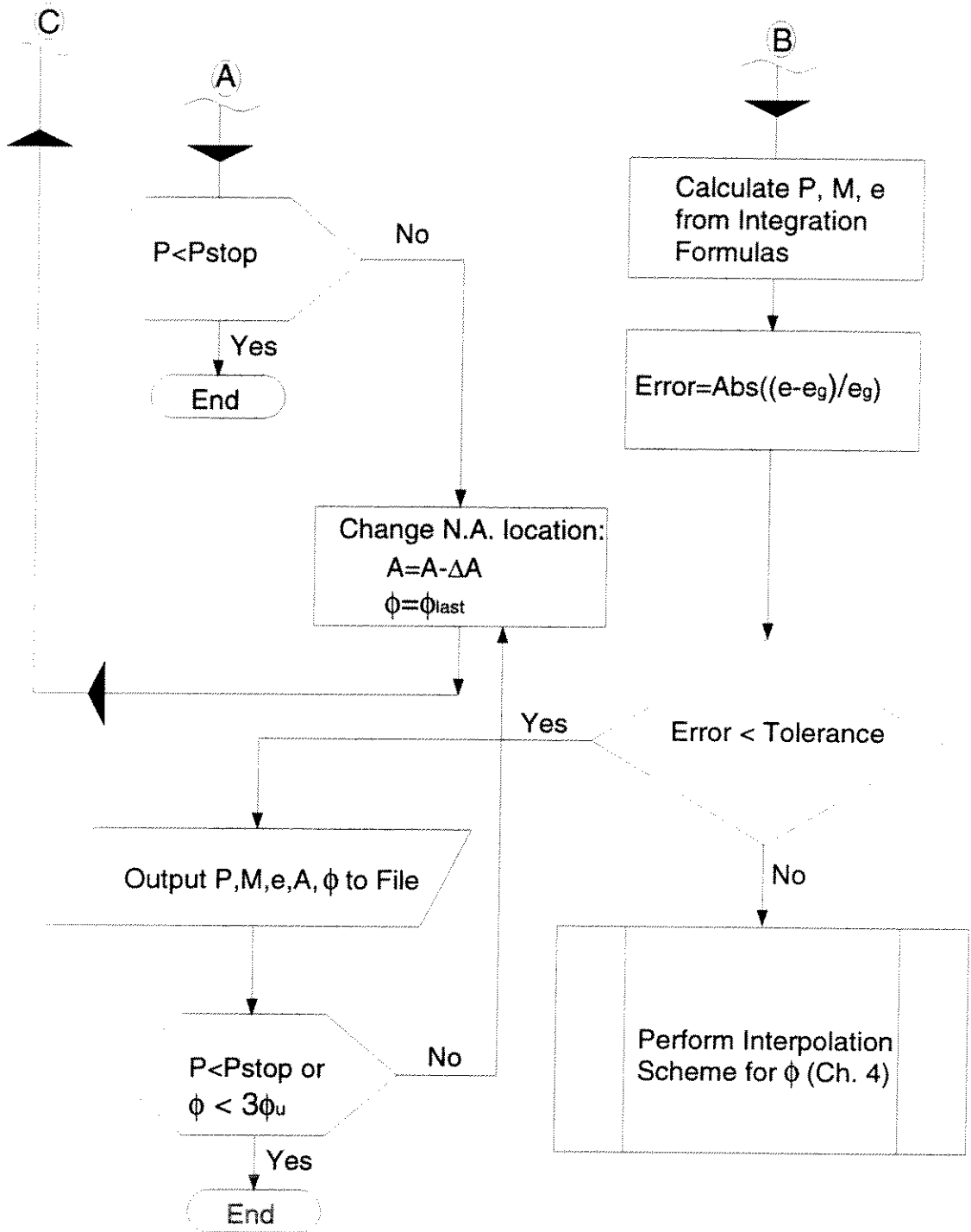
Figure S4-1b: Flowchart of Computer Program, 'SIMGT.F', continued.

P1P 7.5 0.26 30000.0 150.0 3.0 42.7
8/14/94 0.1 0.003 0.05

(SPECIMEN) (THICKNESS) (E_s) (WEIGHT OF GROUT) (f'_g) (F_y)

(DATE)   (e_g/D ratio)   (ϕ_{ult})   (d/D)

Figure S4-2a: Example Input Data File for Program-- Specimen T1-P1P.

Specimen: P1P
Date: 8/14/94

ECCENTRICITY (in.)	NA LOC. (in.)	MOMENT (k-in.)	LOAD (kips)	CURVATURE (1/in.)
0.00	0.00	0.00	0.00	0.00
GROUT ABOVE N.A. HAS YIELDED				
STEEL ABOVE N.A. HAS YIELDED				
1.50	11.52	864.43	576.03	5.490E-05
1.50	11.40	897.1	598.31	5.787E-05
1.50	11.28	920.25	613	6.016E-05
1.50	11.17	943.3	628.58	6.267E-05
1.50	11.05	964.89	643.19	6.520E-05
1.50	10.93	985.8	657.31	6.778E-05
1.50	10.82	1006.6	671.35	7.049E-05
1.50	10.70	1027.8	685.63	7.337E-05
1.50	10.59	1049.9	700.46	7.647E-05
1.50	10.47	1072.7	715.41	7.975E-05
1.50	10.35	1093.3	728.88	8.301E-05
1.50	10.24	1100.7	734	8.524E-05
1.50	10.12	1107.6	737.96	8.735E-05
1.50	10.00	1113.5	742.08	8.964E-05
1.50	9.89	1118.8	745.85	9.197E-05
1.50	9.77	1123.8	749.32	9.437E-05
1.50	9.66	1128.5	752.58	9.685E-05
1.50	9.54	1133	755.65	9.943E-05
1.50	9.42	1137.2	758.57	1.021E-04
1.50	9.31	1141.3	761.36	1.049E-04
1.50	9.19	1145.2	764.05	1.079E-04
1.50	9.07	1148.9	766.64	1.110E-04
1.50	8.96	1152.6	769.16	1.143E-04
1.50	8.61	1163.8	776.04	1.252E-04
1.50	8.26	1174.4	782.65	1.386E-04
1.50	8.03	1180.1	787.43	1.498E-04
1.50	7.79	1186.9	791.79	1.628E-04
1.50	7.56	1194.1	796.15	1.788E-04
1.50	7.33	1201.9	800.63	1.990E-04
1.50	7.21	1204.9	803.28	2.119E-04
1.50	7.10	1196.9	798.7	2.215E-04
1.50	6.98	1182.2	788.52	2.281E-04
1.50	6.63	1127.4	751.49	2.512E-04
1.50	6.28	1052.4	701.44	2.831E-04
1.50	6.05	981.45	654.08	3.184E-04
1.50	5.93	929.96	619.4	3.518E-04
STEEL BELOW N.A. HAS YIELDED				
1.50	5.85	846.19	563.79	4.620E-04
1.50	5.87	809.91	539.74	5.082E-04
1.50	5.91	780.1	519.77	5.590E-04
1.50	5.97	755.96	503.74	6.149E-04
1.50	6.05	736.98	491.29	6.764E-04

Figure S4-2b: Example of Output File from Program.
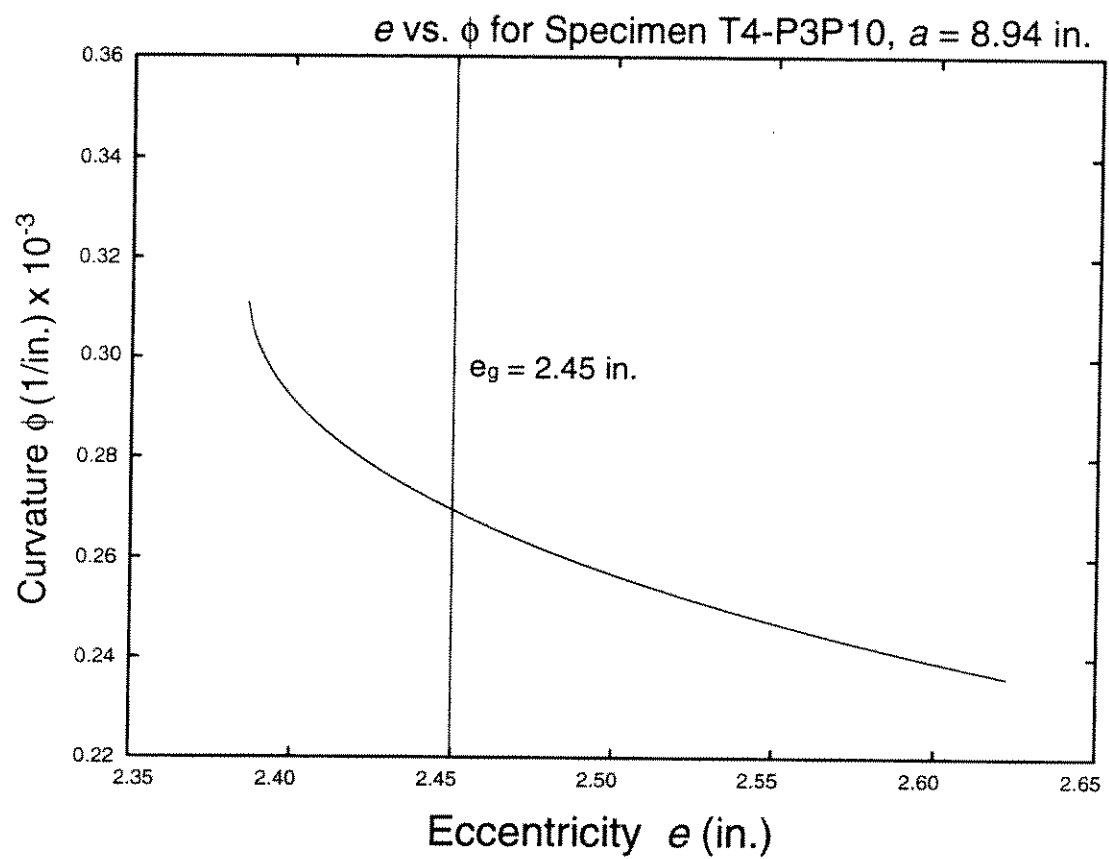
Figure S4-3: Typical e-φ Curve.
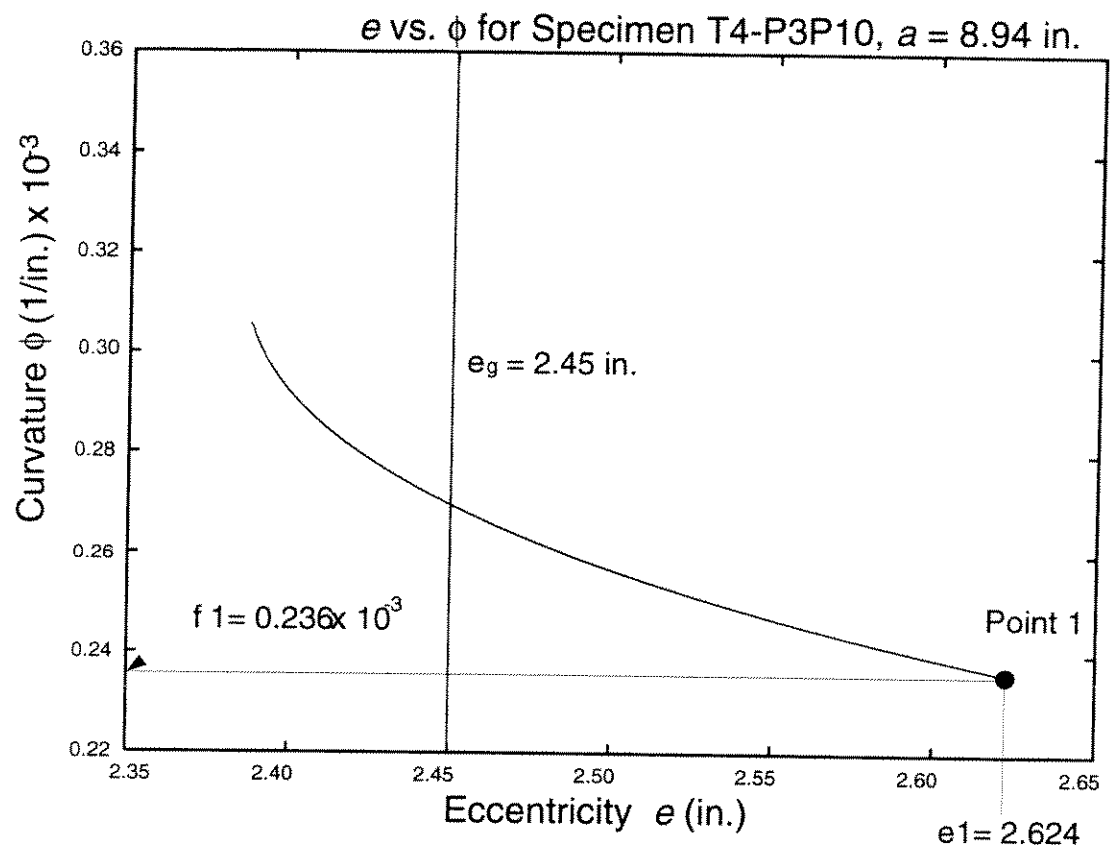
Figure S4-4: First Point of Interpolation Scheme.
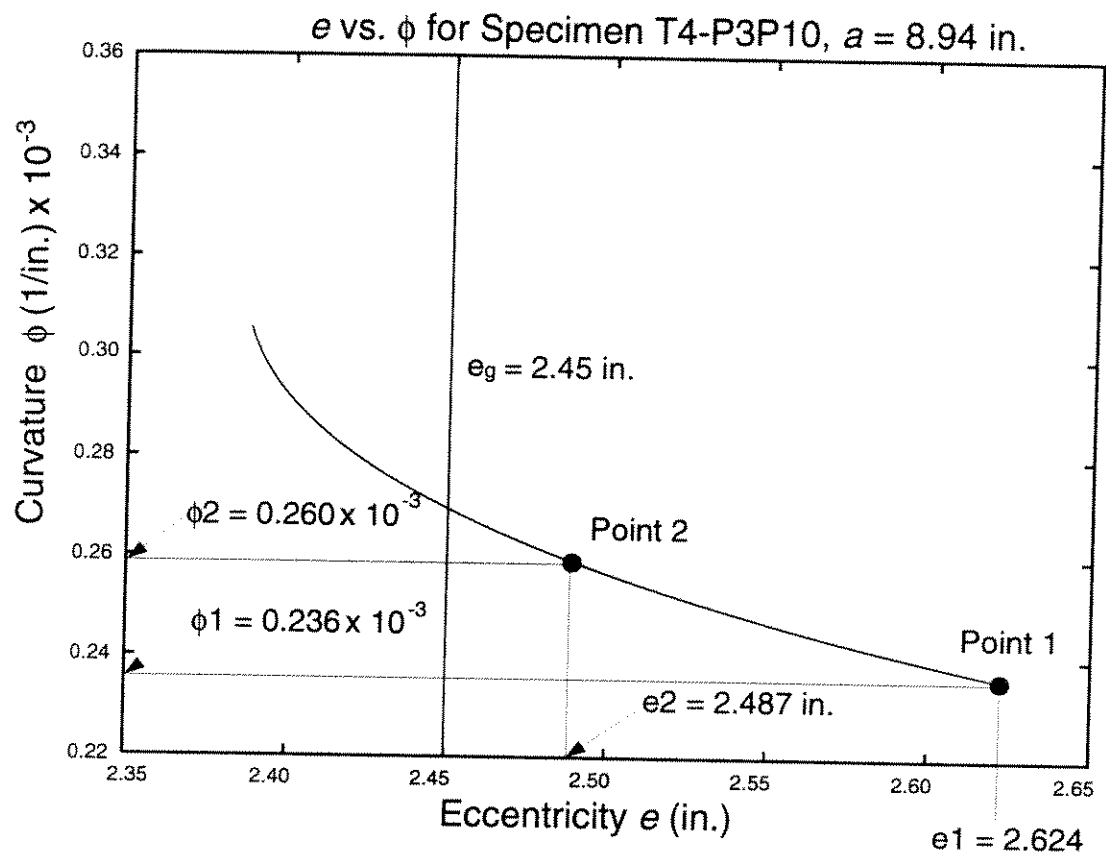
Figure S4-5: Second Point of Interpolation Scheme.
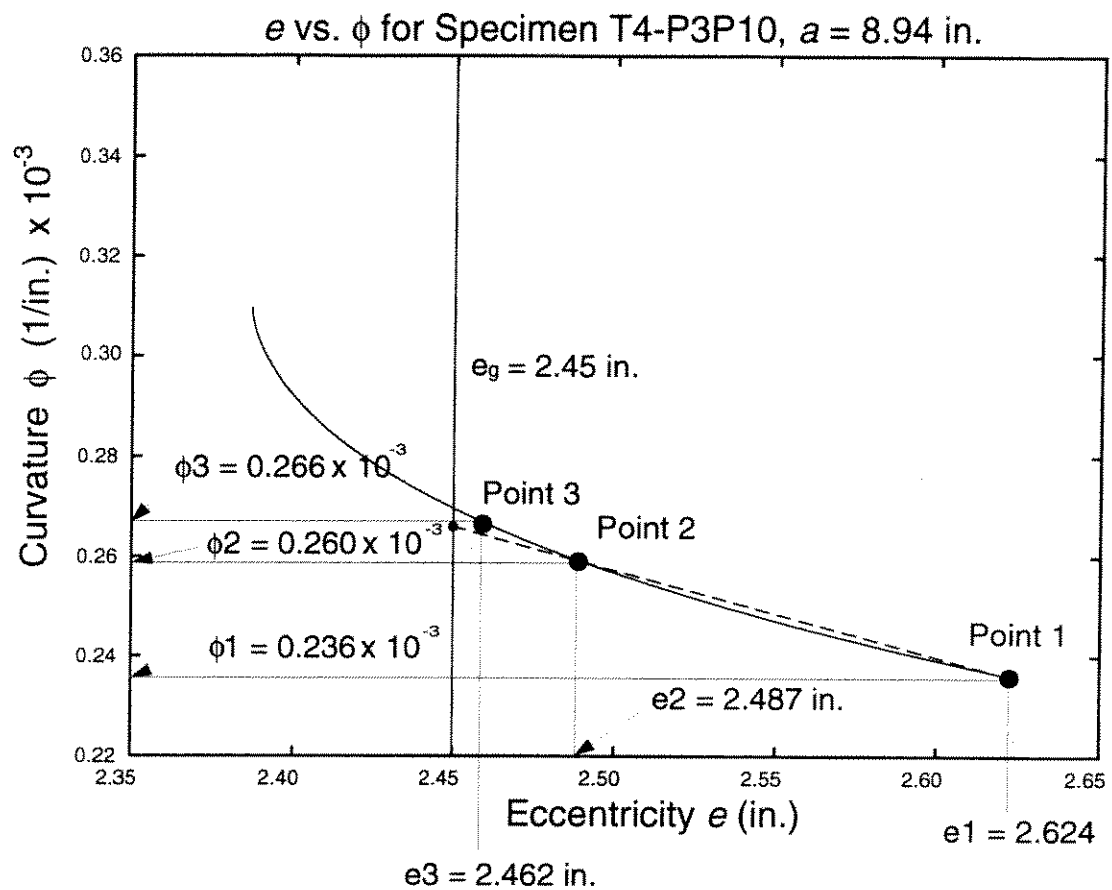
Figure S4-6: Third point of interpolation scheme.
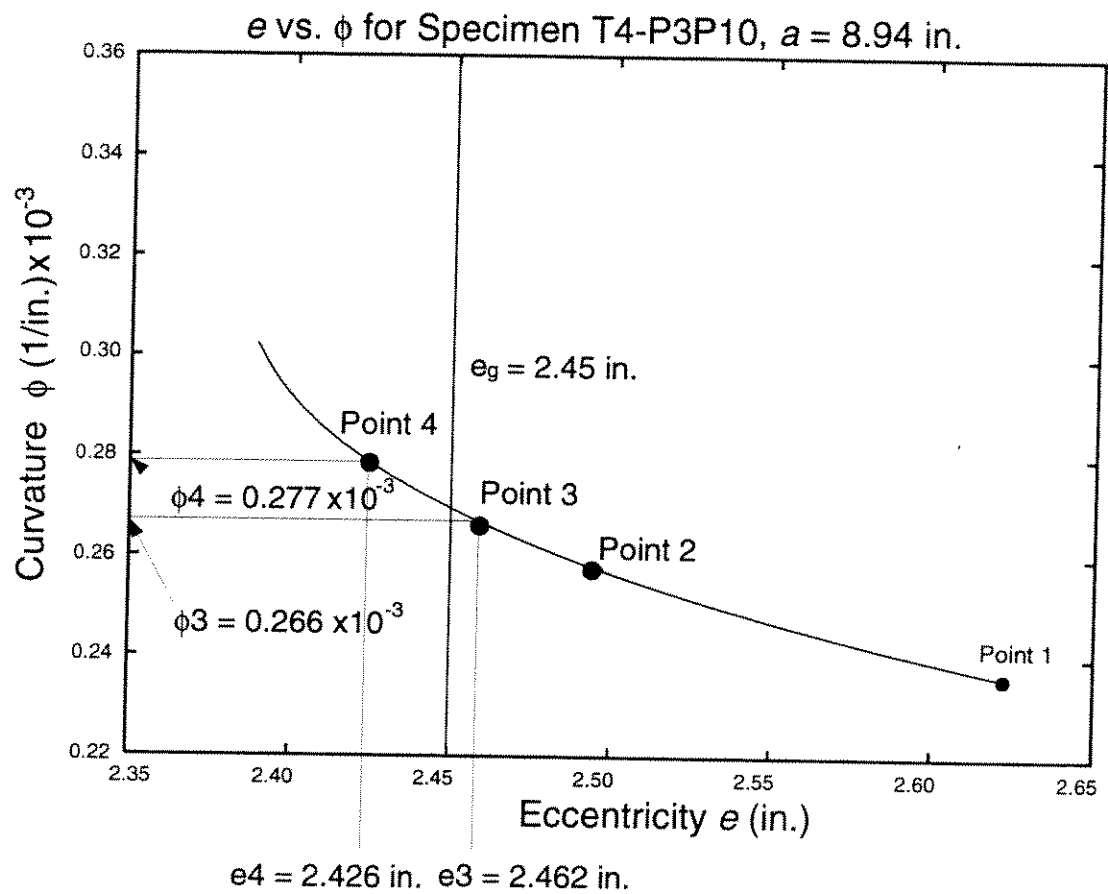
Figure S4-7: Fourth Point of Interpolation Scheme.
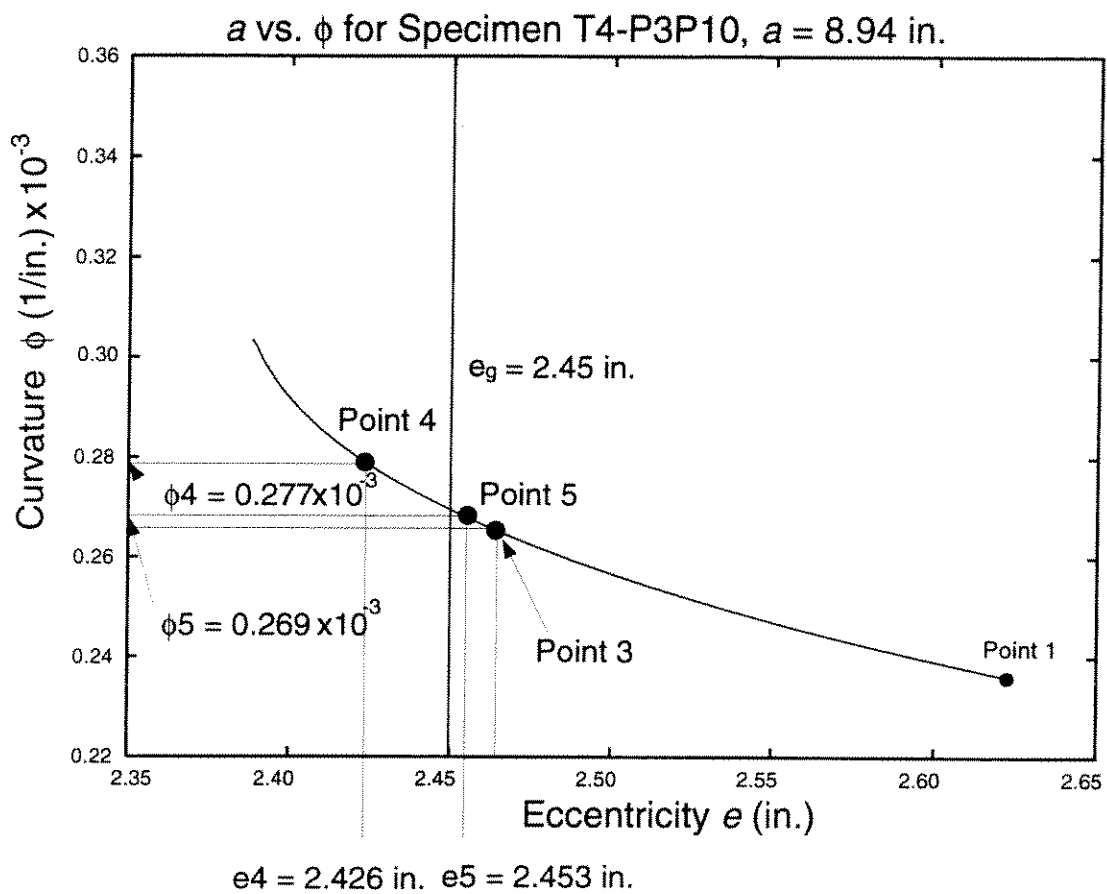
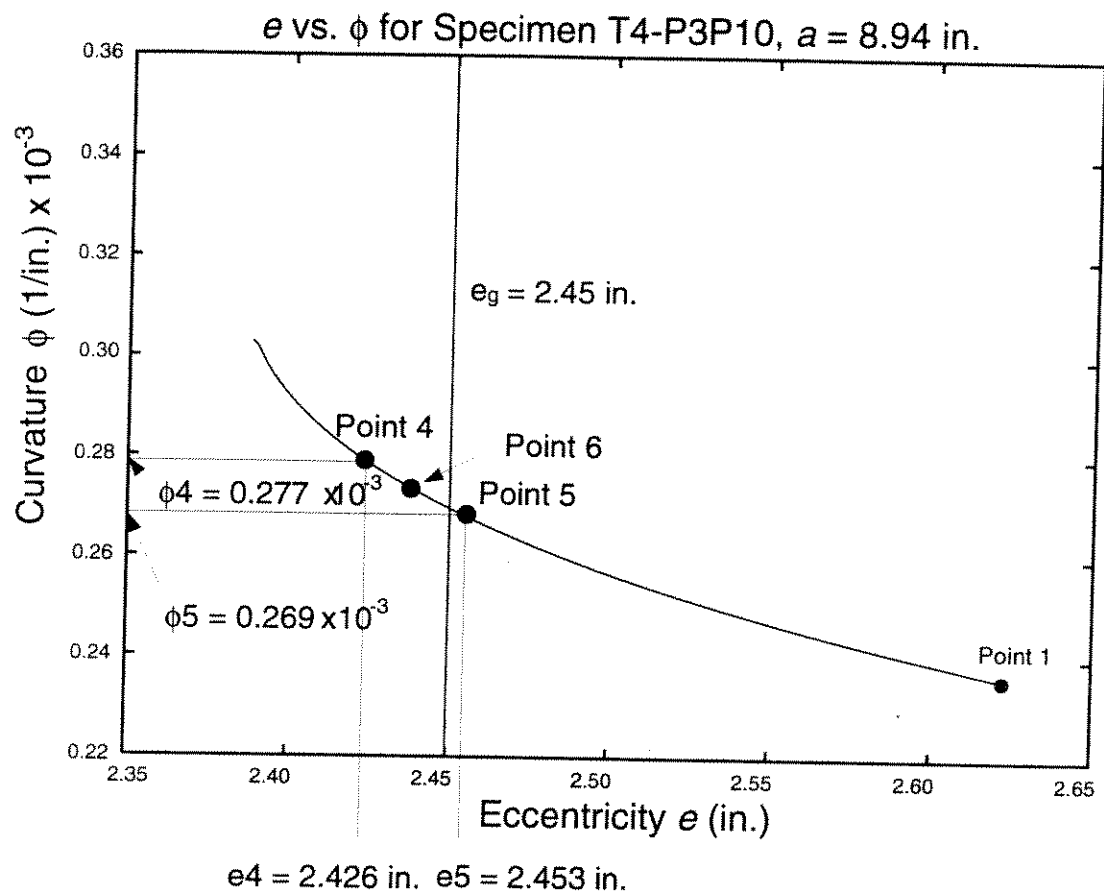Figure S4-8: Fifth Point of Interpolation Scheme.

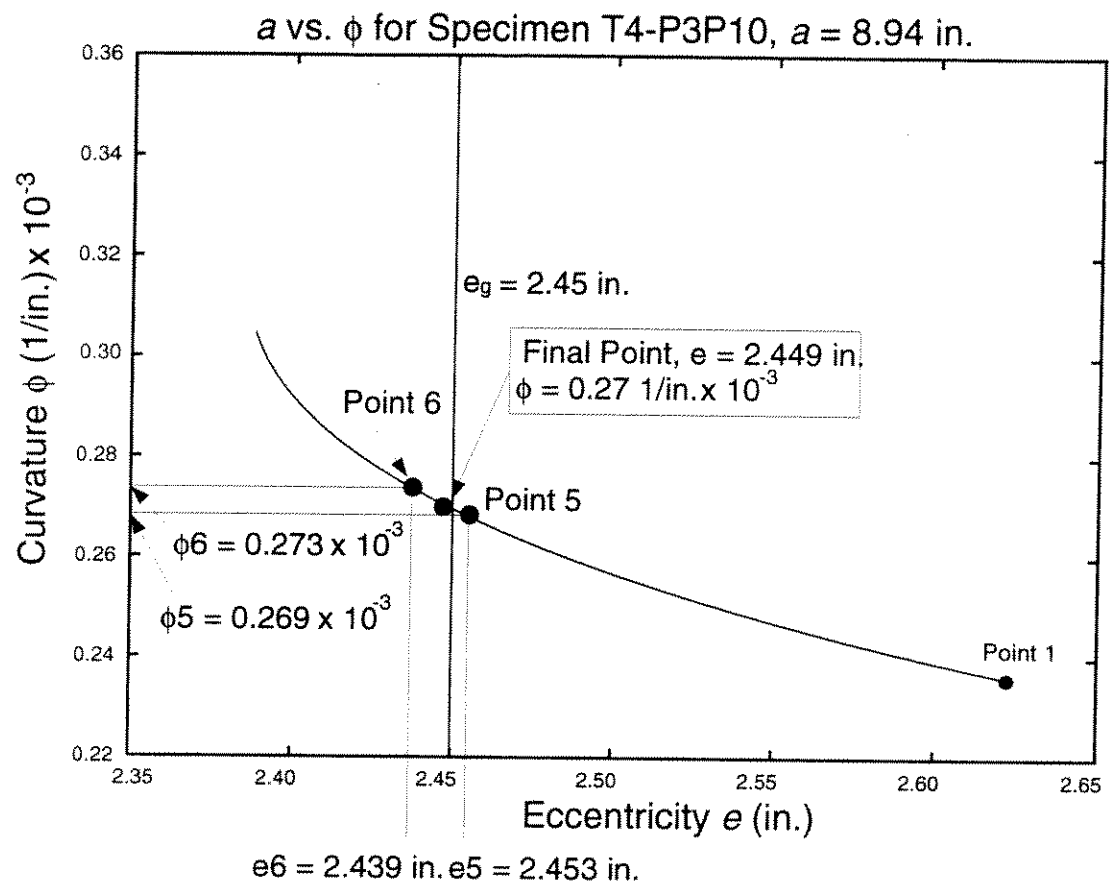Figure S4-9: Sixth Point of Interpolation Scheme.

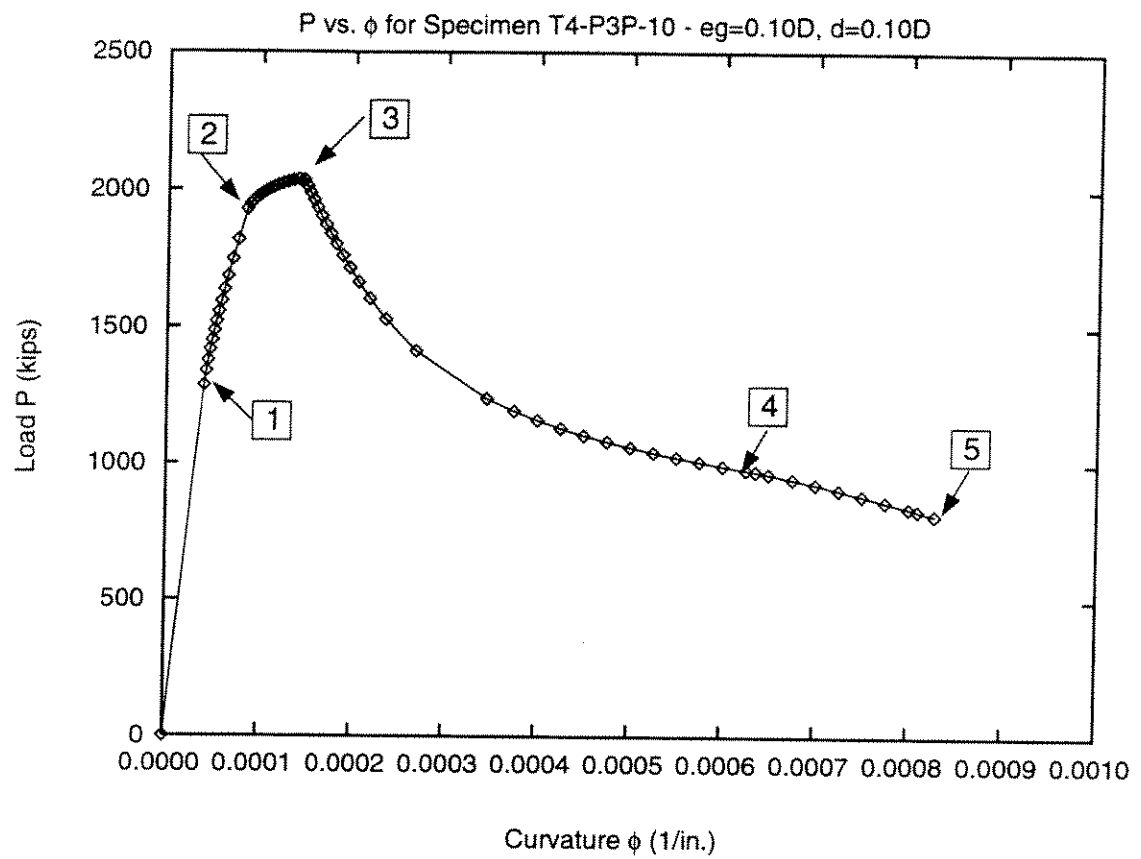Figure S4-10: Final (Converged) Point of Interpolation Scheme.
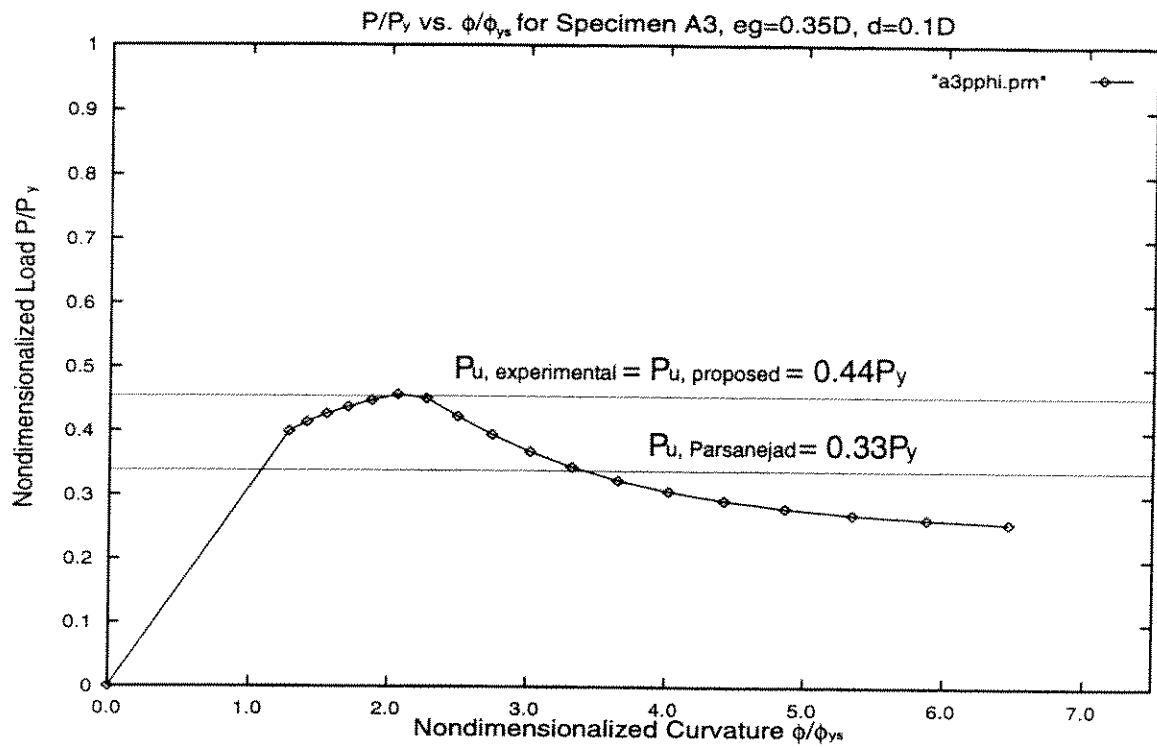
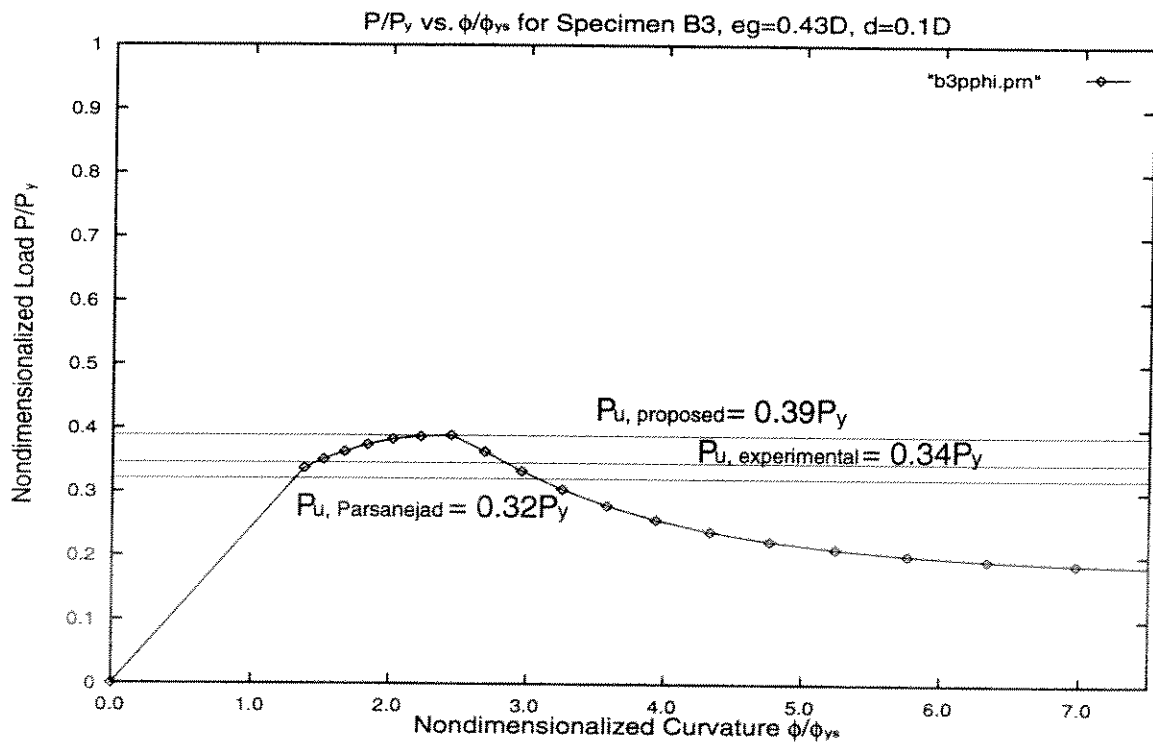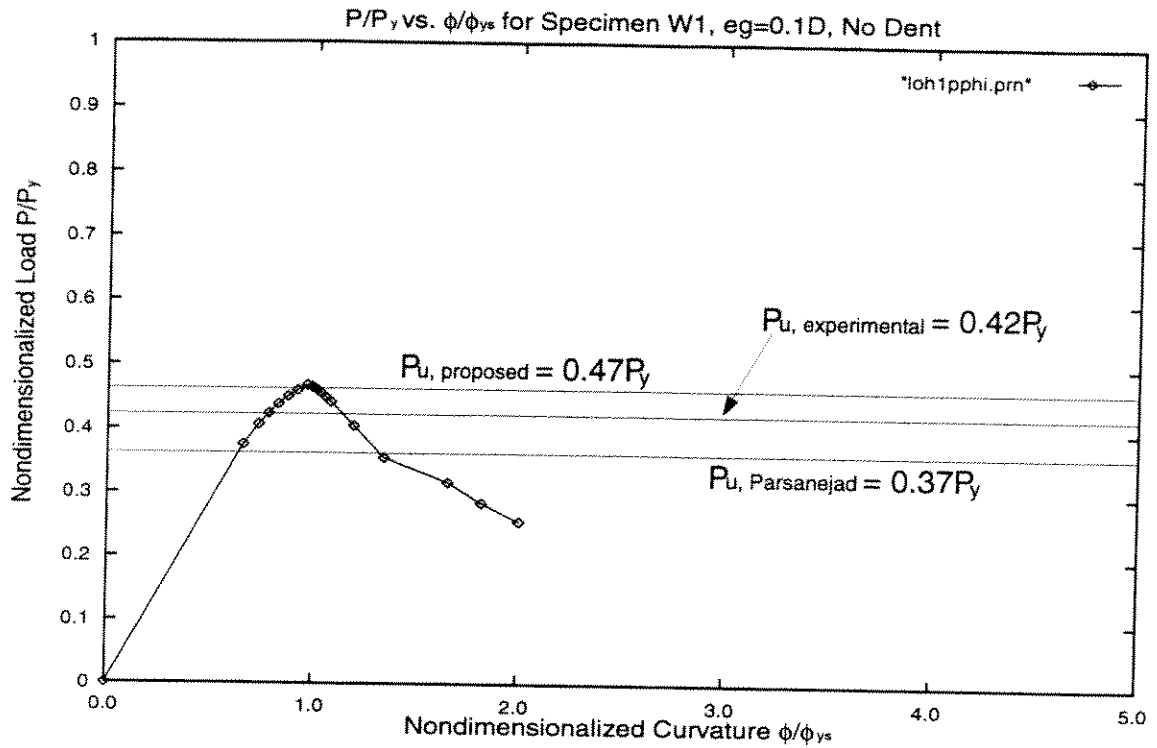Figure S4-11: Typical P- φ Curve.

Figure S5-1: P vs. φ curve for Specimen A3. (Ref. S8)

Figure S5-2: P vs. φ curve for Specimen B3. (Ref. S8)
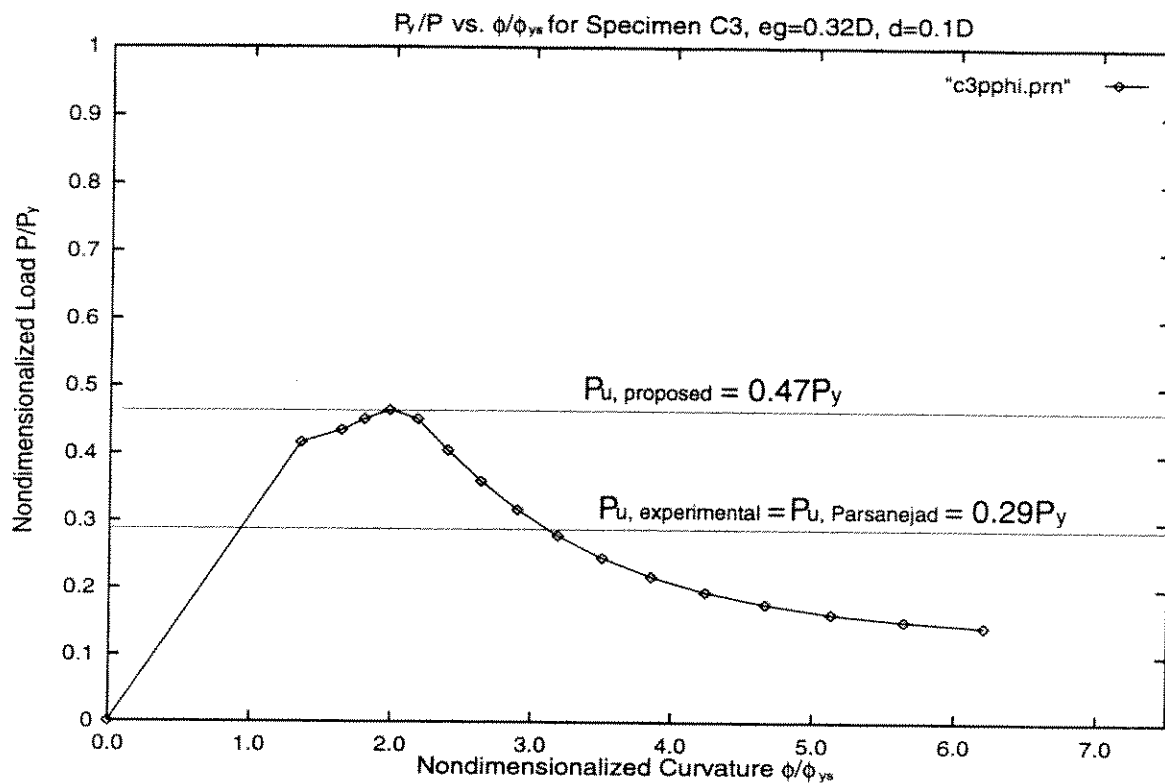
Figure S5-3: P vs. ϕ curve for Specimen C3. (Ref. S8)
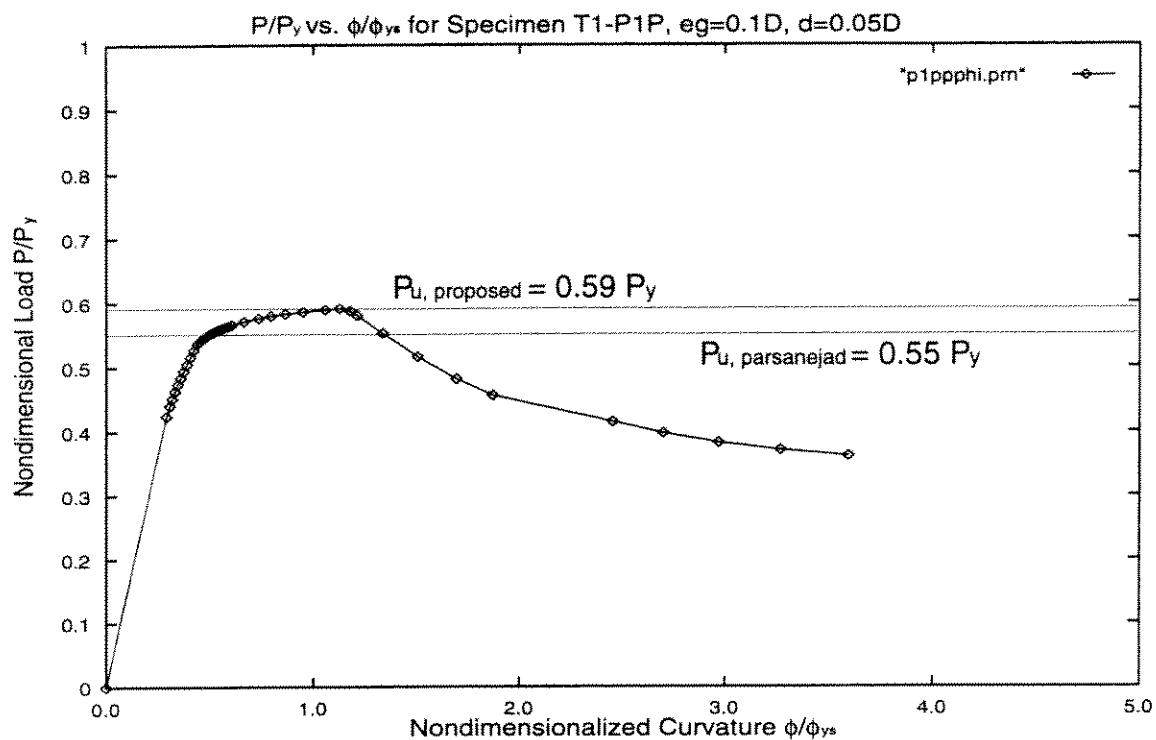
Figure S5-4: P vs. φ curve for Specimen T1-P1P. (Ref. S4)
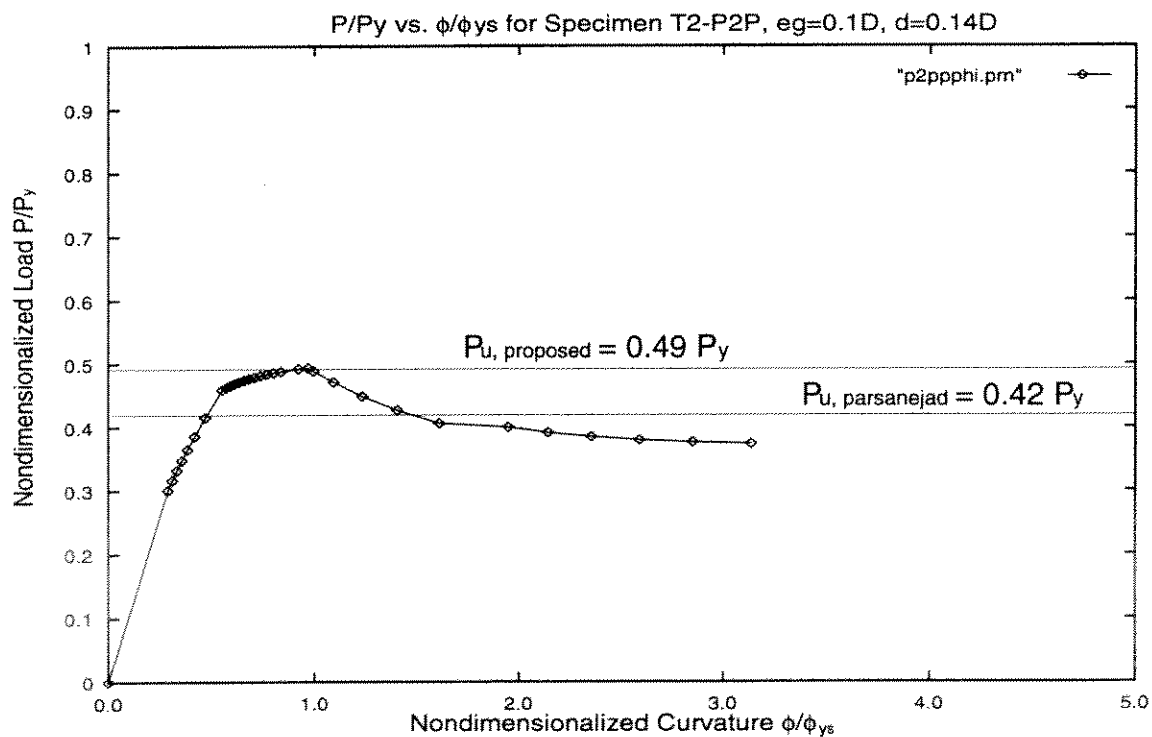


Figure S5-5: P vs. φ curve for Specimen T2-P2P. (Ref. S4)
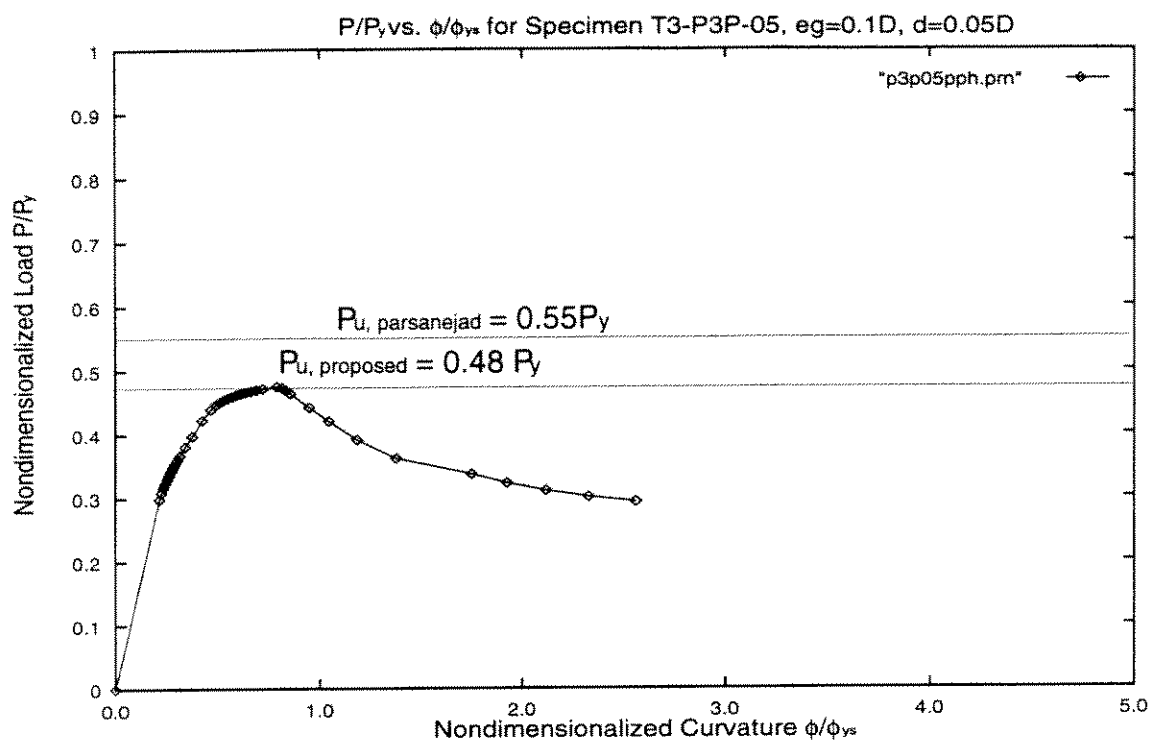
Figure S5-6: P vs. ϕ curve for Specimen T3-P3P. (Ref. S4).
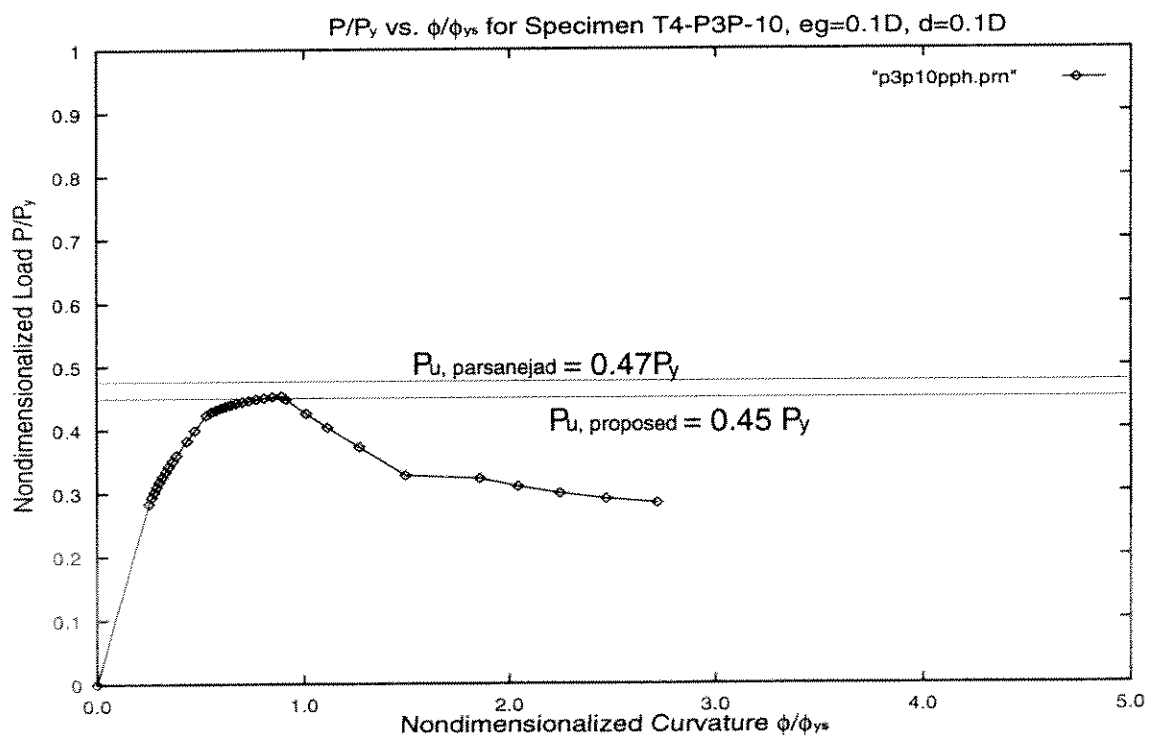
Figure S5-7: P vs. ϕ curve for Specimen T4-P3P. (Ref. S4)
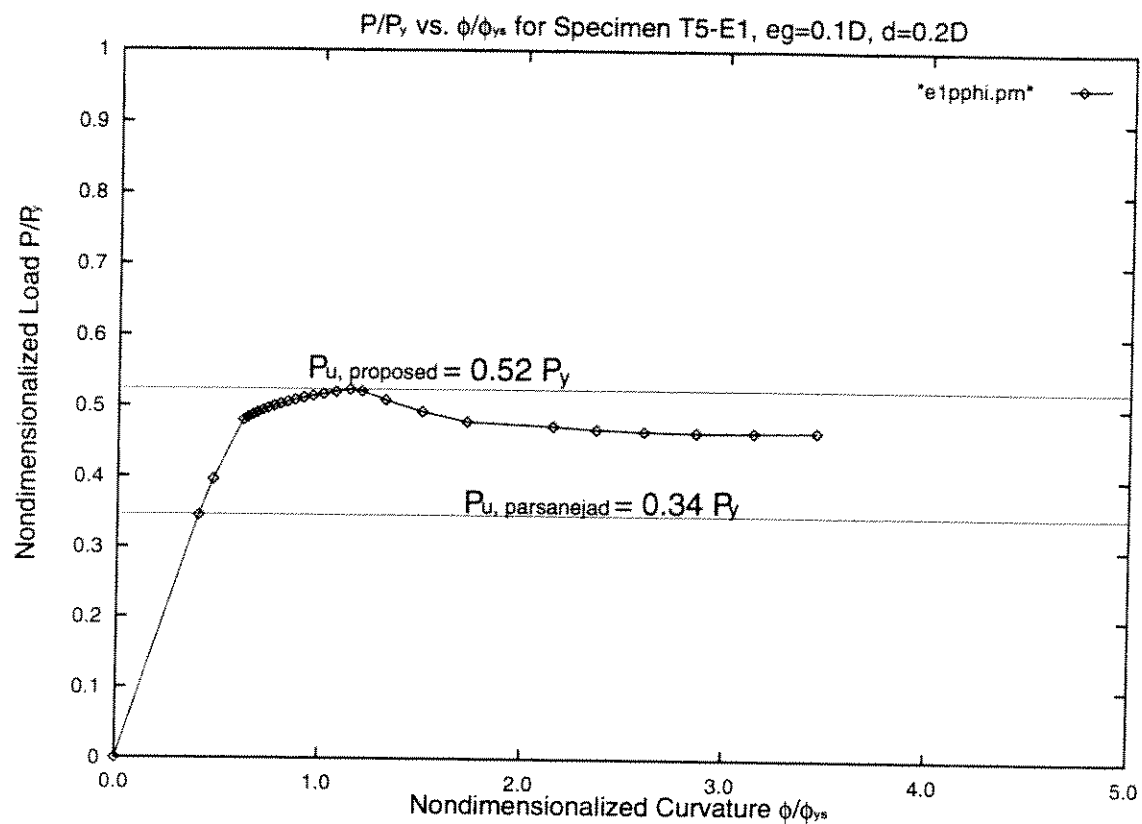
Figure S5-8: P vs. φ curve for Specimen T5-E1. (Ref. S4)

P/Py vs. φ/φ_ys for Specimen T6-D1, eg=0.1D, d=0.15D
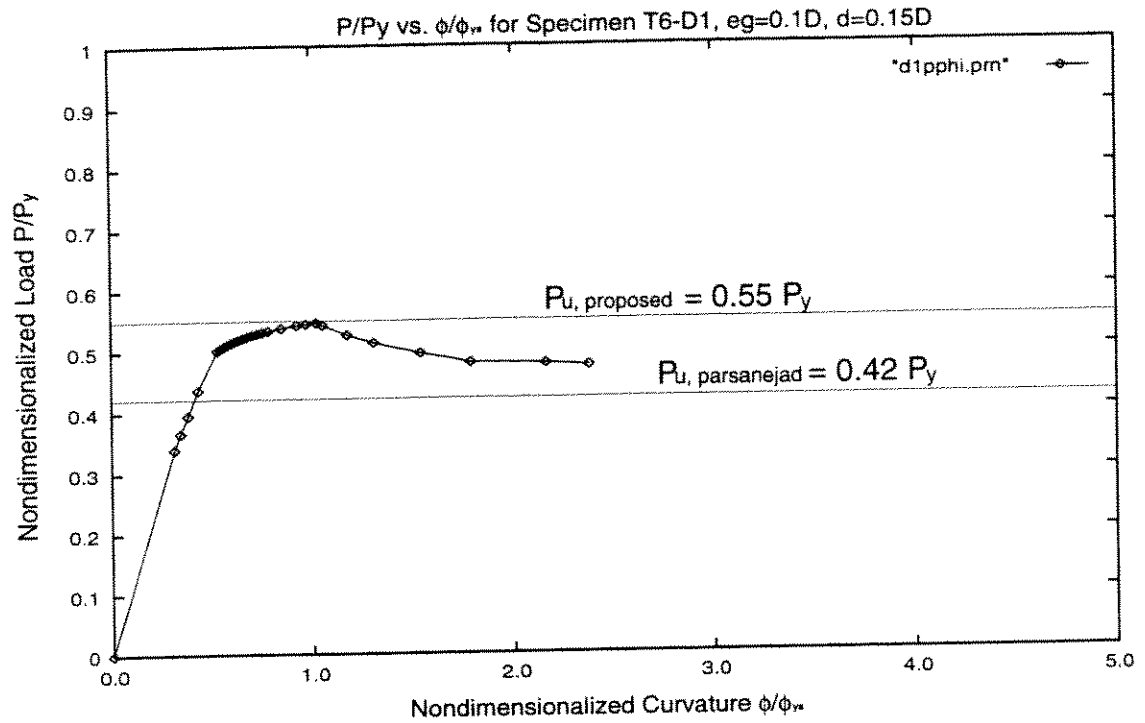
Figure S5-9: P vs. φ curve for Specimen T6-D1. (Ref. S4)

P/Py vs. φ/φ_ys for Specimen T7-D3, eg=0.1D, d=0.16D
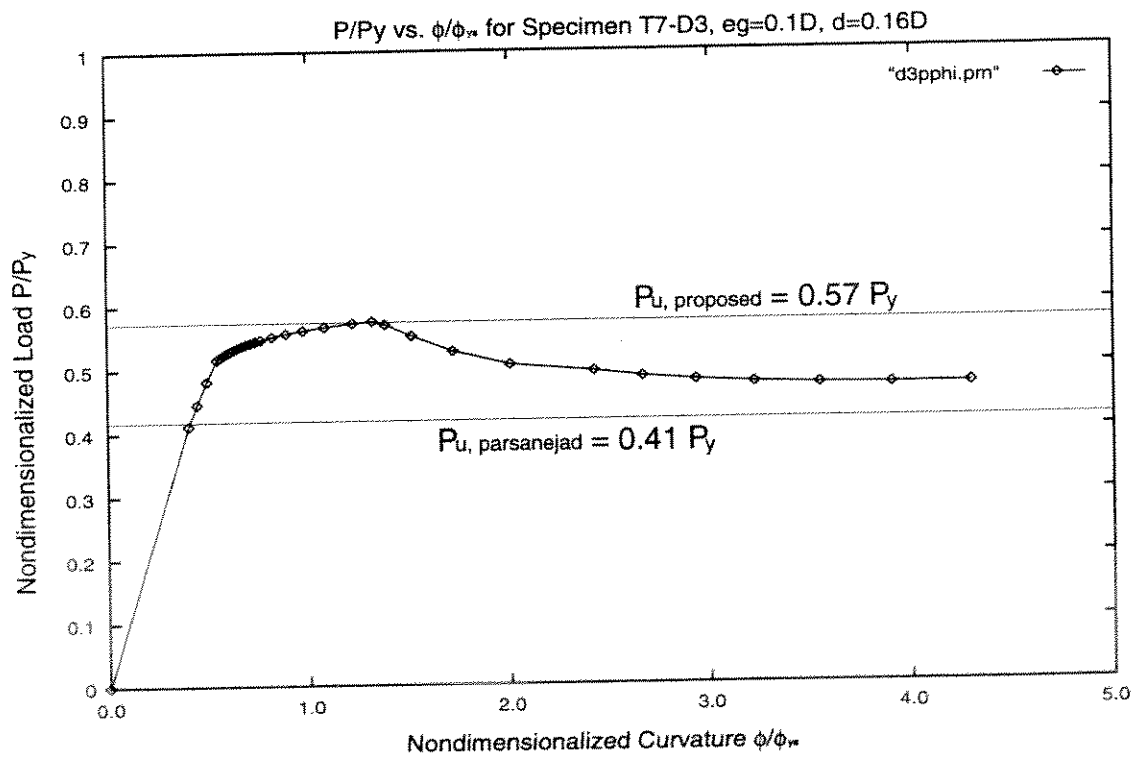
Figure S5-10: P vs. φ curve for Specimen T7-D3. (Ref. S4)

Figure S5-11: P vs. φ curve for Specimen W1. (Ref. S3)
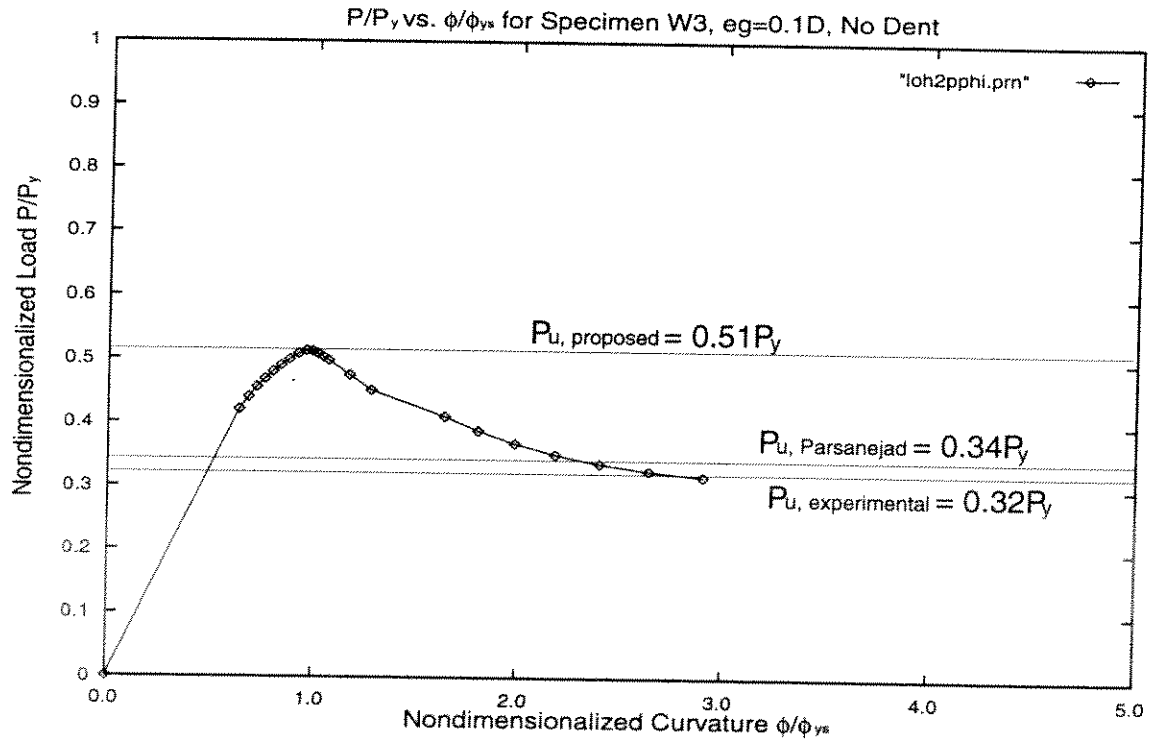
Figure S5-12: P vs. φ curve for Specimen W3. (Ref. S3)
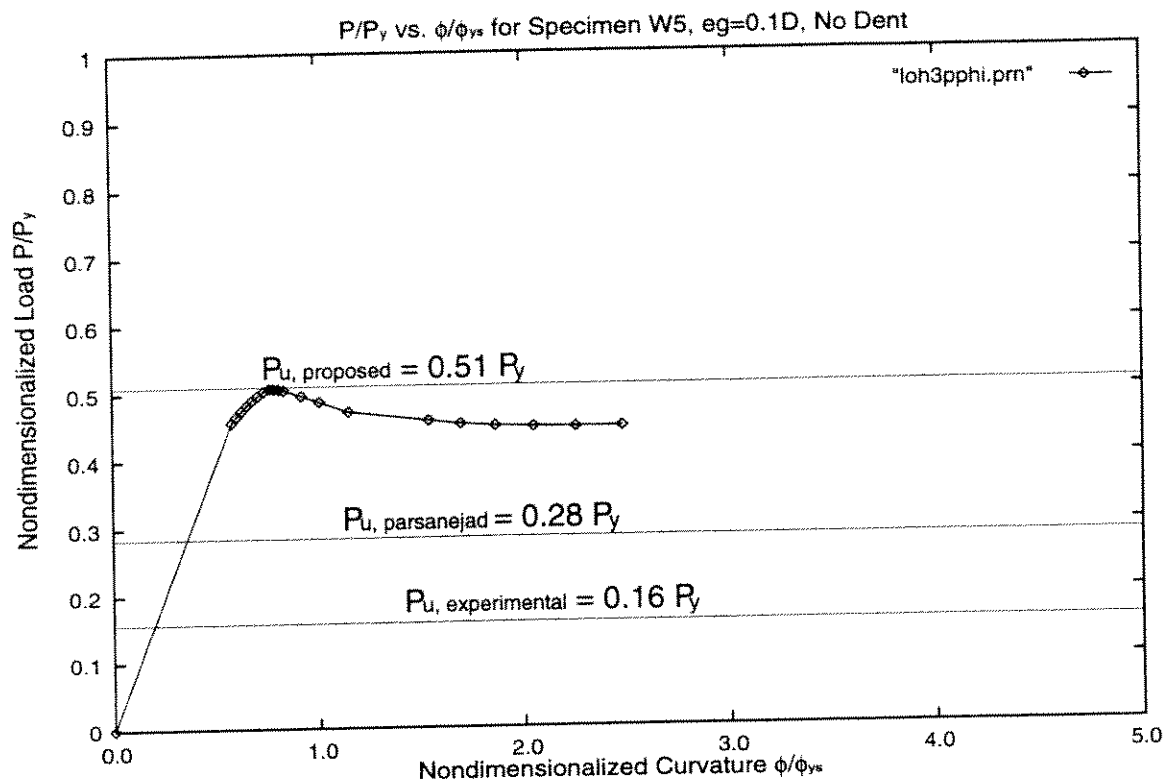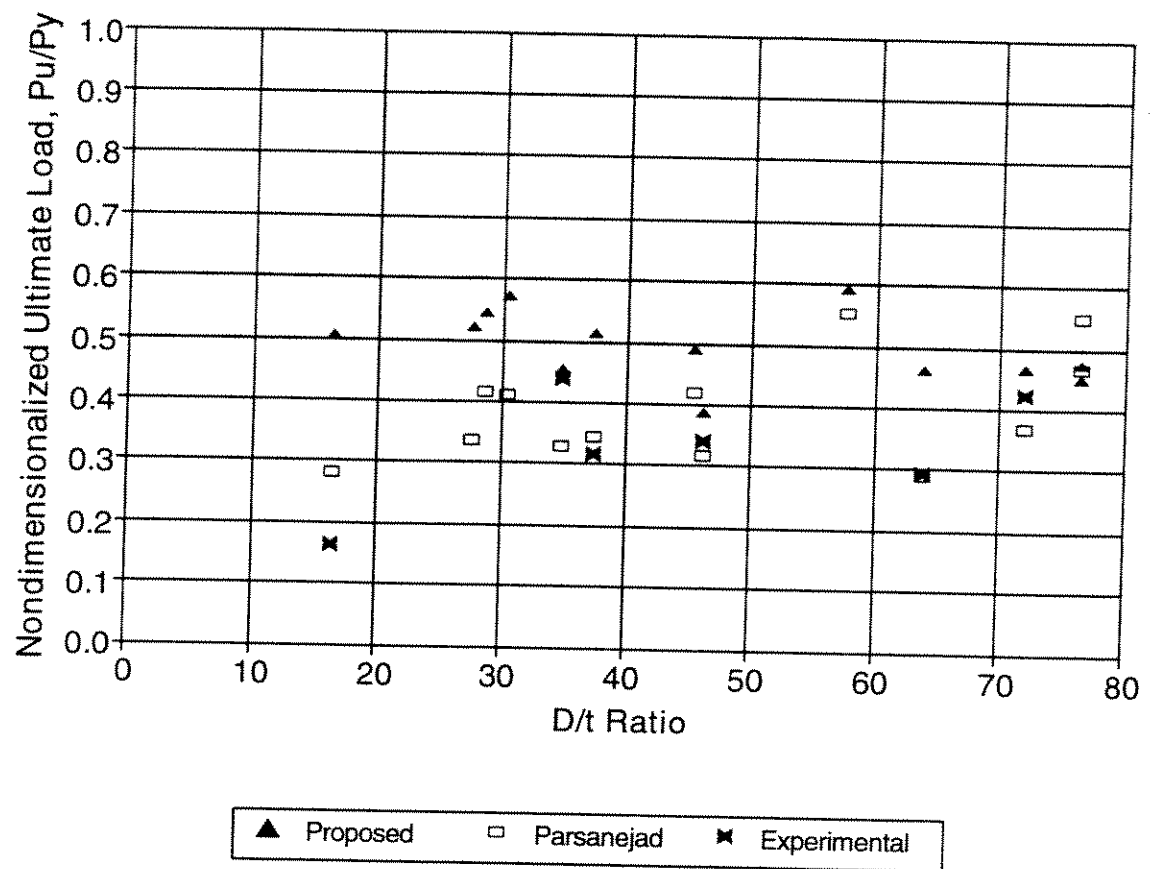
Figure S5-13: P vs. φ curve for Specimen W5. (Ref. S3)

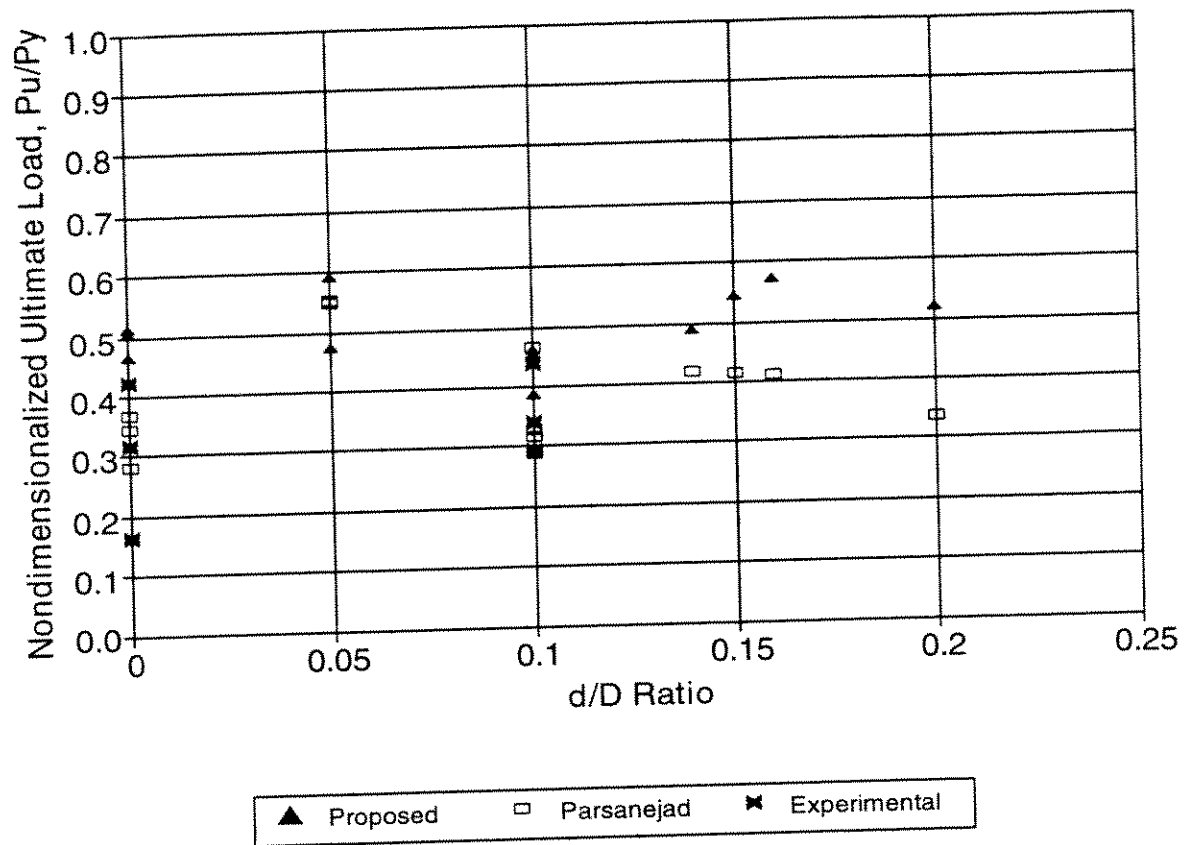Figure S6-1: Nondimensionalized Ultimate Load vs. Diameter-to-thickness ratio, D/t.

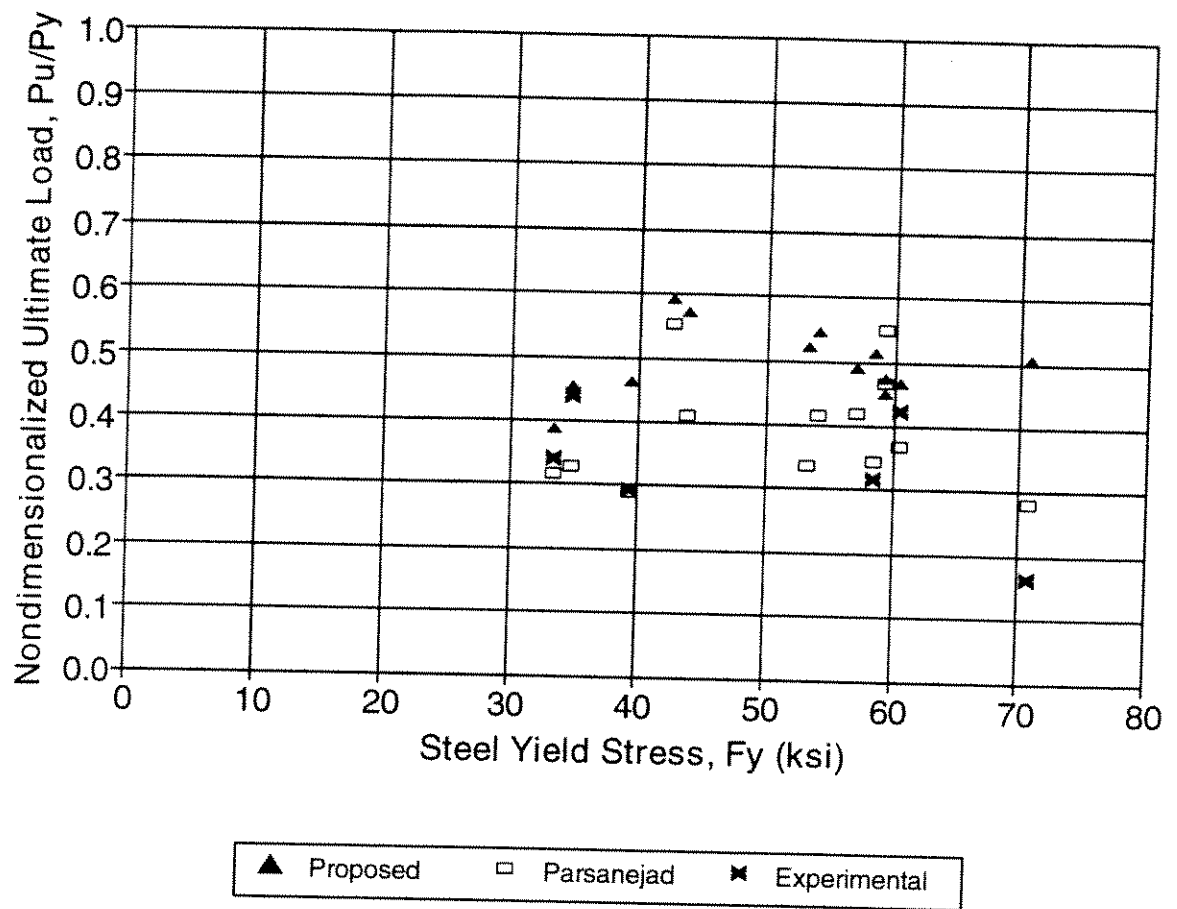Figure S6-2: Nondimensionalized Ultimate Load vs. Dent depth-to-diameter ratio, d/D.

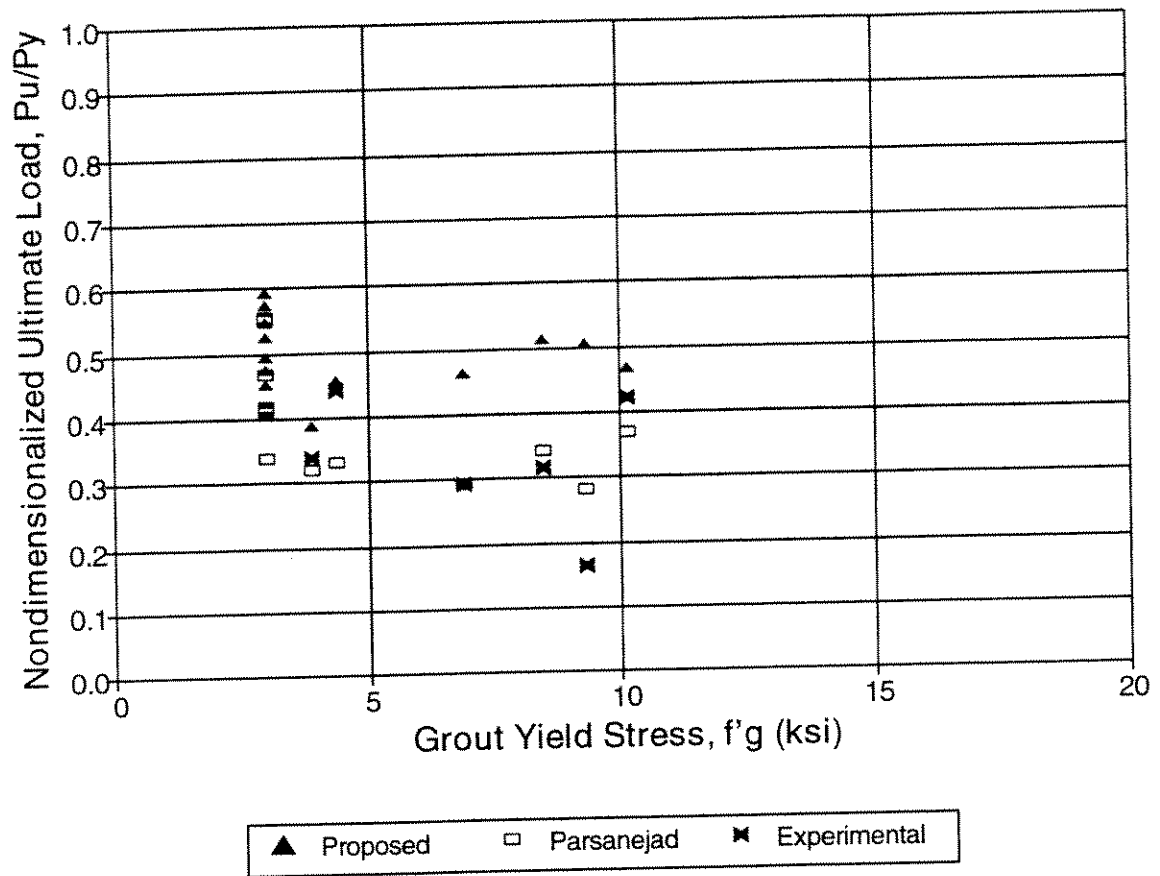Figure S6-3: Nondimensionalized Ultimate Load vs. Steel Yield Stress, F_y

Figure S6-4: Nondimensionalized Ultimate Load vs. Grout Yield Stress, f'g.

Appendix SA: Computer Program 'SIMGTD.F'

Copies of the FORTRAN-77 computer program can be obtained from:

Professor Alexis Ostapenko

Lehigh University

Fritz Engineering Laboratory

13 E. Packer Ave.

Bethlehem, PA 18015

        Tel: (610) 758-3517

        E-mail: ao03@Lehigh.edu